

A SPATIOTEMPORAL PROBE OF THE
HUMAN VISUAL SYSTEM
BY
APPLICATION OF NONLINEAR SYSTEMS IDENTIFICATION THEORY

Thesis by
Michael Jiu-Wei Chen

In Partial Fulfillment of the Requirement
for the Degree of
Doctor of Philosophy

California Institute of Technology

Pasadena, California

1982

(Submitted November 30, 1981)

Acknowledgements

I am deeply grateful to Professor Derek H. Fender, my advisor, for his insight, enthusiasm, inspiration and perspicacity in scientific research, and for his guidance, direction, and support throughout my graduate studies.

I feel thankful to Dr. James P. Ary for his company, assistance in this research, helpful discussions, and experimental expertise to bring this research to fruition. I am thankful to Dr. Gilbert McCann for providing a sound environment for white noise research. Also, my gratitude is due to Dr. Ross Larkin and Dr. Stan Klein for their elucidating discussions on white noise and related topics.

I would like to thank Dr. James Kajiya for his intuitive instructions on digital signal processing, Dr. Lincoln Wood for deepening my interest in systems theory and Dr. John Allman for improving and reviewing this thesis.

I would like to thank Jeffrey K. Eriksen for his company and enthusiastic participation and assistance in numerous experiments; and Dr. Terrance Darcey for imparting his first-hand knowledge on source localization technique in evoked potentials.

Many thanks are also due to Sandy Griffon for her assistance in preparing the manuscript and to Evelyn Johnson for taking care of administrative affairs.

Finally, my special gratitude is extended to my parents and my wife Jennifer for their continuous spiritual support for this Ph.D. program.

ABSTRACT

This thesis describes an attempt to apply signal processing and systems theory to the task of analyzing and interpreting evoked potential data and locating evoked potential sources by physical principles. Random impulse trains were used as inputs to characterize the human visual system. The method is analogous to the Wiener method for a continuous Gaussian white noise input. The restricted-diagonal Volterra series for discrete inputs is used by making certain restrictions on the integrals in a Volterra series. A modification of Lee and Schetzen's method was used in the estimation of the kernels.

Forty-channel first-order kernels were computed for briefly appearing checkerboard patterns placed in left or right visual fields. The measured potential distribution showed a radical dependence on stimulus locus. Equivalent dipoles generally give excellent fits to the measured data, and the mapping between the visual field and these equivalent sources is similar to the commonly accepted mapping between the visual field and the visual cortex. Also, the results resemble those using conventional signal averaging.

First order kernels show better signal-to-noise ratio when compared to conventional signal averaging for the same experiment duration. Multichannel first-order kernels show that sources from early components are deep in the head as expected and in a believable region.

Results for the second-order kernels reveal occlusive interactions in the visual system and are interpreted relative to the first-order kernel.

These inhibitions display different lengths of memories which suggest that they might arise from different neural origins.

CONTENTS

	page
Chapter 1	
SYSTEMS, VISUAL SYSTEMS, AND BRAIN WAVES	1
Chapter 2	
THEORY OF WHITE-NOISE ANALYSIS	29
Chapter 3	
DATA ACQUISITION AND INSTRUMENTATION	64
Chapter 4	
EXPERIMENTAL DATA ANALYSIS AND INTERPRETATION	78
Chapter 5	
DISCUSSION AND CONCLUSION	139
REFERENCES	143

CHAPTER 1

SYSTEMS, VISUAL SYSTEM, AND BRAIN WAVES1.1 SYSTEMS

The problem of finding the functional relationship that determines the output of a system in response to any relevant input is known as the problem of system identification, characterization or estimation. This estimation process is a major step in system modeling. System modeling helps the experimenter to extract from the model insight into the functioning of the system and makes prediction of system behaviour possible.

The techniques of linear systems theory have been used extensively in the study of nonlinear systems because of the completeness and simplicity of the linear approach and the difficulty in linking nonlinear analysis with functional entities such as individual building-blocks defined by transfer-functions. For those nonlinear systems which utilize linear approaches, small signal approximations or certain linearizing assumptions are usually made. Because of their limitations and applicability to a narrow class of systems, they cannot be applied generally to nonlinear systems.

There are essentially two approaches to the characterization of a nonlinear system. In the differential equation (parameter and state estimation) method, the topology of a system is assumed to be known, so that a set of differential equations can be used to represent the system. Identification reduces to the determination of various parameters in the equations. In the integral equation (nonparametric weighting-function, filter, kernel, or func-

tional) method, little or no a priori assumptions are made about the topology of the system. The identification reduces to the determination of the various kernels.

I shall confine myself to the system defined by the stimulus-response relationship of the evoked potentials. This system is assumed to be stationary, finite-memory, and analytic. A system is stationary if its characteristics do not change rapidly with time and the system response to identical stimuli remains similar. Finite-memory means that a stimulus with finite energy will generate a response that decays to an arbitrarily small degree in finite time. Analyticity means that the differential behavior of all orders is continuous within the domain of stimulus values. In general, the functional relation between the stimulus $x(t)$ and the response $y(t)$ can be described by the mathematical notion of a functional:

$$y(t) = T[x(t)]$$

For a physical system like the evoked potential, the causality principle is the first instrument of the analysis process. Under this principle, a system only reacts to the past and present values of the stimulus. Therefore, $y(t)$ can be expressed as

$$y(t) = T[x(t'); t' \leq t]$$

Further, any explicit mathematical expression of the functional T has a certain structural form involving a set of parameters and a set of constants. The set of parameters Q is the object of the identification process.

Therefore, we can denote $y(t)$ as

$$y(t) = T[Q; x(t'), t' \leq t]$$

to demonstrate the existence of the parameter set within the functional expression.

DEVELOPMENT OF WHITE-NOISE NONLINEAR ANALYSIS

Volterra series can be considered as a generalization of the power series representation. Wiener (1949) applied this analysis technique to find the response of a nonlinear device to noise. Bose(1956) has carried the theory further. Following a series of lectures by Wiener, the theoretical framework, higher dimensional transforms, and optimization with Gaussian inputs were studied by Brilliant(1958), George(1959), and Chesler(1960), respectively. Barrett (1963) has treated statistical inputs, while the synthesis problem has been examined by Van Trees(1962). The technique has been extended to discrete systems, and a class of time-variant systems. The theory of convergence has also been treated by Ku and Wolf(1966).

BIOLOGICAL SYSTEMS

Nonlinearities are often necessary for the optimal functioning of biological systems from the behavioral point of view. One typical example is that the transformation of sensory inputs from the physical parameters of the real world to the neural response is usually in a logarithmic fashion to accommodate large ranges of the physical parameters.

Biological systems are often nonlinear even under "small signal" conditions. Moreover, since the signal-to-noise ratio in biological systems is often low, the degree of nonlinearity is also low, i.e. only the first few terms of the Volterra(Wiener) series are required in order to describe the system accurately. This is due to the fact that noise has a linearizing effect. Consider the response of a nonlinear system such as a rectifier or saturation-cutoff to a sinewave input (Fig. 1.1.1). Assume also that the size of the harmonic distortion is directly proportional to the size of the nonlinear kernels. It can be noted by inspection that the effect of contaminating noise is to round off the sharp corners of the response which are caused by the nonlinearity. The higher the noise level, the more linear the response 'appears', i.e. the size of the harmonic distortion decreases. In other words, a system with high noise content limits its analysis to the first few kernels. For a noisy system such as the evoked potential, it might be possible to characterize it by a few kernels.

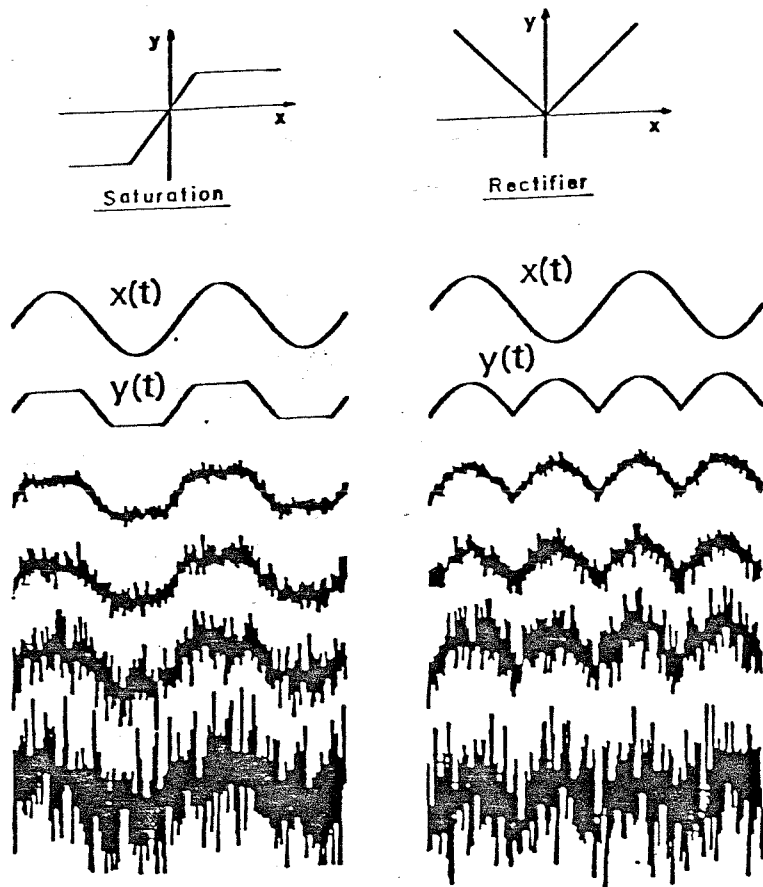


Fig. 1.1.1 Linearizing effect of noise to nonlinear systems.
 (From The Noise about White-Noise: Pros and Cons
 P. Z. Marmarelis, 1975)

1.2 HUMAN VISUAL SYSTEMS

The eye acts as a self-contained outpost of the brain. It collects information, analyzes it, and hands it on for further processing by the brain through the optic nerve. The optic nerve fibers arise from ganglion cells in the retina and end on cells in the lateral geniculate nucleus(LGN) whose axons in turn project through the optic radiation to the cerebral cortex. From here on the progression becomes even more complex.

The anatomy and projections of the human LGN do not appear to differ significantly from those of other primates. When the retinal fibers reach the LGN, they terminate in a number of laminae, each of which receives a topographic projection from a hemiretina and projects to the cerebral cortex. The laminae are stacked in visuotopic register so that there is direct continuity of visual field between adjacent laminae. The thalamus lies near the center of the brain, while the primary visual cortex lies in and around the medial surface of the occipital lobe. Some 70% to 80% of all retinal fibers subserve this pathway.

Figure 1.2.1 shows how the output from each retina divides in two at the optic chiasm to supply the lateral geniculate nucleus and cortex in each hemisphere. As a result, the right side of each retina projects to the right cerebral hemisphere. The right side of each retina receives the image of the visual field on the left side of the animal. Each cerebral hemisphere, therefore, sees the contralateral visual field.

The part of the visual cortex where the optic radiations end consists of a folded plate of cells about 1 or 2 mm thick. This region of cortex, area 17 (also called the striate cortex or visual area I) lies posteriorly in the

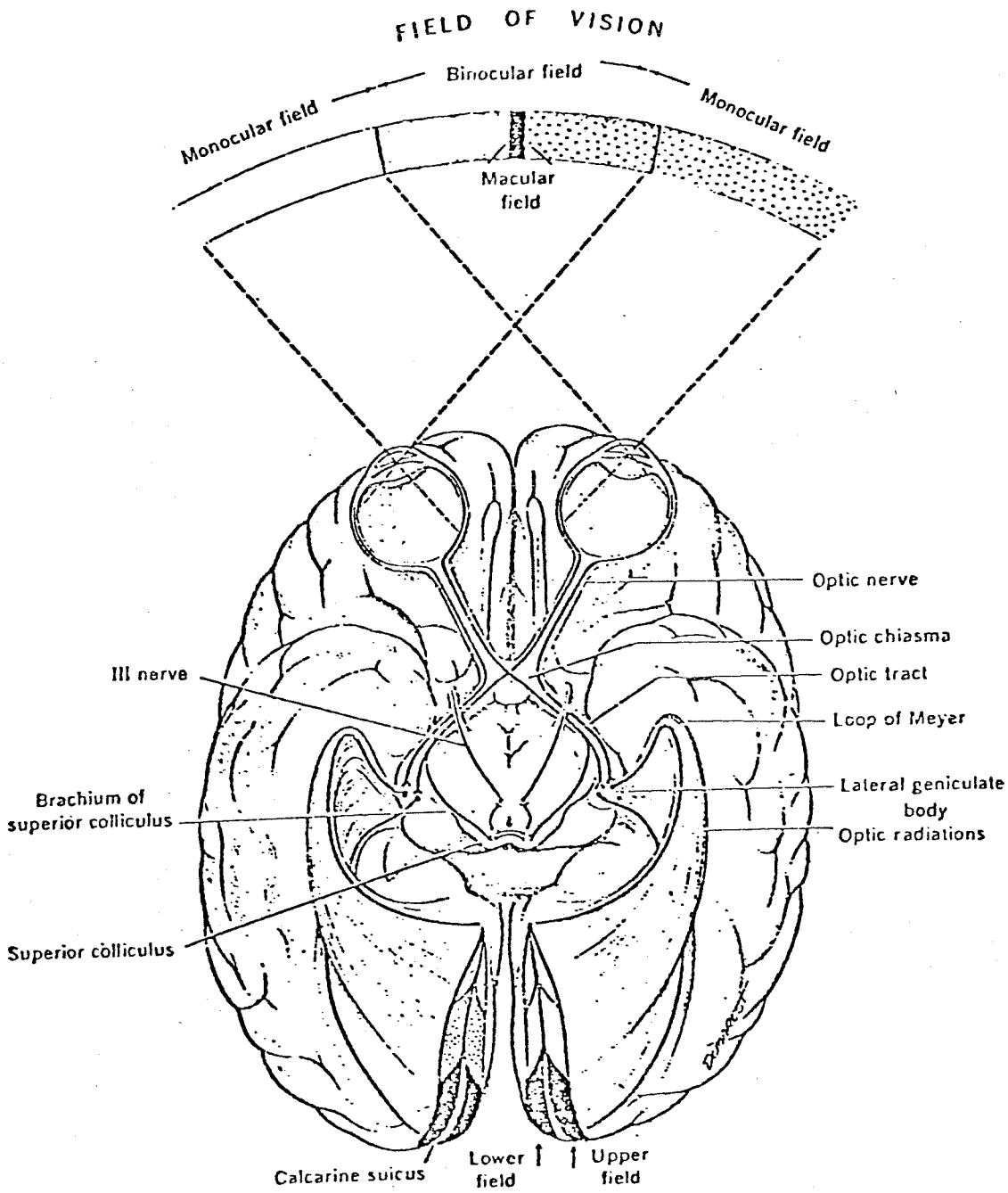


Fig. 1.2.1 The geniculo-cortical pathway of the human visual system

occipital lobe. Around area 17 lie the secondary visual cortices, area 18 and 19, which get their input from area 17. Connections are known from area 17 in one hemisphere through the corpus collosum to area 18 in the other hemisphere.

There are other retinal projections that branch off to the midbrain. In higher vertebrates they are primarily concerned with regulating eye movements and pupillary responses and are not directly relevant for pattern recognition (Sprague et al, 1973). It is also known that there are rich interconnections between midbrain areas and thalamic and cortical areas. The important point here is that the anatomy does support the existence of at least two separate retino-cortical pathways. The retino-geniculo-striate-circumstriate pathway is believed to be concerned with the detailed analysis of visual pattern, while the retino-tectal neocortex pathway is concerned with spatial orientation functions and has only crude discrimination capabilities(Doty, 1973).

In these visual pathways, the neurons converge and diverge extensively at any stage; that is, each cell makes and receives connections with a number of other cells. One purpose of this study is to develop a noninvasive technique to investigate this highly interactive and complicated system through evoked potentials in conjunction with systems analysis.

1.3 ELECTROENCEPHALOGRAPH (EEG)

Electrical recordings from the scalp demonstrate continuous electrical activity which is assumed to have its origin in the brain. The undulations in the recorded electrical potentials are called brain waves, and the entire record is called an electroencephalogram. It has been speculated that both the intensity and patterns of this electrical activity are determined to a great extent by the overall level of excitation of the brain resulting from functions mainly in the reticular activating system.

The amplitudes of the potentials on the surface of the head range from zero to 200 microvolts, and the usual range of recorded frequencies is from 0.1 to 100 Hz to cover the major portion of the spectrum. The character of the waves is dependent upon the degree of activity of the cerebral cortex and subcortical structures, and the waves change markedly between the states of wakefulness and sleep.

Much of the time the EEG are irregular, and no general pattern can be discerned in the EEG. However, at other times, distinct patterns do appear. Some of these are characteristic of specific abnormalities of the brain, such as epilepsy. Others occur even in normal persons and can be classified into alpha, beta, theta, and delta waves. This classification is based mainly on the frequency distribution: alpha(8-13 Hz), beta(14-50 Hz), theta(4-7 Hz), and delta(0.1-3.5 Hz)(Guyton, 1975).

Summaries of current methods in EEG analysis have been published (Gevins et al., 1975, Barlow, 1979).

The following is a brief discussion concerning the statistical aspects of the EEG. Some properties such as the degree of whiteness and stationarity of EEG have direct relevance to white-noise nonlinear analysis of evoked potentials. We are trying to extract characteristics (kernels) of a system by using a white-noise stimulus and measuring responses which are also predominated by white-gaussian noise while its amplitude can be a hundred times larger than the responses. Luckily the EEG possesses certain simple statistical properties. Signal averaging and cross-correlation methods can be performed for signal enhancement but these techniques are only valid for additive white-noise.

At present, almost all methods of time-domain and frequency-domain EEG analysis are based on implicit assumptions regarding the statistical characteristics of the underlying random process, particularly with respect to the extent of stationarity and the degree that the process approximates a Gaussian distribution.

It is generally accepted that the EEG may be regarded as a statistical phenomenon with two components: (1) a stochastic and, in short sections, almost stationary process; and (2) transient components (wave trains, spikes, and sharp waves) that arise sporadically. Some investigators have done EEG modelling based on testing of its statistical properties (Wennberg and Zetterberg, 1971; Johnson et al, 1979).

There is evidence to support modelling of the clinically-recorded EEG as a zero-mean gaussian process. Elul(1969) found that the EEG was Gaussian

distributed two-thirds of the time for a patient in the resting state, while Glass(1969) showed that the amplitude probability density function for the alpha rhythm is approximately zero-mean and Gaussian. The center frequencies, bandwidths and RMS amplitudes of the basic rhythms are estimated from data provided by Kaiser et al.(1964), Obriest and Henry(1958), and Matousek et al(1967). Wennberg and Zetterberg (1971) studied the stochastic component of EEG based on the observation that the auto-correlation function of the EEG has a strikingly simple structure. They showed that the method of parameter analysis of the EEG permits an exact description of the stationary part of the EEG with a few parameters. Johnson et al.(1979) proposed that the EEG can be represented as the superimposed outputs of four slightly damped oscillators (alpha, beta, theta, and delta bands) driven by independent white Gaussian noise processes.

It should be noted that the statistical model only serves as a working hypothesis to efficiently parameterize certain a priori knowledge about sources of variability in the recorded EEG rather than a representation of underlying physiology.

1.4 EVOKED POTENTIALS (EP)

From the results of intracranial recordings on animals, it has been known for some time that sensory stimulation produces distinct, identifiable, electric signals. These signals have been variously referred to as evoked responses (ER), evoked potentials (EP), cortical evoked potentials, etc. If the evoked signals are due to visual stimulation and the measurements are made on the scalp, the potentials can then be referred to as visually evoked scalp potentials (VESP). Until recently, attempts to measure through the intact scalp the details of the changes in brain activity accompanying sensory stimulation have been swamped in a flood of ever-present spontaneous neuro-electric activity. Because of the small amplitudes of the EP signals in comparison with the ongoing EEG and the technical difficulties in extracting them, until the early 1960's, the electroencephalogram (EEG) was one of the few techniques available to the brain physiologist and neuroscientist for the study of electrical activity of the human brain.

Measurement of evoked potentials, on the one hand, constitutes a probe into the cerebral black box of sensory processing. On the other hand, it is a noninvasive and practical means of access to the electrical activities within the sensory pathways of the intact human brain.

DETECTION OF EP SIGNALS:

The main problem in recording evoked potentials is detecting them at all. The signal recorded at the scalp commonly reaches an amplitude of between 50 and 100 microvolts, but evoked potentials are often no more than 5

microvolts and may be as small as 0.5 to 1.0 microvolt. To the evoked potential investigator the EEG signal is unwanted and overwhelming background noise. Some form of signal processing must be applied to improve the signal-to-noise ratio before any interpretation can be done.

The entire history of development in EEG and EP technology reflects the gradual advance in electronics and progressive application of analog and digital signal processing techniques and adoption of new concepts in systems and communications theory. The following is a short summary of this process.

Cruikshank (1937) demonstrated that it was possible to detect a VESP in the ongoing EEG by blocking the spontaneous alpha rhythms due to visual stimulation. Adrian (1941) demonstrated a perturbation detectable in the ongoing EEG activity which was evokable by stimulation of the receptors of any of the various sensory modalities.

Galambos and Davis (1943) superimposed successive amplified responses to auditory stimulation on an oscilloscope face. The lower amplitude and shorter latency components of the cortical response were made evident. Dawson (1954) was able to average a small number of oscillograms. He constructed the first automatic averaging device for recording transient evoked potentials. The device was partly mechanical but nonetheless sufficiently efficient to provide research findings that are still valid today. In 1957, magnetic recordings of brain potentials were used by Barlow. In 1960, Rosner et al. used a tape recorder as a memory device and repetitive triggering in conjunction with an analog amplifier for summation. An all electronic averaging com-

puter was subsequently developed by Clynes and Kohn(1964). Commercial production of this machine enabled hundreds of hospitals and laboratories to embark on research on transient evoked potential in the mid-1960's.

Mainly because of developments in computer technology, we are now able to record stimulus-related evoked potentials in man. The method most often used today incorporates computers and signal averaging and display software.

SIGNAL-TO-NOISE RATIO ENHANCEMENT

The following is a summary of various methods employed for enhancing the signal-to-noise ratio of evoked potentials. Although these methods seem to be different, the first and second methods in theory are special cases of the third. The fourth method encompasses the third since one dimensional cross-correlation can be considered as a special case of the more general multidimensional cross-correlations in kernel estimations.

(1) Conventional Transient Signal Averaging - Time Domain Analysis

When a repetitive sensory stimulus (flash, sound click, or tap) is presented to a subject, a repetitive electrical response is evoked. The stimuli are sufficiently spaced in time such that the system is returned to a resting state between successive stimuli. The evoked waveform is assumed to be time-locked to the occurrence of the stimulus presentation and to be affected by stimulus-parameter variations. A randomized presentation of stimuli helps to minimize locking of the EEG and may improve S/N ratio (Rushkin, 1965). For most applications, it is not feasible to measure the evoked

potential directly on the cortex of the brain and measurements are made by electrodes attached to the scalp. Transient EP waveforms are commonly divided into different latencies ranges in the hope of associating different components with different functions of the central nervous system and/or with different locations in the brain (Kooi and Bagchi, 1964; Ciganek, 1961).

(2) Steady State Evoked Potentials- Frequency Domain Analysis

As the stimulus repetition frequency is progressively increased, transient EPs overlap to an increasing extent. Under this condition, the brain does not have time to regain its undisturbed state between successive stimuli. At sufficiently high repetition frequency, no individual response cycle can be associated with a particular stimulus cycle (Milner et al., 1972). When this steady state is established, it is more appropriate to describe the response in terms of different stimulus repetition frequencies and to analyze the EPs by their harmonic components. A convenient way to present steady state EP data is to plot the amplitude and phase of the various harmonic components of the EP versus stimulus repetition frequency. In some circumstances frequency analysis is more convenient and more effective in extracting responses of small amplitudes than in temporal (transient) analysis. Milner et al.(1972) claimed this method is less influenced, as transient EP's are, by the psychological state of the subject. In other words, a higher S/N ratio enhancement may be attained by using this method. Fourier analyzers are normally used for this method. One purpose of classifying steady-state EPs into different frequency regions is the hope of associating different frequency regions with different brain functions and/or locations within the CNS (central nervous

system).

(3) Cross-correlation Method

This method may be viewed as a generalization of conventional waveform averaging, Fourier analysis and synchronous detection (Ciganek, 1961; Fricker and Sanders, 1974).

(4) White-Noise Systems Analysis

This is the method that this thesis adopts. The information processing system in the brain is treated as a black box. The Input-output transformation can be expanded as a Volterra/Wiener-type functional series. Kernels are computed using one-dimensional or multidimensional cross-correlation methods. A white-noise input is used as a testing function. This method can be considered as the most complete, canonical and exhaustive approach in EP research so far. In essence, this approach encompasses all the concepts and methods previously discussed.

1.5 VISUALLY EVOKED SCALP POTENTIALS (VESP)

HUMAN VESP'S RELATION TO SPATIALLY UNSTRUCTURED AND STRUCTURED STIMULUS FIELDS

It is generally known that patterned stimulus fields can evoke EPs whose amplitudes are as large as, or larger than those evoked by spatially-unstructured stimuli, even though the light energy involved may be ten thousand times less (Clynes and Kohn, 1967, 1968). In other words, pattern stimuli are much more potent stimuli to the EP part of the visual system. This has

been supported by evidence from many single cell studies also (Hubel and Wiesel, 1962, 1965, 1968). There are a number of investigations of pattern EPs in which various types of patterns have been flashed (Rietveld et al., 1967; Spehlmann, 1965).

Using the EP, the mapping between the visual field and visual cortex in the human has been studied by several investigators (Michael and Halliday, 1971; Jeffreys and Axford, 1972; Darcey, 1979; Darcey et al., 1980). Local stimuli are required for selective stimulation of specific areas of the visual field.

For pattern stimulation, the issue of the contribution of the fovea, parafovea and periphery to the VESP is clearer than for a blank flash stimulus. Pattern VESPs are believed to have major contributions from the central 6 degrees or so of the visual field (Michael and Halliday, 1971; Jeffreys and Axford, 1972; Jeffreys, 1971; Nakamura and Biersdorf, 1971).

Darcey, Ary, and Fender (1980) explored the problem of VESP dependence on retinal location in great detail. Previous studies often disagreed both in results and interpretation. Typically, the methods used differed in stimulus regime, referencing scheme, electrode layout, and data analysis. Darcey et al. showed that the detailed spatiotemporal measurements can reconcile some of the differences and elucidate the character of the generators.

ABOUT THE STIMULUS USED IN THIS THESIS

One reason why I used (randomly) flashed pattern in this study is that

it is easier to present a brief, impulse-like patterned stimulus by transilluminating flash through a checkerboard pattern than by other methods. Presenting pattern-appearance or pattern-reversals in an impulse fashion is more difficult on our system because of the longer switching time involved. Pattern instead of blank field was used because pattern is a stronger stimulus in evoking responses of reasonable size as explained before. Another reason is that the typical response parameters such as latencies, magnitudes, and potential distributions to checkerboard pattern by using conventional signal averaging on several subjects in this laboratory are known from results of previous experiments. They can be used as a comparison to responses obtained from white-noise analysis.

1.6 NONLINEAR BEHAVIOURS OF VESP SYSTEM

Recall that in systems analysis using a sinusoidal input, a system is linear when the response only contains a sinewave of the same frequency as the input signal. When the response also contains other frequencies, the system is nonlinear. For example, a zero-memory nonlinear system, such as a rectifier, introduces higher harmonics. When this nonlinearity can be expanded in a Taylor series, the nonlinearity is said to behave in a quasi-linear manner. At decreasing modulation depths (small signal analysis), the response of the system could become more linear, if the amplitudes of the higher harmonics decrease faster than the amplitude of the fundamental frequency. A zero memory nonlinearity is called an "essential nonlinearity" when the response contains higher harmonics even at the lowest modulation depths.

EVIDENCE OF NONLINEARITY FROM STEADY STATE EVOKED POTENTIALS

De Lange(1957) introduced the use of sinusoidally modulated light(SML) in vision research. This stimulus is given by: $L(t) = I(1 + m \sin wt)$, where the modulation depth m is A/I , A is the amplitude of the sinewave, I is the average light intensity of the light source, and $w = 2\pi f$, f is the frequency of the sinewave.

Kamp et al.(1968) found that the occipital EP behaves nonlinearly to sinusoidally modulated light. Even at the lowest modulation depths, the response in a certain frequency region contains second harmonics, so the EP system may contain an essential nonlinear element.

Clynes et al. (1964) studied the brain wave response to step, ramp, and sinewave light stimuli. The step response allowed them to obtain the transient response of the system, and the sinewave stimuli allowed them to obtain the steady state response. They reported a nonlinearity in the VESP for dark and light flashes on a background. Both dark and light flash responses show the same polarity. They also mentioned an essential nonlinearity in the EP system.

When the luminance of a diffuse field is sinusoidally modulated it is found that only very small EPs result for modulation frequencies below 3 Hz (Fig.1.5.1). However, a stimulus frequency which lies within a range centered near 10 Hz evokes a response of large amplitude compared with that at neighboring frequencies. A number of characteristics of this 10Hz response are closely related to corresponding characteristics of the spontaneous EEG. The

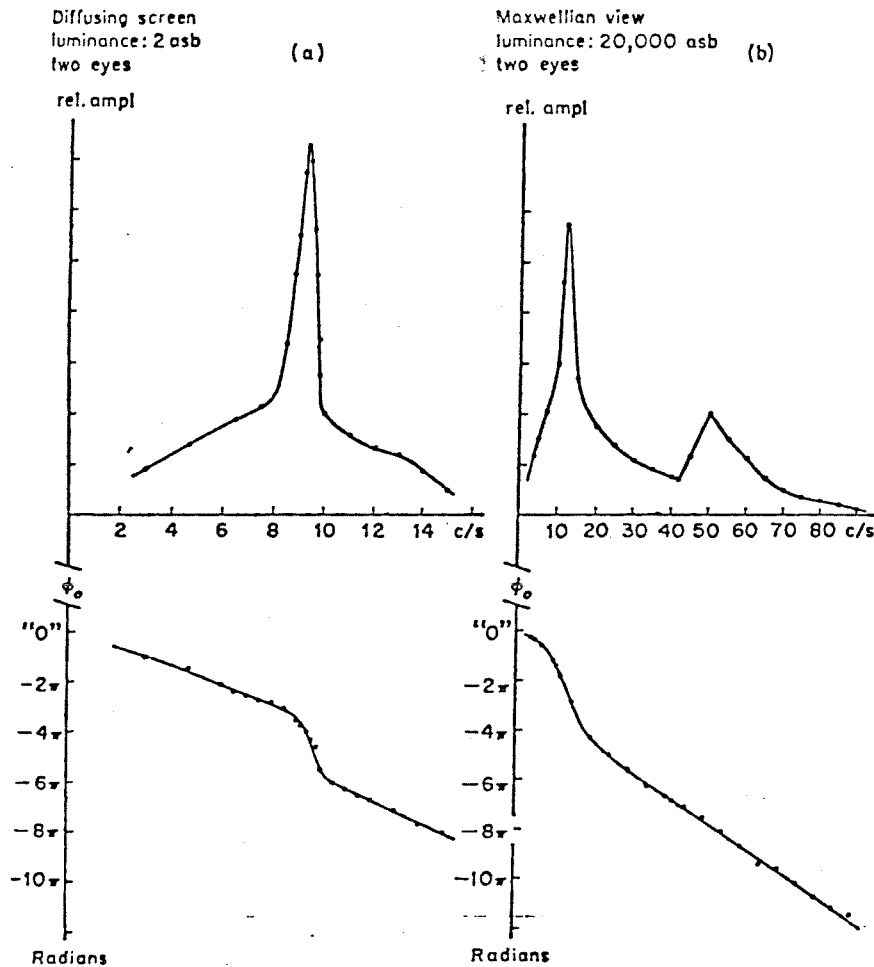


Fig. 1.5.1 Amplitude and phase characteristics for two subjects with sinusoidally modulated light; the frequency scale is linear; amplitudes in relative units.

- (a) Both the amplitude and phase characteristics of subject A show resonance properties.
- (b) The amplitude spectrum of subject B shows two preference regions. Neither amplitude nor phase characteristics shows resonance properties. The phase characteristic shows that the latencies in the low frequency range are longer than in the high frequency range.

From H. Spekreijse (1966), *Analysis of EEG Responses in Man*. Junk Publishers, The Hague.

large 10 Hz EP component can be evoked by a stimulus modulation frequency of 5 Hz as well as one of 10 Hz.

A plot of the lag of the phase of the EP versus stimulus modulation frequency is fairly close to a straight line except at frequencies near the center frequency of the amplitude peak where there is a well-defined step.

The findings described above led to the suggestion of a simple serial processing model of the form illustrated in Fig.1.5.2. It must be emphasized that the model is not unique. This model is a sequential processing model and does not involve any feedback or feedforward element, nor does it involve any more parallel pathways. It can be considered as one of the early attempts in combining engineering and system concepts with physiological structures. In this figure, we do observe there are nonlinear elements such as rectification and saturation combined with frequency tuning devices. Evidence of correspondencies between peripheral stages of the model and neuroanatomy has been reported by Spekrijse(1966). The frequency selective peak near 10Hz has been modelled by a centrally-located linear filter. The physiological correlate of such a filter is not clear yet. For example, it might arise from the reverberation between cortex and thalamus according to Anderson and Anderson(1958). Spekrijse and Oosting(1970) introduced a technique to separate a nonlinear system into linear and nonlinear parts, knowing only the input and output signals of the whole system. The nonlinearity is linearized by means of an auxiliary signal added to the input signal. Using this method with sinusoidally modulated light, Spekrijse proposed the above model for the evoked response system. He could distinguish two parallel channels, a long-latency system with

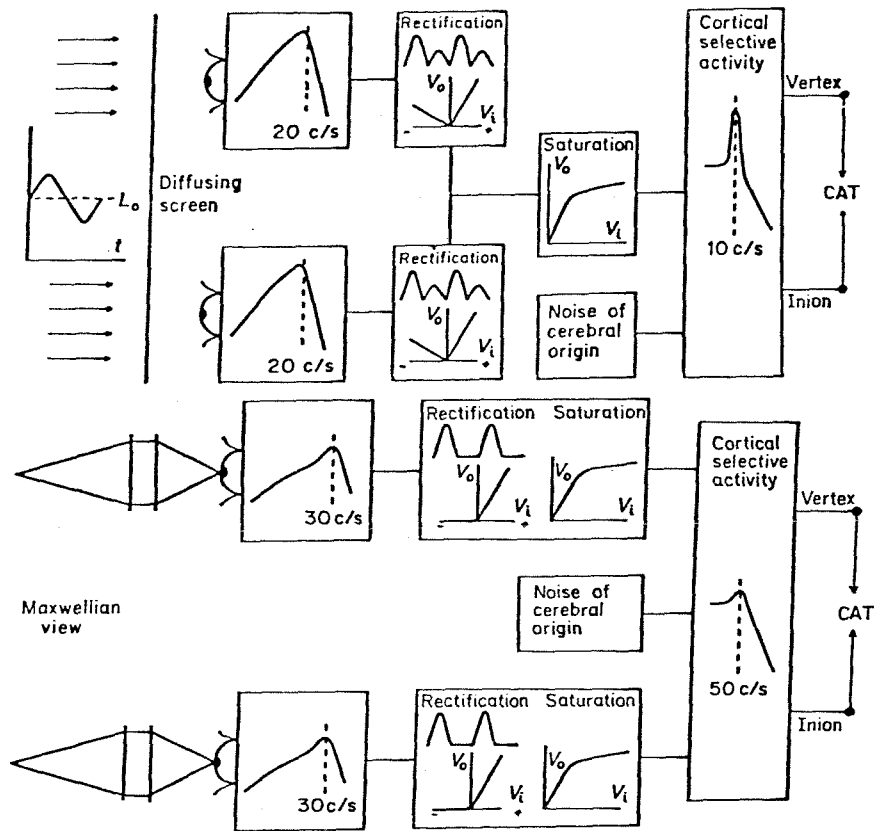


Fig. 1.5.2. Upper half: a simplified model of the retina-cortex system of long latency (i.e. low frequency region).

Lower half: a simplified model of the retina-cortex subsystem of short latency (i.e. high-frequency region).

From H. Spekrijse (1966). Analysis of EEG Responses in Man. Junk Publishers, The Hague.

the largest response in the region of the alpha-frequency(10Hz) and a short-latency system with the largest response in the 45-60 Hz region.

In many, but not all subjects, the harmonic components of steady-state EPs which fall in the range 45 to 60 Hz (high-frequency components) have several features in common with the 10Hz (low-frequency components) described above. A frequency selective process gives an amplitude peak in this frequency region, which can be evoked as a fundamental component or as a second harmonic component. This behaviour is similar to that of the 10Hz class of evoked potentials.

Their results, as well as the work of other investigators (Donker, 1975; Montagu, 1967; Van der Tweel and Verduyn-Lunel, 1965) have demonstrated the nonlinear nature of steady state evoked potentials.

One of the most striking effects observed for subjects with pronounced alpha-activity is the appearance of a second harmonic component for a stimulus frequency of about half of the alpha-frequency. In these same subjects the fundamental component dominates in the response when stimulating with a frequency near the alpha rhythm. It has been shown that the amplitude of the fundamental component in the response is proportional to the modulation depth of the sinusoidal input, up to a certain value that depends on the size of the visual field, average luminance etc. Such a linear relationship holds also for the second harmonic in the response except for a small deviation at modulation depths approaching zero. This deviation can be explained by the influence of quantal noise (Van der Tweel and Spekrijse, 1969). These findings

indicate that the distortions in the human evoked responses can be described, to a first approximation, as linear rectification.

The above evidences from steady-state evoked potentials support the nonlinear nature of visually evoked potentials. Sinusoidally modulated light was generally used as the stimulus. The nonlinearity was interpreted with respect to the luminance effect of the visual stimulus. One purpose of this thesis is to probe into nonlinear effect due to pattern stimulation. In other words, the rapid adaptation effect of one pattern stimulus to a subsequent pattern stimulus separated by a small time interval will be discussed.

1.6 APPLICATIONS OF WHITE-NOISE NONLINEAR SYSTEMS ANALYSIS

As with most scientific endeavors, the application of white-noise nonlinear systems identification theory lags far behind the theoretical development. In the last ten years there has been an outburst of applications in biological, physical and engineering systems. Most biological applications are in neurophysiology.

In general, applications in biology have been reported in such diverse systems as neurons(Marmarelis and Naka, 1974; McCann, 1974; Marmarelis and McCann, 1973), pupillary systems(Sandberg and Stark, 1968; Watanabe and Stark, 1975; Hung et al, 1977; Hung and Stark, 1977(a)), eye-movement systems(Hung and Stark, 1977(b)), synapses(Krausz, 1975), central nervous system (CNS)(Reits, 1975; Ho, 1973), electroretinogram (ERG)(Koblaz and Fender, 1975; Larkin, 1979; Larkin, Klein, Ogden and Fender, 1979) and manual control in biology (French and Butz, 1973).

PREVIOUS ATTEMPTS OF WHITE-NOISE ANALYSIS OF EVOKED POTENTIALS

Beatty(1971) used the Lee-Schetzen cross-correlation method to obtain the 1st-degree transfer function associated with a Poisson-distributed temporal light stimulus and the EEG recorded over the midline occipital cortex.

Ho (1973) calculated the kernels associated with the human visual evoked response(VER) by recording with electrodes placed 3 cm forward from theinion on the midline. One-hundred epochs were averaged, resulting in 5 sec of data sampled at 5msec. For flashing-diffuse-light stimulus input, the shapes of the envelopes of the resulting first- and second-degree kernels of the

second-degree VESP kernel model are highly convoluted. The model responses appear to simulate the experimental responses fairly well.

Reits(1975) used a correlation technique for the noise-modulated input analysis of visual evoked potentials recorded at 9 electrodes which are distributed in a cross, 5 vertically from theinion to the vertex and 4 horizontally, intersecting at theinion. He analyzed the cross mono- and bi-correlation functions of the EP and deduced that the human visual system can be separated into a number of linear and nonlinear parts. From this and other experimental results he concluded that " all components share the first linear part, which consists of a band filter with maximal transmission in the frequency range of 8-11 Hz which produces the alpha component. The output of the half-wave rectifier branches again to two filters, one of which has a maximal transmission near 40-50 Hz and the other has a passband from 14-25 Hz. The output of the high frequency filter produces the early component and that of the intermediate filter produces the late component. " His result was incomplete because he did not calculate the entire time domain second order kernel. This is necessary to fully understand the system's quadratic nonlinearity.

Sciabassi et al.(1977) used electric stimulation in a Poisson impulse train to investigate the somatosensory evoked responses in normal subjects and in multiple sclerosis patients. The use of functional power series to characterize the somatosensory modality shows that the responses to temporally interactive stimuli are nonlinear, decrease with increasing stimulus rate, and degenerate in the advanced state of the disease. The kernels that they obtained revealed a generally occlusive interaction.

Trimble and Phillips (1978), using bandlimited Gaussian noise and time-domain correlation techniques, obtained the first- and second-order kernels for the human VESP system. They found that the first-order kernels have a memory of approximately 250 msec. The second-order kernels indicated a quadratic nonlinear element with a memory less than 20 msec. They found that the nonlinear kernel played a major part in the VESP but that there were no significant contributions from kernels higher than second-order. Further tests of reproducibility suggested that the kernels are reliable describing functions. They also examined the predictive power of the kernel set for transient and steady state responses, as well as how they were altered by changes in stimulus parameters such as luminance and chromaticity.

Coppola (1979) used band-limited Gaussian noise to study the human visual system. He claimed that the prediction of the VESP from the identified kernels was quite good. Prediction of the response to sine wave modulated light was in close agreement with the actual responses. He did not use any mathematical method to justify the closeness of match. Neither did he present enough kernels to verify the repeatability of his estimates.

I handled the nonlinear analysis of VESP in a different manner. First of all, a stronger pattern stimulus was used instead of noise-modulated light. Secondly, since Gaussian stimulus is a weak stimulus both statistically and psychophysically, Poisson white noise was used to avoid this disadvantage. Through a combined effect of the above two factors, kernel estimates turned out to be more stable. Most importantly, a large number of channels were used to investigate the spatial distribution of these kernels. Comparisons were

then made between white-noise results with those obtained by conventional methods due to partial-field effect. The problem of equivalent sources was also considered. These are some aspects that previous investigators never addressed.

CHAPTER 2

THEORY OF WHITE-NOISE ANALYSIS

The theory of white-noise system analysis is in general complicated and requires some background in statistical communications and signal theory. This chapter serves as an overview of the theory without rigorous mathematical proofs. It starts from the concept of auto- and cross-correlation, their past utilization in evoked-potential research, to Volterra and Wiener kernels and functional series, Lee-Schetzen's cross-correlation method for kernel estimation, different kinds of white noise, and finally the Poisson impulse train, RDV(restricted diagonal Volterra) series, and a kernel-estimation method similar to the approach of Lee and Schetzen.

2.1 AUTO-CORRELATION AND CROSS-CORRELATION FUNCTION ANALYSIS

Since multidimensional cross-correlation plays an important role in kernel estimation for identification of nonlinear systems, it is necessary to discuss briefly the correlation methods used in systems and signal theory. Although white-noise nonlinear analysis is still a new approach in EP research, correlation analysis has already been applied to the EEG for some time. Also, techniques used in conventional signal averaging can be considered as special cases of cross-correlation, although such terminology is not used.

Auto-correlation and cross-correlation are methods of analysis which have been developed in statistical communication theory for the study of randomly varying processes, and have found wide applications in radar and communications data processing and in infrared and nuclear magnetic resonance

spectroscopy (Whalen 1971; Becker and Farrer, 1972). Basically, the voltage-time graph of the signal is considered as a time series, and some aspects of its statistical behavior are examined. With appropriate limitations, the EEG can similarly be considered as a time series, and its statistical behavior studied by means of these techniques.

AUTO-CORRELATION AND CROSS-CORRELATION

The cross-correlation function is defined as

$$R_{xy}(T) = E\{x(t)y(t-T)\}$$

where $E\{ \}$ denotes the expected value or statistical average. This function is dependent upon the time shift between the two signals. If ergodicity holds, then time and ensemble averages are interchangeable. In experimental situations, one does not usually have the statistical data necessary for computation of ensemble averages. Thus correlation functions are computed by time averaging. Therefore,

$$R_{xy}(T) = \overline{x(t)y(t-T)} = \lim_{P \rightarrow \infty} \frac{1}{P} \int_0^P x(t)y(t-T)dt \quad (2-1-1)$$

where P (the period of observation) is large but not necessarily infinite.

Similarly the auto-correlation function is defined as

$$R_{xx}(T) = E\{x(t)x(t-T)\} \quad (2-1-2)$$

This function reflects the degree of time-connectedness of the same sample function. It should be carefully noted that $R_{xx}(T)$ is a deterministic function even though $x(t)$ is random.

Implemented on a discrete system such as a digital computer, the above formula can be expressed as

$$R_{xx}(m) = \frac{1}{N} \sum_{n=0}^{N-m-1} x(n)x(n+m) \quad (2-1-3)$$

There are two reasons to consider the auto-correlation function of a random signal. First, the auto-correlation function $R_{xx}(T)$ in its own right provides useful information about $x(t)$. It is a measure of both time variation and statistical dependence. Second, by the Wiener-Kinchine theorem, the frequency-domain description of a random signal is its power spectral density $G_{xx}(f) = F[R_{xx}(T)]$, where $F[\cdot]$ indicates Fourier transform.

We can similarly define the n -th order auto-correlation function of a signal as

$$R_n(T_1, \dots, T_n) = E\{x(t-T_1) \dots x(t-T_n)\}$$

In white-noise system analysis, the "whiteness" of a signal is determined by the degree to which its auto-correlation properties approximate the ones of ideal white-noise. In the case of ideal white-noise, the auto-correlations of odd orders are uniformly zero, while the even-order ones are zero everywhere but on the full-diagonal points; where the arguments T_1, \dots, T_n form exhaustive pairs of identical values (Lee and Schetzen, 1965). For Gaussian white-noise,

$$E\{x(t-T_1) \dots x(t-T_n)\} = \begin{cases} \binom{n}{2}^p \prod_{i,j=1}^n \delta(T_i - T_j) & \text{if } n \text{ is even} \\ 0 & \text{if } n \text{ is odd} \end{cases}$$

where p is the power density of the Gaussian white noise.

An application of cross-correlation is the detection of the presence

of a periodic signal buried in noise. A disadvantage of this technique is that the signal must be known ahead of time. Stated another way, the signal cannot be recovered; only its presence (if periodic) can be detected. For this reason, investigators studying the VESP or any other evoked response have very seldom used correlation function analysis in detecting periodic signals. In the following sections, the cross-correlation method will be used to extract signals from random stimuli and their responses buried in noise. System kernels can be characterized by this method. This method is found to be powerful and intuitively understandable. I foresee in the near future that this technique will be received by more and more researchers in evoked potentials.

RELATIONSHIP BETWEEN CORRELATION ANALYSIS AND FREQUENCY ANALYSIS

The results of auto-correlation and cross-correlation analysis, with their corresponding displays in the time domain, contain information that is theoretically equivalent to that obtained by frequency analysis as represented in the power density spectrum for a single signal, and the cross-power density spectrum for a pair of signals.

The choice of frequency analysis versus correlation analysis is largely predicated on the appropriateness of the output display of the analysis relative to the immediate physiological problem. For example, if the specific question being asked is one of time relationships (latencies), then correlation analysis is especially appropriate. On the other hand, if the question is related to the presence of a specific frequency component, then

the power density spectrum of frequency analysis is the method that gives this type of answer explicitly. For the present study, latencies and amplitude distributions are more important than frequency components; therefore we shall only consider the time-domain behavior of the system.

CROSS-CORRELATION AND SIGNAL AVERAGING

The evoked potential obtained from conventional waveform averaging is a special form of the more general procedure of cross-correlation (Lee 1960; Perry and Childers 1969; Whalen 1971 ; Regan 1972). It is equivalent to the cross-correlation between a pulse train with a constant interstimulus period and the measured EEG waveform.

Fourier analysis techniques (Milner et al. 1972) were used in conjunction with higher frequency constant stimulation rates. The method of synchronous detection has also been used (Fricker 1974; Padmos and Norren 1972). The above method involves several periods of stimulation at various specified frequencies, usually in the 10-50 Hz range. This type of signal processing is analogous to very narrow band filtering and integration, with outputs of amplitude and phase at each separate frequency. The phase-frequency data can be used to determine a time delay for the frequency range tested. This is another specialized example of cross-correlation where one waveform is the noisy signal waveform at any stimulus frequency, and the other waveform may be either a sinewave or a square wave at the same frequency, depending on the particular technique used.

All the methods described above, conventional signal averaging,

Fourier analysis and synchronous detection, may be regarded as extreme aspects of cross-correlation techniques. We can now clearly see the generality of the cross-correlation technique.

2.2 VOLTERRA FUNCTIONAL SERIES

FRECHET-VOLTERRA SERIES

Frechet (1910) showed that every continuous functional F on a set of functions x which are continuous on a finite interval (a,b) can be represented by a power-series type functional

$$\begin{aligned}
 F(x) = & k_0 + \int_a^b k_1(T)x(T)dT + \iint_a^b k_2(T_1, T_2)x(T_1)x(T_2)dT_1 dT_2 \\
 & + \iiint_a^b k_3(T_1, T_2, T_3)x(T_1)x(T_2)x(T_3)dT_1 dT_2 dT_3 \\
 & + \dots
 \end{aligned} \tag{2-2-1}$$

A functional is a function whose argument is a function and whose value is a number. The convolution integral for linear systems,

$$y(t) = \int_{-\infty}^t h(t-T)x(T)dT$$

is an example of a functional.

Volterra is credited with applying the concept of a functional to expanding the input-output relationship of a nonlinear system in a power series with functionals as terms.

For the class of systems described before, F can be expanded in a functional power series, known as the Volterra series.

$$y(t) = \sum_{n=0}^{\infty} \int_{-\infty}^{\infty} \int_{-\infty}^{\infty} k_n(T_1, \dots, T_n)x(t-T_1)\dots x(t-T_n)dT_1 \dots dT_n$$

or expressed in another way,

$$y(t) = \sum_{n=0}^{\infty} \int_{-\infty}^{\infty} \int_{-\infty}^{\infty} k_n(T_1, \dots, T_n) \prod_{i=1}^n x(t-T_i) dT_i \tag{2-2-2}$$

The Volterra series can be thought of as the limiting case of Taylor

series expansion of a function with multiple arguments. The Volterra functionals are a generalization of convolution techniques for linear systems to nonlinear systems which have finite memory and are time-invariant.

Bedrosian and Rice (1971,1975) showed that the Volterra series can be expanded in a slightly different way in a suitable region of convergence.

$$y(t) = \sum_{n=1}^{\infty} \frac{1}{n!} \int_{-\infty}^{\infty} \int_{-\infty}^{\infty} k_n(T_1, \dots, T_n) \prod_{i=1}^n x(t-T_i) dT_i \quad (2-2-3)$$

The function $k(T_1, \dots, T_n)$ is known as the "nth-order Volterra kernel" and is assumed to be a symmetric function of its arguments. If it is not given in such a form, it can be symmetrized by taking $1/n!$ times the sum of the kernels obtained by permuting the arguments. The constant term ($n = 0$) is omitted because we are only interested in the passive systems, while the factorial is introduced to simplify some of the results.

Writing out the first two terms in (2-2-3) yields

$$\begin{aligned} y(t) &= \int_{-\infty}^{\infty} k_1(T) x(t-T) dT \\ &+ \frac{1}{2!} \int_{-\infty}^{\infty} \int_{-\infty}^{\infty} k_2(T_1, T_2) x(t-T_1) x(t-T_2) dT_1 dT_2 \\ &+ \dots \end{aligned}$$

from which it is seen that the leading term is the familiar response of a linear filter and $k_1(T)$ is simply the impulse response. The resemblance of the second term to the first suggests that the 'nth-order Volterra kernel' $k_n(T_1, \dots, T_n)$, can be viewed as a sort of 'nth-order impulse response'. This concept is important for later discussion of the significance of the kernel

method in system identification.

VOLTERRA TRANSFER FUNCTION

The n-dimensional Fourier transform of the Volterra kernel leads to similar observations. Letting

$$K_n(f_1, \dots, f_n) = \int_{-\infty}^{\infty} \dots \int_{-\infty}^{\infty} k_n(T_1, \dots, T_n) \exp[-j(w_1 T_1 + \dots + w_n T_n)] dT_1 \dots dT_n \quad (2-2-4)$$

and

$$k_n(T_1, \dots, T_n) = \int_{-\infty}^{\infty} \dots \int_{-\infty}^{\infty} K_n(f_1, \dots, f_n) \exp[j(w_1 T_1 + \dots + w_n T_n)] dw_1 \dots dw_n \quad (2-2-5)$$

denote the n-dimensional Fourier transform pair, where $w_i = 2\pi f_i$, and substituting in (2-2-3) yields

$$y(t) = \sum_{n=1}^{\infty} \frac{1}{n!} \int_{-\infty}^{\infty} \dots \int_{-\infty}^{\infty} df_1 \dots df_n K_n(f_1, \dots, f_n) \exp[j(w_1 + \dots + w_n)t] \prod_{i=1}^n X(f_i) \quad (2-2-6)$$

where $X(f)$ is the Fourier transform of $x(t)$, assuming for the moment that $X(f)$ exists. The Fourier transform of the output then becomes

$$\begin{aligned} Y(f) = & \frac{1}{1!} K_1(f)X(f) + \frac{1}{2!} \int_{-\infty}^{\infty} K_2(f_1, f-f_1)X(f_1)X(f-f_1)df_1 \\ & + \frac{1}{3!} \int_{-\infty}^{\infty} \int_{-\infty}^{\infty} K_3(f_1, f_2, f-f_1-f_2)X(f_1)X(f_2)X(f-f_1-f_2)df_1 df_2 \\ & + \dots \end{aligned} \quad (2-2-7)$$

from which it is again seen that the first term is the familiar response of a linear filter and that $K_1(f)$ is simply the conventional linear transfer

function. By analogy, $K_n(f_1, \dots, f_n)$ can be regarded as an 'nth-order Volterra transfer function'. The symmetry of k_n assures the symmetry of K_n .

Although the results are in the form of infinite series whose terms rapidly increase in complexity, useful approximations can be obtained by using only the leading terms in these expansions when dealing with systems that have only nonlinearities of low orders.

The point of the above derivation is that there is a correspondence between the Volterra kernels in the time domain and the Volterra transfer functions in the frequency domain for nonlinear systems. This kind of symmetry is evident in linear systems and again revealed in nonlinear systems. Also, it is important to understand how the multidimensional Fourier transform plays a role in this relationship.

2.3 WIENER THEORY OF NONLINEAR SYSTEM IDENTIFICATION

Norbert Wiener is considered as the single individual who above anyone else is responsible for the conception of system theory. For it was Wiener who, starting in the twenties and thirties, introduced a number of ideas, concepts, and theories which collectively constitute the core of present-day system theory. Among his contributions, to name just a few, are his theory of prediction and filtering, his representation of nonlinear systems in terms of a series of Laguerre polynomials and Hermite functions, his generalized harmonic analysis, the Paley-Wiener criterion, and the Wiener process. It was Wiener who laid the foundation for cybernetics - the science of communication and control in the animal and the machine.

Wiener developed a canonical representation of a large class of nonlinear systems and proposed its experimental determination in terms of the system response to Brownian motion inputs.

In much the same way that Legendre polynomials are formed to make an orthogonal function set useful for curve fitting, so can a set of orthogonal functionals for nonlinear system characterization be formed. This was first done by Wiener and his work further simplified by Lee and his co-workers.

CHARACTERIZATION OF NONLINEAR SYSTEM

Cameron and Martin (1947) and Wiener (1958) have shown that a broad class of nonlinear systems can be characterized by input-output relationships of the form

$$y(t) = \sum_{n=0}^{\infty} A_n X_n(t) \quad (2-3-1)$$

where the $X_n(t)$ represents products of Hermite functions of various order in the variables z_1, z_2, \dots , which in turn are linearly related to u (the input) through Laguerre functions. Note that the operations involved in this representation are (1) linear with memory, viz., the relations between the z 's and u ; (2) memory-less nonlinear, viz., the relations between the X_n and z_1, z_2, \dots ; and (3) linear with no memory, viz., the summations. In this connection, it should be pointed out that the basic idea of representing a nonlinear input-output relationship as a composition of an infinite number of (1) memory-less nonlinear operations and (2) linear operations with memory, is by no means a new one. It had been employed quite extensively by Volterra and Frechet near the turn of the century.

WIENER FUNCTIONAL SERIES AND KERNELS

As discussed before, a nonlinear analytic system can be described through a Volterra functional expansion by introducing a set of orthogonal functions which completely characterize the system. Wiener's functionals and their associated kernels are constructed with respect to a Gaussian white-noise (GWN) input. He used a method very similar to the Gram-Schmidt orthogonalization procedure to make the functionals orthogonal to each other. At each step he normalized the resulting functional.

Wiener showed that the output $y(t)$, of an unknown nonlinear system can be approximated by a series of functionals, $G_i[h_i, x(t)]$, of the input $x(t)$, where P is the constant power spectral density of the random input.

$$y(t) = G_0[h_0, x(t)] + G_1[h_1, x(t)] + G_2[h_2, x(t)] + \dots$$

$$= \sum_{n=0}^{\infty} G_n[h_n, x(t)] \quad (2-3-2)$$

where

$$\begin{aligned} G_0[h_0, x(t)] &= h_0 \\ G_1[h_1, x(t)] &= \int_{-\infty}^{\infty} h_1(T)x(t-T)dT \\ G_2[h_2, x(t)] &= \int_{-\infty}^{\infty} \int_{-\infty}^{\infty} h_2(T_1, T_2)x(t-T_1)x(t-T_2)dT_1 dT_2 - P \int_{-\infty}^{\infty} h_2(T, T)dT \\ G_3[h_3, x(t)] &= \int_{-\infty}^{\infty} \int_{-\infty}^{\infty} \int_{-\infty}^{\infty} h_3(T_1, T_2, T_3)x(t-T_1)x(t-T_2)x(t-T_3)dT_1 dT_2 dT_3 \\ &\quad - 3P \int_{-\infty}^{\infty} \int_{-\infty}^{\infty} h_3(T_1, T_2, T_2)x(t-T_1)dT_1 dT_2 \quad (2-3-3) \end{aligned}$$

in which $\{h_n\}$ is the set of Wiener kernels for the nonlinear system, and $\{G_n\}$ is a complete set of orthogonal functionals.

He showed that when $x(t)$ is Gaussian white-noise, the functionals G_i , are mutually orthogonal in the sense of time averages. Namely

$$\overline{G_i[h_i, x(t)]G_j[h_j, x(t)]} = 0 \quad \text{for } i \neq j \quad (2-3-4)$$

Because of orthogonality, the Wiener series can be truncated after n functionals, giving the best n th order polynomial nonlinear approximation to the system output in the sense of least mean square error. The Wiener kernels $h_n(T_1, T_2, \dots, T_n)$ characterize a given system and allow prediction of its output to any input $x(t)$.

The class of nonlinear operators amenable to the Wiener technique is the class of functionals that are Lebesgue square integrable over the sample space of realizations of Gaussian white noise signals. In other words, the

output at time t when the input varies over all possible samples of Gaussian white noise has a finite variance. In practice, any continuous time-invariant nonlinear system with a finite memory and limited bandwidth can be identified using Gaussian white noise as the input. The kernels will be finite and continuous.

WHITE-NOISE

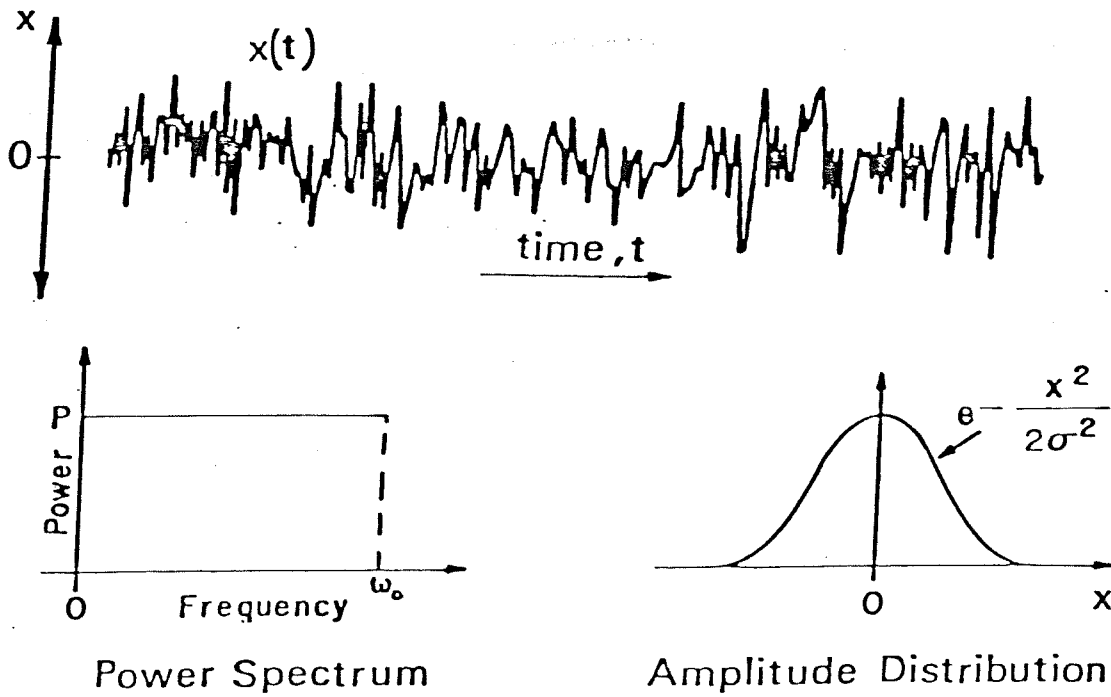


Fig. 2.3.1. Power spectrum and amplitude distribution function for Gaussian white-noise signal.

2.4 CORRELATION AND TRANSFORM METHOD FOR WIENER-KERNEL ESTIMATION

TIME DOMAIN: CORRELATION

Lee and Schetzen (1965) showed that because of orthogonality, the various Wiener kernels could be measured by cross-correlating the system's response with moments of the Gaussian noise input because of orthogonality, specifically,

$$h_n(T_1, T_2, \dots, T_n) = \frac{1}{n! P} \overline{y(t)x(t-T_1)x(t-T_2)\dots x(t-T_n)} \quad (2-4-1)$$

where P is the power density spectrum of the white noise $x(t)$. It can be obtained by

$$E\{x(t-T_1)x(t-T_2)\} = P \delta(T_1 - T_2) \quad (2-4-2)$$

In practice, when computing kernels, it is desirable to subtract from the response the contribution from lower-order kernels before cross-correlation is applied. This is due to the fact that we deal with signals of finite length for which the averages may deviate somewhat from the ones obtained in theory (p.164, Marmarelis and Marmarelis, 1978)

$$h_n(T_1, T_2, \dots, T_n) = \frac{1}{n! P} E\left\{[y(t) - \sum_{k=0}^{n-1} G_k(t)]x(t-T_1)x(t-T_2)\dots x(t-T_n)\right\} \quad (2-4-3)$$

Therefore, the first three kernels can be obtained using

$$h_0 = E\{y(t)\}$$

$$h_1(T) = \frac{1}{P} E\{[y(t) - h_0]x(t-T)\}$$

$$h_2(T_1, T_2) = \frac{1}{2!P} E\left\{[y(t) - h_0 - \int_0^{\infty} h_1(T)x(t-T)dT]x(t-T_1)x(t-T_2)\right\}$$

Integrations are replaced by summations in discrete digital computations. The actual formulas implemented on the digital computer for zero, first- and second-order kernel estimation in the GAS(General Analysis System- a software package for signal processings)are as follows:

$$h_0 = \frac{1}{N} \sum_{n=A}^{A+N-1} y(n)$$

$$h_1(T) = \frac{1}{PN} \sum_{n=A}^{A+N-1} x(n-T)y(n)$$

$$h_2(T_1, T_2) = \frac{1}{2!P^2 N} \sum_{n=A}^{A+N-1} x(n-T_1)x(n-T_2)[y(n)-f(n)]$$

where

$$f(n) = h_0 + \Delta T \sum_{m=0}^M h_1(m)x(n-m)$$

P = the power level of the stimulus

$$= \Delta T \frac{1}{N} \sum_{n=A}^{A+N-1} \sum_{m=-H}^H x(n)x(n-m)$$

H = the time it takes for the auto-correlation of the stimulus to go to zero, M = the maximum time shift of interest, ΔT = the sampling interval, and N = total number of samples used in averaging.

The cross-correlation method is much simpler computationally because it does not involve the cumbersome Laguerre and Hermite transformations. However, because the kernels are multidimensional and therefore require multidimensional cross-correlations for their elucidation, the amount of necessary data processing is still formidable. The main difficulty in the computational

process is the calculation of the higher order correlation functions. The amount of computation increases with the order of the length of the record, the length to which each kernel is computed, and the order of the computed correlation.

FREQUENCY DOMAIN: FFT METHOD

The fast Fourier transform (FFT) algorithm has found wide application since its rediscovery by Cooley and Tukey in 1965.

Since the Wiener kernel theory involves multidimensional convolutions, French and Butz (1973) thought it was possible to apply the FFT to the measurement of the kernels. They showed that it is possible by substituting complex exponential filters in place of Wiener's Laguerre filters. The resulting network evaluates the Fourier transforms of the kernels instead of the coefficients in a Laguerre series expansion.

Such a procedure is an expression of the "duality" which exists in the Fourier transform theory.

Assume that the cross-correlation is obtained by

$$\phi_{yx}(T) = E[y(t)x(t-T)] \quad (2-4-4)$$

Since the Fourier transform of a function $x(t)$ is

$$X(w) = F[x(t)] = \int_{-\infty}^{\infty} x(t)e^{-iwt} dt$$

and the inverse transform is

$$x(t) = F^{-1}[X(w)] = \frac{1}{2\pi} \int_{-\infty}^{\infty} X(w)e^{iwt} dw$$

then the FT of the cross-correlation

$$\Phi_{yx}(w) = F[\phi_{yx}(T)] = F\{E[y(t)x(t-T)]\} = Y(w)X^*(w) \quad (2-4-5)$$

Thus, to compute the cross-correlation, or the kernel $h_1(T)$, the steps can be described as follows:

- (1) Compute $Y(w)$ and $X^*(w)$ via FFT.
- (2) Multiply $Y(w)$ and $X^*(w)$ to obtain $\Phi_{yx}(w)$.
- (3) Compute $(1/P)\phi_{yx}(T) = h_1(T)$ through FFT of $\Phi_{yx}(w)$.

Similarly, with the aid of two-dimensional Fourier transform, the second-order kernel can be estimated as follows:

- (1) Compute $Y_0(w)$ and $X(w)$ via FFT ($Y_0(w) = F[y(t)-h_0]$).
- (2) Form the product $Y_0(w_1+w_2)X^*(w_1)X^*(w_2)$.
- (3) Obtain the time domain inverse of this product by FFT.

The frequency domain method is mentioned here for completeness. For the data computed in chapter 4, only the time-domain cross-correlation method was used.

2.5 QUASI-WHITE AND NON-GAUSSIAN STIMULUS SIGNAL

One practical problem in white-noise system analysis arises from the unrealizability of truly white signals. Real white-noise, by definition, has infinite spectral range, infinite energy, and infinite levels of magnitude in the time domain. Several investigators introduced and studied quasi-white signals that approximate ideal white-noise to a determinable degree. Two such signals are band-limited gaussian white-noise and pseudorandom signals based on m-sequence.

The Wiener-Lee-Schetzen scheme of using Gaussian white-noise to test a nonlinear dynamical system can be extended in two ways (Klein and Yasui, 1979; Marmarelis V. Z., 1977a, 1978): (1) An arbitrary non-Gaussian white-noise stationary signal can be used as the test stimulus. (2) An arbitrary function of this stimulus can then be used as the analyzing function for cross-correlating with the response to obtain the kernels characterizing the system.

Klein and Yasui (1979) also developed a formalism to handle the most general white-noise test stimulus. They theoretically clarified how the kernels obtained with non-Gaussian stimuli are related to the basic Volterra and Wiener kernels. They also considered the case in which the output is cross-correlated not with the stimulus, but with a nonlinear function of the stimulus. They developed a new set of dual-space kernels and dual-space functionals which preserve orthogonality. The dual-space kernels were expanded in terms of Volterra kernels and then related to Wiener kernels. The mathematics involved in their derivation was complicated and will not be reproduced here.

There are many types of white-noise which are different in their

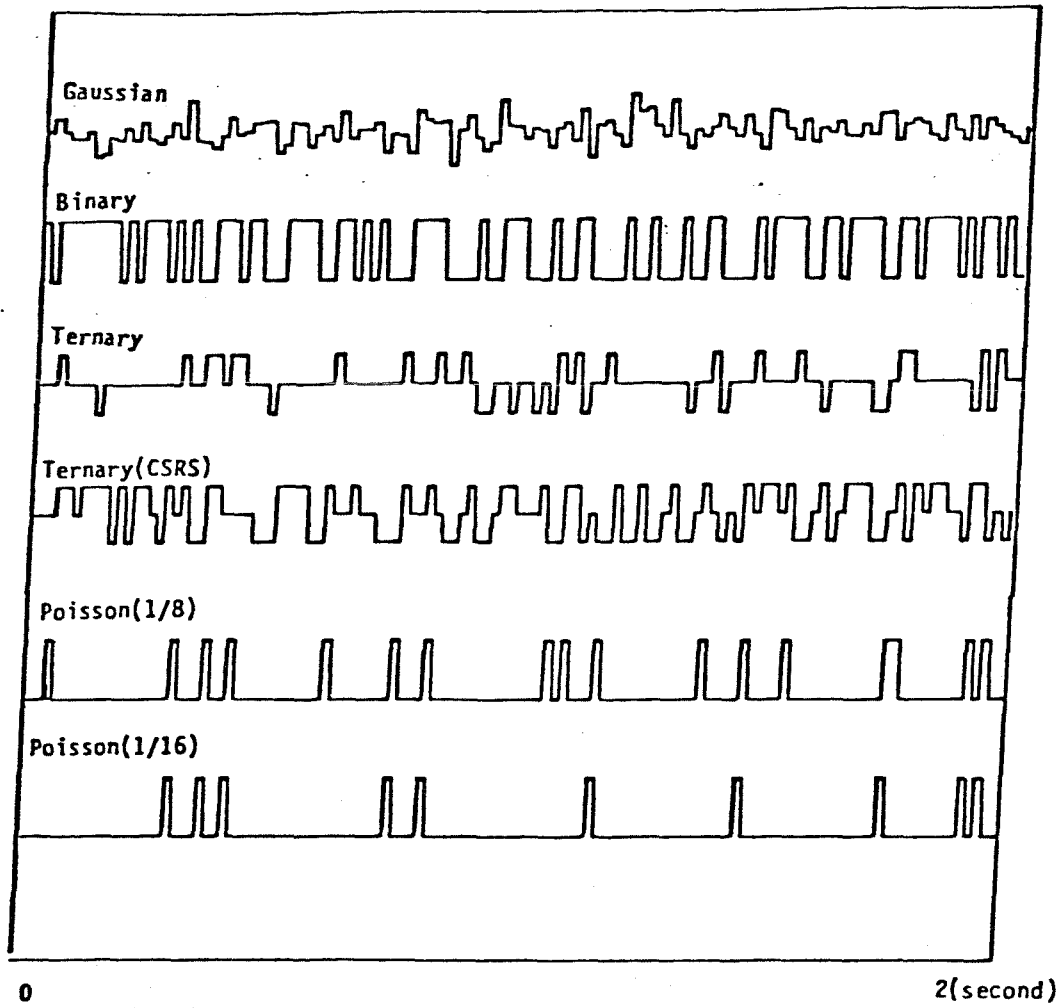


Fig. 2.5.1 Gaussian, binary, ternary, ternary (CSRS) and Poisson white-noise.

amplitude probability distributions and their generation statistics. Binary, ternary, and Poisson are some examples. Another example is the constant-switching-pace symmetric random signals (CSRS - introduced and studied by Marmarelis, V. Z.(1977a)). One example of this kind of signal is a 4-level equi-random CSRS. Figure 2.5.1. shows several types of white-noise. Each of them has different auto-correlation functions of all orders. These lead to different powers and different functional forms. Among them the binary stimulus has the maximum power, while the gaussian stimulus has the minimum power.

2.6 POISSON IMPULSE TRAIN

The probability distribution of m occurrences and $n-m$ non-occurrences in n trials of an experiment, if the probability of a success is p and the probability of failure is $(1-p)$, is known as the binomial distribution.

$$P(m) = C(n,m)p^m (1-p)^{n-m}$$

The limit of the binomial distribution which is of interest to us results when $n \rightarrow \infty$ and $p \rightarrow 0$ in such a way that the product $np = a$ remains finite.

Under this condition, with $m \ll n$,

$$\frac{n!}{(n-m)!} \rightarrow n^m \quad \text{and} \quad (1-p)^{n-m} \rightarrow (1-p)^{a/p} \rightarrow e^{-a}$$

$$P(m) = \frac{n^m}{m!} \left(\frac{a}{n}\right)^m e^{-a}$$

Therefore,

$$P(m) = \frac{a^m}{m!} e^{-a} \quad (2-6-1)$$

This is known as the Poisson distribution. Note that $\sum_{m=0}^{\infty} P(m) = 1$ as it should.

The Poisson distribution applies when a very large number of experiments is carried out, but the probability of success in each is very small, so that "a", the expected number of success, is a finite number.

Let us assume that on the stimulus channel during an experiment, n samples are produced. Among these n samples, the probability of occurrence of a stimulus-event (a flash impulse) is p . If the probability of the stimulus is made smaller and smaller, but the record is long enough to keep the total

number of stimuli finite ($np = a$), one approaches a Poisson stimulus.

Several investigators, including McShane (1962), Hida and Ikeda(1965), Ogura(1972), Krausz(1975) and Kroeker(1977) have dealt with the construction of orthogonal functionals of the Poisson process. Krausz presented a method which is very intuitive and mathematically simple. He described a new series, analogous to the Wiener series, referred to as the "restricted diagonal Volterra (RDV) series". For Poisson impulse trains (where the times of randomly occurring impulses are given by a Poisson process), the functionals of the RDV series are orthogonal.

In order to derive an orthogonal series expansion for the input of a system when the system input is a Poisson train of impulses, it is first necessary to determine the input moments of all orders. The moments of a train of impulses take a simpler form when the train is adjusted to have zero mean amplitude. Let $x(t)$ denote the binary process. Krausz showed that when $x(t)$ is the zero mean Poisson impulse train previously defined, the functionals, $G_i[h_1, x(t)]$, are mutually orthogonal.

MOMENTS OF THE POISSON IMPULSE TRAIN

The moments of the input to a polynomial nonlinear system determine the form of the orthogonal expansion for its output. The Poisson impulse train input is defined by

$$x(t) = \lim_{\substack{\Delta T \rightarrow 0 \\ r \rightarrow \infty}} x(r\Delta T)$$

$$x(r\Delta T) = \frac{1}{\Delta T} \quad \text{with probability } L\Delta T$$

(2-6-2)

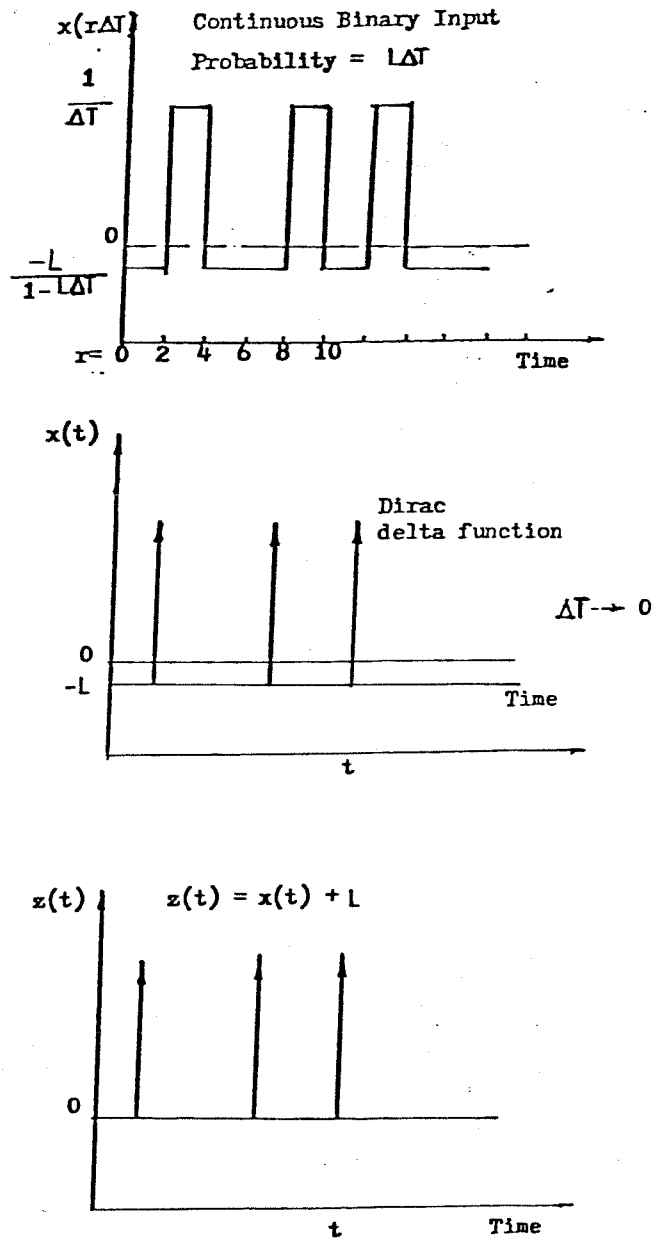


Fig. 2.6.1 Random impulse train input. (a) continuous binary input. (b) limiting case as $\Delta T \rightarrow 0$. (c) the input actually delivered to a real system.

$$- \frac{L}{1 - L\Delta T} \quad \text{with probability } (1 - L\Delta T)$$

where $x(t)$ is a zero-mean input, ΔT is the sampling interval and L is the mean rate of impulses (Fig.2.6.1).

As $\Delta T \rightarrow 0$, $r\Delta T \rightarrow t$, the binary signal $x(r\Delta T)$ approaches a train of impulses superimposed on a baseline of $-L$. The impulses in $x(t)$ are Dirac delta functions since they have unit area.

The mean, or first moment is

$$\overline{x(t)} = \lim_{\Delta T \rightarrow 0} \overline{x(r\Delta T)} = \frac{1}{\Delta T}(L\Delta T) - \frac{L}{(1-L\Delta T)}(1 - L\Delta T) = 0 \quad (2-6-3)$$

The second moment, the auto-correlation of $x(t)$ is $\overline{x(t)x(t-T)}$.

From (2-6-2), it can be proved that

$$\int_{-\infty}^{\infty} x(t)x(t-T)dT = L$$

Therefore,

$$\overline{x(t)x(t-T)} = \begin{cases} 0 & T \neq 0 \\ \infty & T=0 \end{cases}$$

Therefore, since the auto-correlation vanishes for all values of T except at one point where it becomes infinite, and since its integral is a finite constant, L , the auto-correlation is proportional to the Dirac delta function $\delta(t)$. Namely

$$\overline{x(t)x(t-T)} = L\delta(T) \quad (2-6-4)$$

By definition, $x(t)$ has a zero mean and values of $x(t_1)$ and $x(t_2)$ are independent for $t_1 \neq t_2$. Therefore for $T_1 \neq T_2 \neq \dots \neq T_n$, the n th moment of $x(t)$ is

$$E[x(t-T_1)\dots x(t-T_n)] = E[x(t-T_1)]\dots E[x(t-T_n)] = 0$$

since $E[x(t)] = 0$

The third moment $\overline{x(t-T_1)x(t-T_2)x(t-T_3)}$ equals zero by the independence and zero mean properties of $x(t)$ unless $T_1=T_2=T_3$

It is easy to prove that

$$\overline{x^3(t)} = \lim_{\Delta T \rightarrow 0} \overline{x(r\Delta T)^3} = \infty$$

And it follows by the same reasoning as above that

$$\int_{-\infty}^{\infty} \int_{-\infty}^{\infty} \overline{x(t-T_1)x(t-T_2)x(t-T_3)} dT_1 dT_2 = L$$

So we find that the integrand is a two-dimensional Dirac delta function, and the third moment is

$$\overline{x(t-T_1)x(t-T_2)x(t-T_3)} = L\delta(T_1-T_2)\delta(T_2-T_3) \quad (2-6-5)$$

Finally consider the fourth moment

$$\overline{x(t-T_1)x(t-T_2)x(t-T_3)x(t-T_4)}$$

There are three cases to consider. First, if any one of the T_i 's differs from all the others, then the average is zero by independence. The second case is where there are two pairs of equal T_i 's but not all four are equal. There are three such sub-cases, one of which is $T_1=T_2, T_3=T_4, T_2 \neq T_3$ giving

$$\begin{aligned} \overline{x(t-T_1)x(t-T_2)x(t-T_3)x(t-T_4)} &= \overline{x(t-T_1)x(t-T_2)} \overline{x(t-T_3)x(t-T_4)} \\ &= L^2 \delta(T_1-T_2)\delta(T_3-T_4) \end{aligned}$$

The other two sub-cases give permutations of the above. If all T_i 's

are equal, we get, analogous to the third moment case,

$$\overline{x(t-T_1)x(t-T_2)x(t-T_3)x(t-T_4)} = L\delta(T_1-T_2)\delta(T_2-T_3)\delta(T_3-T_4) \quad (2-6-6)$$

The moments of the zero-mean input $x(t)$ are mentioned here because they were useful in the orthogonalization process of the Volterra series listed in the following section.

ORTHOGONALIZATION OF THE VOLTERRA SERIES FOR POISSON IMPULSE TRAIN INPUT

According to Krausz (1975), using functionals from the Volterra series, and using the moments of $x(t)$, the orthogonal series for the output of the system can be expressed as follows.

$$y(t) = G_0[h_0, x(t)] + G_1[h_1, x(t)] + G_2[h_2, x(t)] + \dots$$

where

$$\begin{aligned} G_0 &= h_0 \\ G_1 &= \int_{-\infty}^{\infty} h_1(T)x(t-T)dT \\ G_2 &= \int_{-\infty}^{\infty} \int_{-\infty}^{\infty} h_2(T_1, T_2)x(t-T_1)x(t-T_2)dT_1 dT_2 \\ &\quad - \int_{-\infty}^{\infty} h_2(T, T)x(t-T)dT - L \int_{-\infty}^{\infty} h_2(T, T)dT \\ &\quad \dots \end{aligned} \quad (2-6-7)$$

McShane (1962) derived a similar series but in a different notation.

If $z(t)-L$ is substituted for $x(t)$ into the above equations, then the functionals agree with those derived by Ogura(1972) using Charlier polynomials.

RESTRICTED DIAGONAL VOLTERRA SERIES

Lee and Schetzen demonstrated that the restriction against equal T_i 's in the cross-correlation relation can be removed by a sequential calculation of the kernels. But this is not possible for the above functionals because

the even moments of zero-mean Poisson impulse train $x(t)$ do not decompose into sums of pairwise products of second moments as for Gaussian white noise.

Krausz proved that these difficulties can be avoided by restricting the T_i 's to be unequal in the integrations of the functionals of (2-6-7), resulting in the series (2-6-8) below which he showed to be 'equivalent' to the series formed by the functionals in (2-6-7). The resulting series was Restricted Diagonal Volterra (RDV) series.

$$y(t) = \sum_{n=0}^{\infty} G_n[h_n, x(t)] \quad (2-6-8)$$

where

$$G_0 = h_0$$

$$G_1 = \int_{-\infty}^{\infty} h_1(T)x(t-T)dT$$

$$G_2 = \int_{-\infty}^{\infty} \int_{\substack{\infty \\ T_1 \neq T_2}}^{\infty} h_2(T_1, T_2)x(t-T_1)x(t-T_2)dT_1dT_2$$

In general,

$$G_n = \int_{-\infty}^{\infty} \dots \int_{\substack{\infty \\ T_1 \neq \dots \neq T_n}}^{\infty} h_n(T_1, \dots, T_n)x(t-T_1) \dots x(t-T_n)dT_1 \dots dT_n \quad (2-6-9)$$

CROSS-CORRELATION TO RECOVER KERNELS FOR POISSON IMPULSE TRAIN INPUTS

The RDV kernels can be found by cross-correlation in an analogous manner to that used by Lee and Schetzen, except for the case when two or more of the T_i 's are equal. The kernels are given by

$$h_0 = \overline{y(t)}$$

$$h_1(T) = \frac{1}{L} \overline{y(t)x(t-T)}$$

$$h_2(T_1, T_2) = \frac{1}{2!L} \overline{y(t)x(t-T_1)x(t-T_2)} \quad T_1 \neq T_2$$

...

In general,

$$h_n(T_1, T_2, \dots, T_n) = \frac{1}{n!L} \overline{y(t)x(t-T_1)\dots x(t-T_n)} \quad T_1 \neq T_2 \dots \neq T_n \quad (2-6-10)$$

It is obvious that the above formula is in the same format as in (2-4-1) except that P is now replaced by L . Equations (2-6-4) and (2-4-2) show that the auto-correlations of the stimuli are both expressed by delta functions. Thus Lee-Schetzen's formula would still be valid for a zero-mean Poisson impulse train input except for the restriction on equal T_i 's. The VESP kernels presented in chapter 4 were computed based on (2-6-10).

2.7 DISCUSSIONS: ABOUT POISSON IMPULSE TRAINS AS A SYSTEM PROBING SIGNAL

For nonlinear systems, the use of a Poisson impulse train input is analogous to the use of Gaussian white-noise for continuous input systems. The system characterization is in terms of orthogonal series, whose kernels are determined by the input-output cross-correlations with the random input. Systems known to be second-order can be identified with paired impulses more easily than with a Poisson train. But for higher order systems, a second-order kernel calculated from a Poisson train experiment gives the best second-order approximation to the system output.

For systems whose input could be either continuous or discrete, use of the Poisson impulse train can still have some advantages over the Gaussian white-noise method. Listed below are a few examples.

(1) The most significant advantage is increased speed in the computation of kernels. Since only the input values at discrete points where impulses occur contribute to the cross-correlations, kernels are calculated faster than for the continuous input case. (2) Kernels can be reasoned with intuition and interpreted more easily when thinking of the input as a train of impulses rather than a continuous white-noise. (3) The random impulse train input imitates every possible impulse train input (pairs, triplets,...) given an infinite amount of time.

The major disadvantage of Poisson impulse inputs concerns the identification times required to obtain kernel estimates whose variances are comparable to those obtained with GWN inputs. The estimate of the second-order

kernel, $h_2(T_1, T_2)$, for example, is an average over all pairs of input impulses occurring $T_1 - T_2$ seconds apart in the Poisson train. The number of sweeps contributing to the average is proportional to the number of impulses in the input train. If the sweeps are independent, then the variance of an average of n sweeps is proportional to $1/n$. Therefore, the variance of kernel estimates depends roughly inversely on the number of input impulses.

INTERPRETATION OF KERNELS

If a system S is characterized by a second order RDV series, then the second kernel of S describes the nonlinear effect on the response to the second(test) impulse of a pair of impulses from the occurrence of the first (test)impulse. This effect, known to biologists as facilitation or inhibition (depending on sign), is expressed as

$$f(t) = y_s(t) - [y_1(t) + y_2(t)] \quad (2-7-1)$$

where $y_1(t)$ is the response of S to a single impulse at time t_1 , $y_2(t)$ is the response of S to an impulse at t_2 , and $y_s(t)$ is the response to the pair of impulses. When the RDV series expansion for $y_1(t)$, $y_2(t)$, and $y_s(t)$ are substituted into above formula, the facilitation is found to be

$$f(t) = 2h_2(t-t_1, t-t_2) \quad (2-7-2)$$

Thus the second-order kernel, $h_2(t-t_1, t-t_2)$ gives one-half the facilitation at time t measured in a two impulse experiment with input impulses occurring at times t_1 and t_2 . By performing two pulse experiments with a variety of temporal separations between the pulses, it is possible to estimate the

second-order kernel of an unknown system, but only when the system is second-order.

If the system has higher-order kernels than the second-order then the facilitation is only partially described by the second kernel and (2-7-2) does not hold. Although third-order systems can be experimentally characterized by their responses to all possible triplets of input impulses, and so on, this method soon becomes inefficient. So the advantages of the use of Poisson impulse train rather than pairs, triplets or other impulse inputs are: (1) The random input imitates every possible impulse train input given an infinite amount of time. In finite time it statistically samples the various possibilities. (2) Since the RDV series is orthogonal for Poisson train inputs, a second-kernel gives the best second-order fit to the system output, in the sense of minimum mean square error. Unless the system has no higher kernels, a second-order model constructed from paired impulse experiments will therefore be less accurate. (3) If a sufficiently long random impulse train experiment is performed, it is possible to calculate higher kernels as they become needed without changing the estimates of lower-order kernels already obtained. No new experiments need be performed.

For experiments with the Poisson train input, a close examination of the second-order kernel reveals that it is equal to half of the average facilitation T_2 seconds after the second impulse and averaging over all pairs $(T_1 - T_2)$ seconds apart in the input train, regardless of intervening impulses. In general then, it is necessary to consider the facilitation at all times during a response in order to evaluate the second-order kernel for all positive T_1 and

T₂.RELATIONSHIPS BETWEEN POISSON IMPULSE TRAIN AND GAUSSIAN WHITE NOISE

A Poisson impulse train relates to Gaussian white-noise in the following way. If a Poisson impulse train is generated at a very high mean rate and then smoothed slightly, it will resemble a physical approximation to GWN. That is because the amplitude distribution of this new process approaches a Gaussian distribution when the smoothed versions of a large number of impulses are added (by the central limit theorem).

So it would seem that the kernel variance in a GWN experiment should be the same as the kernel variance in a Poisson train experiment when the mean impulse rate is so high that the Poisson impulse imitates GWN. At such high rates, even the longest intervals between impulses are shorter than the response time of the system. But in order to explore the interesting range of a system's behavior, the Poisson impulse train will normally have a much slower mean rate than the rates that imitate GWN. Since the kernel variances depend on the total number of impulses, it follows that identification may take longer with Poisson impulse train input than with GWN. This nevertheless is offset by the fact that the Poisson impulse train has a stronger power than GWN.

Like the Wiener theory, the theory of nonlinear systems identification using Poisson impulse trains can readily be extended to multi-input systems.

VOLTERRA, WIENER AND RDV SERIES REPRESENTATION

The Volterra series is equivalent to the Wiener series, in the sense that they both span the same function space. However, the Wiener kernels depend on the power level of the G.W.N. with which they have been estimated. The specific value of the power level determines the region of orthogonality of the Wiener G-functionals. Therefore, a system is completely described either by the set of Volterra kernels, or by the set of the Wiener kernels plus the corresponding power level P . Clearly, the overall model given by the Wiener series is independent of P ; however, both the individual Wiener kernels and the G-functionals depend on P . The Volterra kernels, on the other hand, must be thought of as a set of invariant characteristics of the system.

It must be emphasized that, in practice, we usually have to truncate the Wiener series and, consequently, the obtained model depends on P . This dependence on P is explicable in the sense that it determines the range of the stimulus values within which the corresponding Wiener series is orthogonal.

Now suppose an unknown system S can be stimulated with either GWN or a train of impulses. What will be the relation between Wiener series and the two RDV series and their respective sets of kernels? The Wiener series differs from (2-6-8) in both its functionals and its kernels. If S is approximated by both an n th order Wiener series and a series (2-6-8) then the output of Wiener series expansion to a Poisson impulse train input will be unequal to the output of (2-6-8) for the same input. The reason is that the Wiener series is the best n th order fit to the response of S to GWN, while (2-6-8) is the best fit to the Poisson impulse train response. But in the unlikely event that S is actually an n th order polynomial nonlinear system, the output of both

Wiener functional series and (2-6-8) to a Poisson impulse train must agree.

It is then possible to write down the relation between the Wiener kernels and the kernels in (2-6-8).

CHAPTER 3

DATA ACQUISITION AND INSTRUMENTATION3.1 EXPERIMENTAL SETUP

A schematic of the experimental setup is shown in Fig. 3.1.1. A double Faraday cage was used to reduce electromagnetic interference and for sound isolation. A xenon flash unit was placed outside the screened room. The flash stimulus passed through a small hole in the wall of the screened room. The flash unit was triggered at random intervals determined by a random interval generator.

The data collection system consisted of a 128 channel, 100 kHz multiplexer, an A/D converter and a dual buffered digital tape recording system. Data were stored on standard 9-channel 800 b.p.i. digital tapes which are readable by any of the digital computers on campus for further data analysis. The data were sampled at 4 msec intervals, yielding a sampling frequency of 250 Hz. Continuous digital recordings were used for each channel. Acquired data included ground, average-reference, standard-waveform synchronization and calibration signal, a record of the random impulse train stimulus and active brain-wave channels.

A custom-designed multichannel CRT monitor was used to display all electrode channels during experimental sessions. Detached, noisy, and unstable electrodes could be easily detected during the session by the experimenter. Abnormal potential drifts due to body movements, eye blinks and movements could also be noticed and corrective measures taken. A four-channel real-time signal averager (Nuclear Data Model ND-801 Enhancetron) was used to

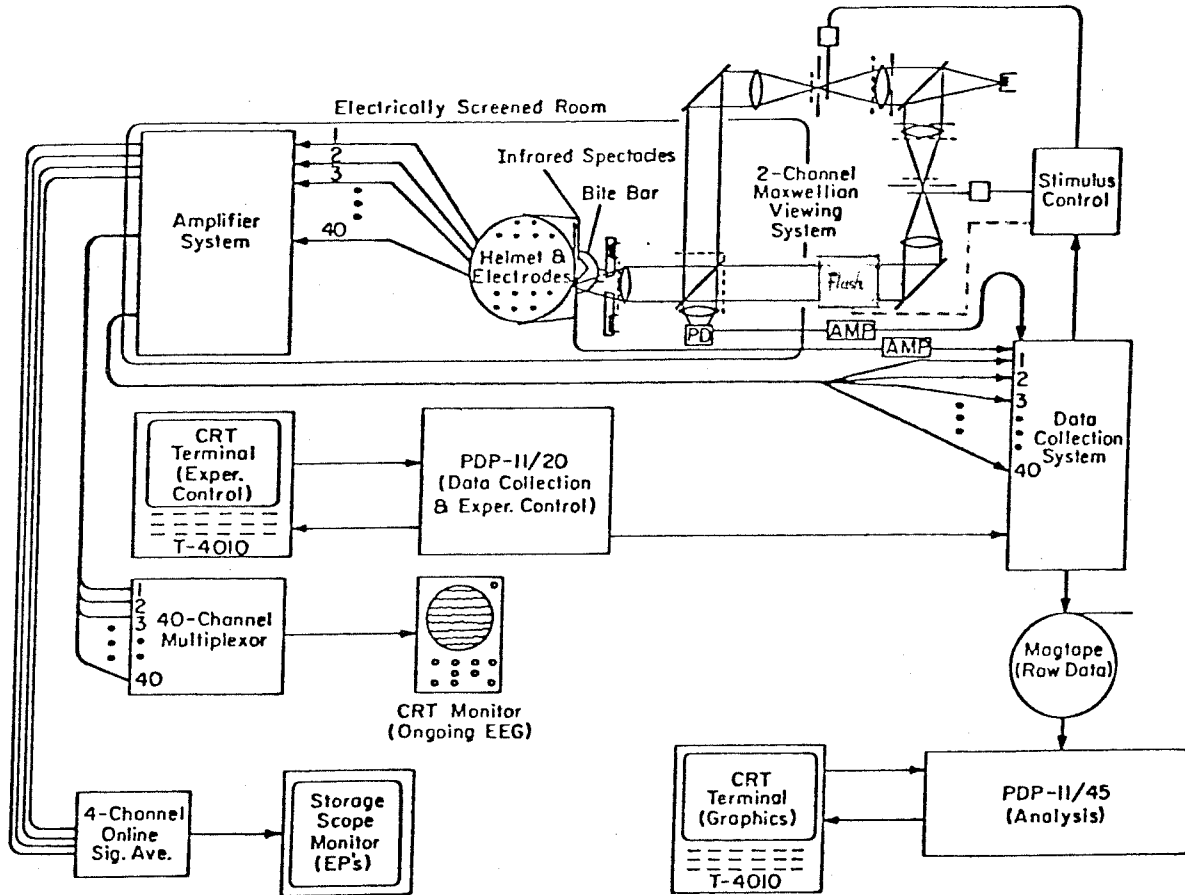


Fig. 3.1.1 General experimental setup.

display averaged evoked potentials from selected channels on a storage oscilloscope. This enabled the experimenters to assess the repeatability of evoked potentials from different runs and to estimate or ascertain the length of time required to extract reliable responses for a fixed probability of stimulus presentation.

An experimental session consisted of three 3.5 minute runs using a given stimulus. The repetitions allowed estimation of the reproducibility of the evoked potentials. Any variation in stimulus parameters was considered to generate a unique stimulus. These stimulus parameters were left or right field checkerboard patterns with or without psychophysically matched right or left background illumination for controlling stray light.

3.2 SIGNAL AMPLIFICATION SYSTEM

Physiological signals acquired by either electrodes or transducers are typically below 10mv in amplitude and must therefore be amplified to be compatible with display devices and common data acquisition systems. This necessitates the usage of physiological amplifiers. A physiological amplifier usually has a high input impedance and a low output impedance and provides either a fixed or a variable voltage gain. Among different kinds of physiological amplifiers, the design criteria of a multichannel EEG amplifier system are most critical.

In almost all physiological measurement situations, the physiological signal of interest is accompanied by an interference signal. The interference is typically 60 Hz due to electrically coupled or magnetically induced interference from the line supply. Measures such as using a screened room are very helpful in reducing electromagnetic interference. Differential amplification provides another level of noise rejection. In EEG or EP research it is a common practice to use a differential amplifier to reject the interference signal and to magnify the desired physiological signal. The desired signal of interest that appears between the two input terminals of the differential amplifier is referred to as the 'differential signal'. The interference signal that appears between both inputs of the differential amplifier and ground is referred to as the 'common mode signal'. Common mode rejection ratio (CMRR) is defined as the ratio between the amplitude of the common mode signal and the amplitude of an equivalent differential signal that would produce the same output from the amplifier. This common mode rejection ratio of an

amplifier is a quantitative measure of the ability of an amplifier to reject common mode signals. Usually, a high CMRR is desired.

MULTICHANNEL AMPLIFIER SYSTEM

A custom-designed multichannel amplifier system was constructed to provide appropriate amplification and referencing for the EEG signals on each of the (40) electrodes. The inherent interaction in a multichannel EEG system operating at high gains and using the same reference in all channels is a major design and implementation problem. Stability is the first requirement for the system. Amplifier cross-talk must be very low, less than 40db at 100 Hz. The amplifiers must have high gain (10,000 to 100,000), high common mode rejection ratio, high input impedance (greater than 10 at 100 Hz), and a roughly uniform bandpass that covers the desired signal frequency range. In the system used, dual-FET input instrumentation amplifiers constitute the front-end preamplifier stage. They provide high input impedance, have a CMRR with a 20k source imbalance of greater than 60 dB in the frequency range of interest, have an adequate linear frequency response. These amplifiers provide the first stage of amplification. The system provides a switch between monopolar and average reference. High and low-pass filters are also included for signal filtering and amplification. A variable gain stage enables changing the gain of this stage, and therefore, of the whole system. Opto-isolation is also included for subjects' protection from electric shock. The entire low-pass filtering system is switchable to one of three upper 3dB points: 30, 60, or 90 Hz. The overall gain of each amplifier was set at 45000. The data acquisition system provides us with another stage of amplification. Therefore

in conversion of units for evoked potential signals, both were taken into account.

3.3 ELECTRODE REFERENCING

In recording the VESP, one determines the algebraic difference in potential between two electrodes, an active electrode and an inactive or reference electrode. Ideally, the active electrode picks up neural signals plus other potentials (muscle, interference and artifact) while the inactive electrode is picking up all potentials except neural signals. The differential result of this ideal situation is a VESP that reflects solely the neural activity of a specified region of the brain since all other potentials would be common to both electrodes and therefore not present in the final waveform. In practice, it is difficult to prove that a truly inactive reference exists.

Therefore in EEG, we desire to find a reference which is relatively indifferent to neural activities resulting from stimulus occurrence. The common mode rejection property of the amplifiers rejects undesired physiological signals from remote sources such as electrocardiograms and 60 cycle power-line noise, but one must optimize the tradeoff between proximity of active and reference electrodes (to minimize common mode noise) and distance (to ensure indifference of reference to active signal).

Monopolar, bipolar, and average referencing are the three usually used reference schemes in EEG or EP research. Monopolar referencing refers to any condition in which one electrode is located over an active region and the second (reference) electrode is located in an inactive region such as the ear-lobe or the mastoid. Bipolar referencing refers to the condition in which two electrodes are placed over active areas, and the resulting waveform reflects the difference between these two regions. Average-referencing refers to the

condition in which the average of the active electrodes is used as the reference. The relative merits and disadvantages of these three reference schemes have been discussed by several researchers (Osselton, 1965; Goldman, 1950; Offner, 1950; Darcey, 1979). Average referencing was used as the electrode reference scheme for forty-channel recording in this thesis because the scheme is a compromise between the competing problem of noise rejection and reference indifference (Darcey's thesis). Also, negative feedback used in average reference helps to stabilize multichannel amplifier systems (Ary, 1977). Without this feedback, high-gain amplifier systems will have a greater tendency to oscillate or otherwise become unstable.

This average referencing method can only be used when a large number of electrodes is applied, since it is based on the assumption that the activity which gives rise to the scalp potentials involves electronic charges which sum to a constant. Recall the Gauss law, which states that the sum of potentials over a closed surface bounding a fixed number of charges is some constant. This method can thus only be exploited when the recording method uses enough electrodes so that the integral of the potential over a closed surface can be approximated. This is another reason that this method was used for the series of forty-channel experiments performed (section 4.2). The single (monopolar) reference scheme was used for the series of five-channel experiments (section 4.1) because of the small number of electrodes used.

3.4 ELECTRODE, ELECTRODE HELMET AND ELECTRODE LAYOUT

Custom-fitted plexiglass helmets were constructed for each subject and were used to support the electrodes and to facilitate their rapid and repeatable placement in spherical coordinates. The electrodes were laid out at 15 degree spacing over the surface of the sphere which best approximated the back of the subject's head. The center and radius of the sphere were determined by using a center-finding device, similar to that used by a machinist in conjunction with the plexiglass mold of the subject's head. Electrode positions ranged from 15 degrees below the inion to 135 degrees above the inion and from 75 degrees left of the vertical plane through the center of the sphere to 75 degrees right of the plane. Angles measured ear-to-ear were designated negative towards the left ear and positive towards the right ear. Angles measured along the midline were designated zero at the inion level and positive above. Inion, nasion, and vertex were used as landmarks of the helmets for accurate and repeatable placement. The helmet was drilled with a 17mm diameter hole at each electrode location. The helmet was applied and strapped under the subject's chin, then the hair was parted through each hole in the helmet and the scalp prepared following conventional techniques. HP Redux Paste was used as an abrasive to reduce skin resistance. A rubber grommet with a 4.5 mm central hole was then plugged into each hole in the helmet. The electrodes are brass cylinders 5 mm in diameter and 15 mm long with one cupped-end. The cylinders are silver plated and chlorided. An electrode was pressed through the hole in each grommet until it seated against the head in a bead of electrode paste. To increase conductivity between electrode and scalp, Type EC-2 electrode paste was usually used. A Grass Model EZM1D Electrode Impedance

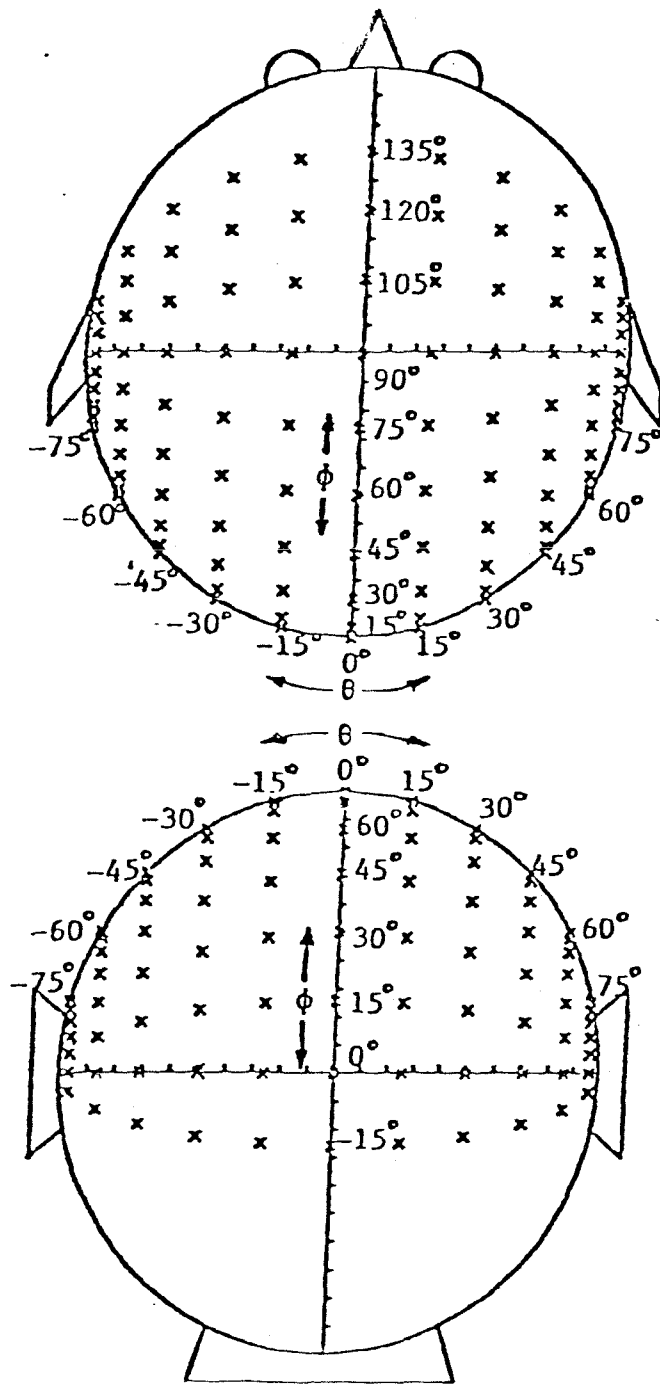


Fig.3.4.1- Equiangular electrode layout (15° spacing)

Meter was used to measure impedance of each electrode after it was applied. A reading below 20 k was considered as acceptable.

3.5 STIMULUS PRESENTATION

XENON FLASH

A xenon flash unit (Strobex model #136 with a model #70 head, Chadwick-Helmuth Co., Inc.) was used for presenting a rapid random flash stimulus through a checkerboard pattern in a Maxwellian view. In general, xenon flash tubes can be used for continuous operation (arcs) or for periodic/apperiodic flashing. Randomized trigger pulses, from a random interval generator, were fed to the trigger circuitry in the flash unit. It was verified that the light flux did not vary from flash to flash, and that the mean light flux did not vary with frequency. Thus identical luminance effects in each stimulus presentation were guaranteed. It is known that very short xenon flashes presented on a background of low adaptation level are likely to excite scotopic as well as photopic mechanisms. Using a small, bright field, the area of the retina that is directly illuminated responds photopically, but the rest of the retina will adapt and respond to the scattered light scotopically. The scotopic response from the scatter could be added to the photopic part of the evoked potentials.

The evoked response to the clicks which accompany xenon flashes was suppressed by playing a radio during experimental sessions to mask the sound of the strobes. The screened room also provided partial effect of sound proofing.

MAXWELLIAN VIEWING SYSTEM

The viewing system had two optically superimposed channels which could

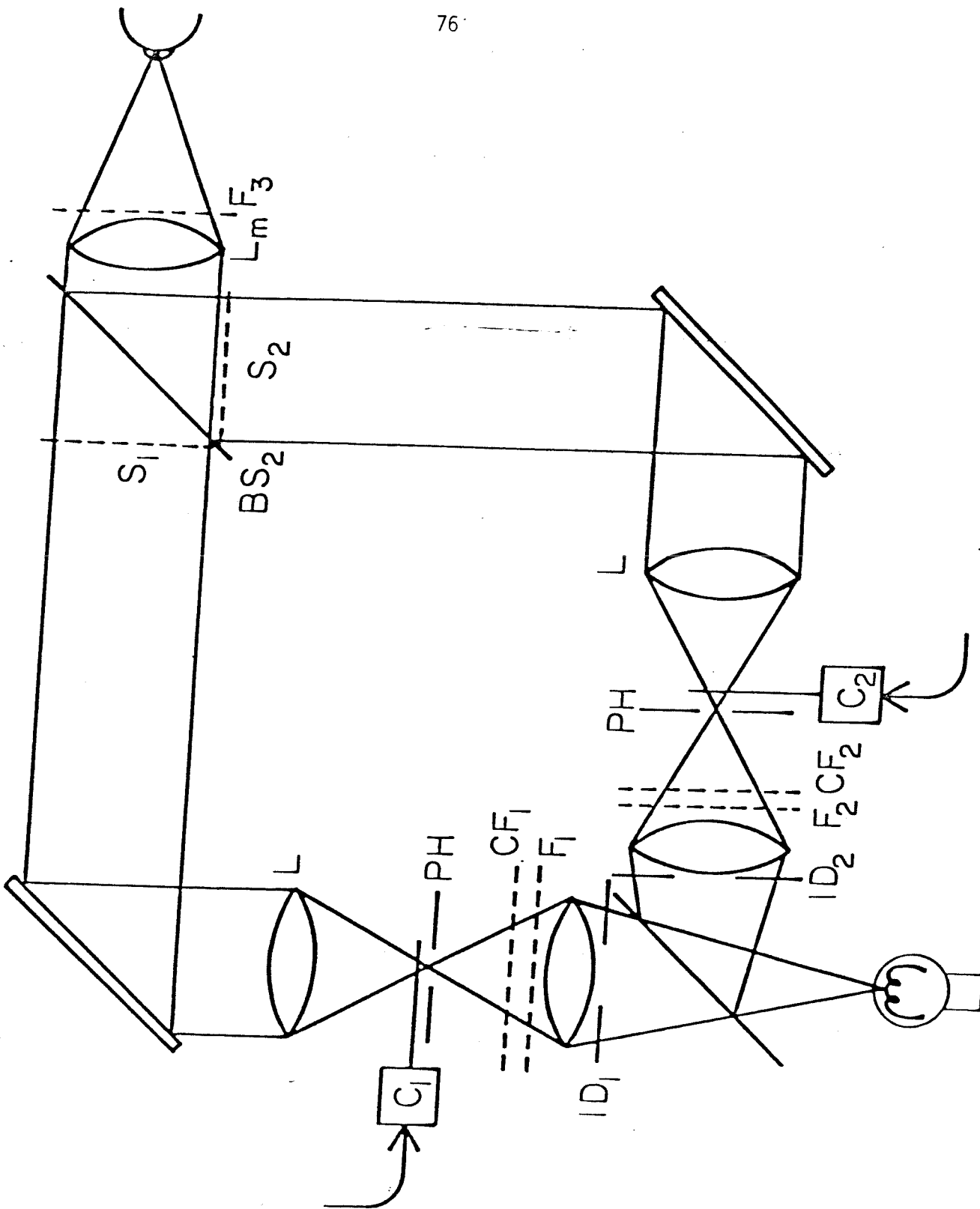


Fig.3.5.1 Optical stimulation system.

be used singly or be exchanged with a switching time of 3 ms. The switching could be accomplished by two linear motion transducers (C1,C2) driven in anti-phase. The transducers moved knife-edges over 1mm pinholes (PH). Using collimating lenses (L), each channel could produce a beam of parallel light incident on separate slides (S1,S2) which were mounted in x-y movements for alignment purposes. The two images could be superimposed by a pellicle beam-splitter (BS2) and presented in Maxwellian view at optical infinity to the right eye of the subject by use of an intervening lens (LM). The intensities of the two beams could be adjusted using iris diaphragms (ID1,ID2) and neutral density filters (F1,F2). In the experiments carried out for this research, one channel was used for flashing half-field pattern. Another channel provided the opposite half-field with psychophysically matched luminance as stray-light control for some experiments. A Gamma Scientific (model 2000) telephotometer was used to measure the luminance of the matching field. The entire pattern was viewed through a red Wratten filter #25(F3). The channel in use carried a fixation target and a checkerboard pattern (10 min arc checksize). The other channel carried a similar fixation target. The two channels were optically aligned. Luminance balance was also periodically checked psychophysically by adjusting the background light beam for a brightness that matched with the average flash intensity. The stimulus was masked so that it occupied the left or right half of a 20 degree circular area. The fixation mark was at the center of the circle.

CHAPTER 4

EXPERIMENTAL DATA ANALYSIS AND INTERPRETATION4.1 FIRST ORDER KERNELS

A series of preliminary experiments was performed to evaluate and ascertain various optimal experimental parameters before the final experiments mentioned in this thesis. These parameters included the optimal time-length per run, probability of stimulus, flash intensity, suitable background luminance, etc. The experiences gained from those early experimental sessions brought about the eventual fruition of this research.

There are two major groups of experiments performed and results presented in this thesis. The first group was done by using five electrodes in a row on four subjects (Fig.4.1.0). The purpose was to compare kernels computed from random impulse train inputs with results obtained from conventional signal averaging under half-field pattern stimulation (Darcey, 1979). Another purpose was to compare intra-subject variability. For the first set of experiments, a left-half field stimulus (10 minute checks, 10 degree field) was viewed by all the subjects through a Maxwellian view with matching right-half field of subjectively equal luminance to reduce stray-light effect. The probability was fixed at 12.5%. Three runs were usually done for each experiment for studying reproducibility of the signals. The second group of experiments consisted of a series of forty-channel ones done on one subject, particularly, subject 1. The first-order kernels obtained from the first set of experiments will be introduced and discussed in this section. The results from the second set of experiments will be displayed in equipotential-map

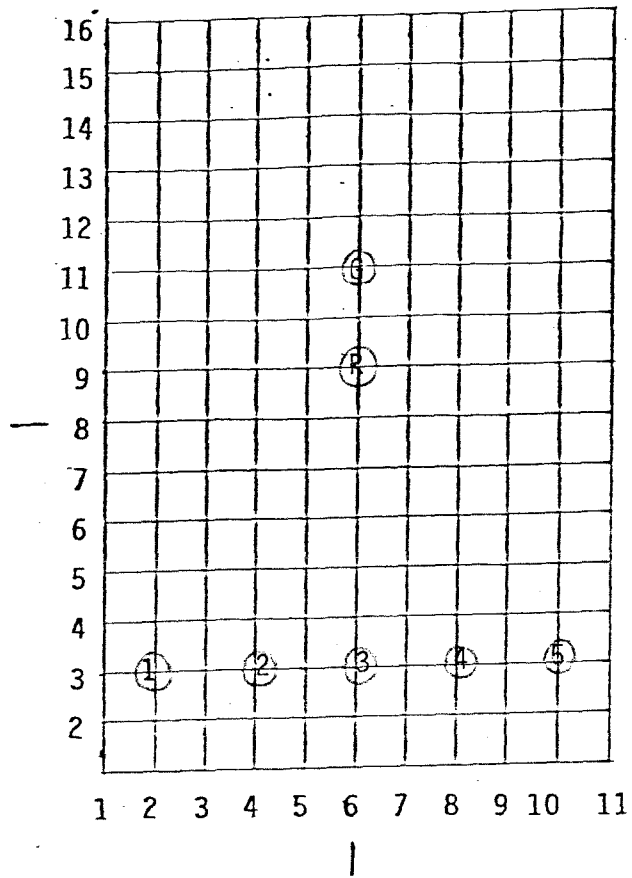


Fig. 4.1.0. Helmet-index for the series of 5-electrode experiments in this section. Coordinate (6,2) is the inion. Vertical line that passes 6 is the midline on subjects' heads. (G = ground, R = reference on the figure)

format, to be introduced and discussed in the second section of this chapter.

SIGNAL PROCESSING METHODS FOR KERNEL COMPUTATION

Following an experimental session, the recorded data on magnetic tapes were taken to the IBM 370, VAX 11-780 or PDP 11/45 computer for analysis depending on the set-up conditions of the programs, the number of channels used and availability of the systems. Data-processing software was written for various purposes on these systems. For these experiments with small number of electrodes, the GAS (General Analysis System) signal processing package on PDP 11/45 was usually used. Correlation, FFT, convolution, kernel computation, and other signal processing operations can be performed on this system. The data on magnetic tape were routinely first transcribed to 24-megabyte Diva disks which served as the primary data storage device. The CHARM program is the first analysis step. It demultiplexed the channels and converted the data from eight-bit binary format into floating-point numbers for further processing. One channel in one run of experiment usually took up 650 kilobytes of storage space. Therefore, large-capacity storage devices were necessary in this kind of analysis. Fig. 4.1.1. shows three channels of EEG response and their stimuli channel. The evoked potentials are in general so small and overwhelmed by EEG that they can not be discerned by human eyes at all if signal-extraction operation is not performed.

Fig. 4.1.2. shows the general flow-chart of signal-processings for the computation of first- and second-order kernels. CHARM, XYLIN, ... are names of programs for the series of operations done on the data. Following CHARM, the

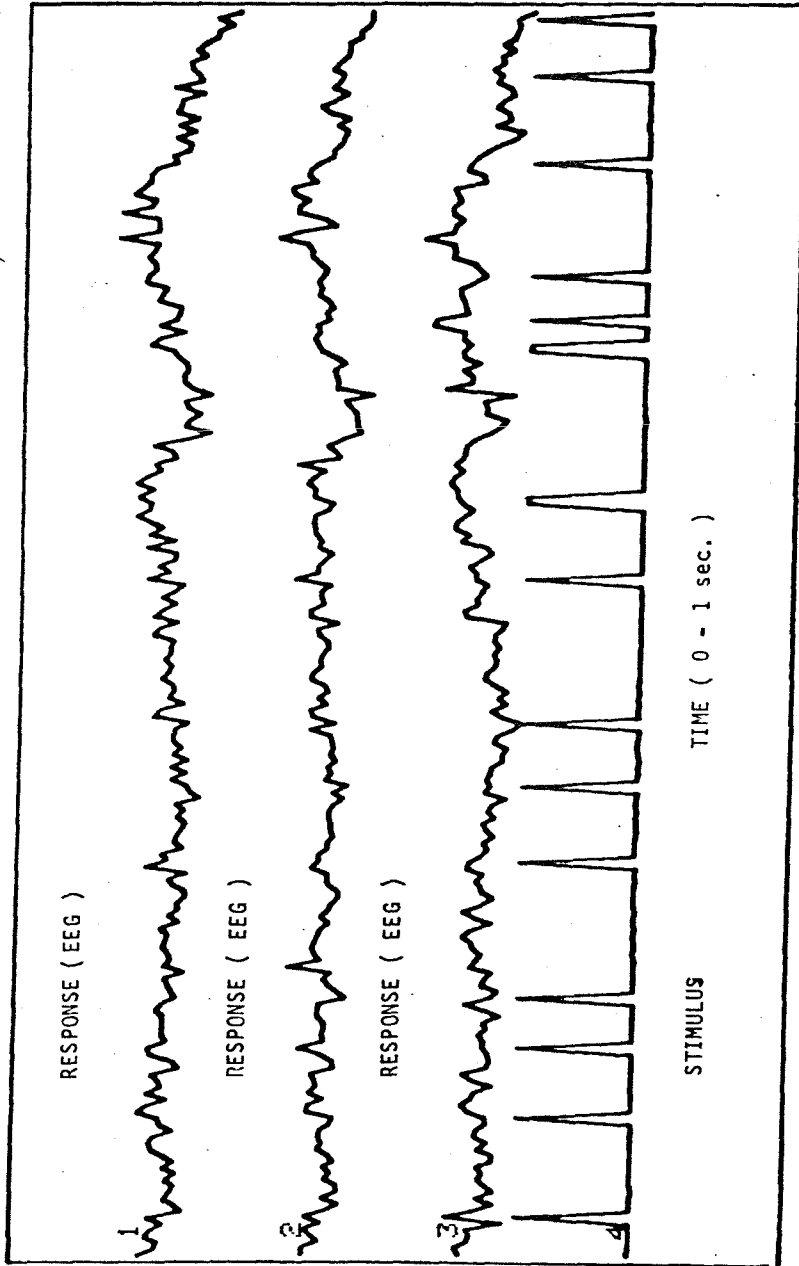


Fig. 4.1.1 One second of experimental record which shows stimulus and three response channels.

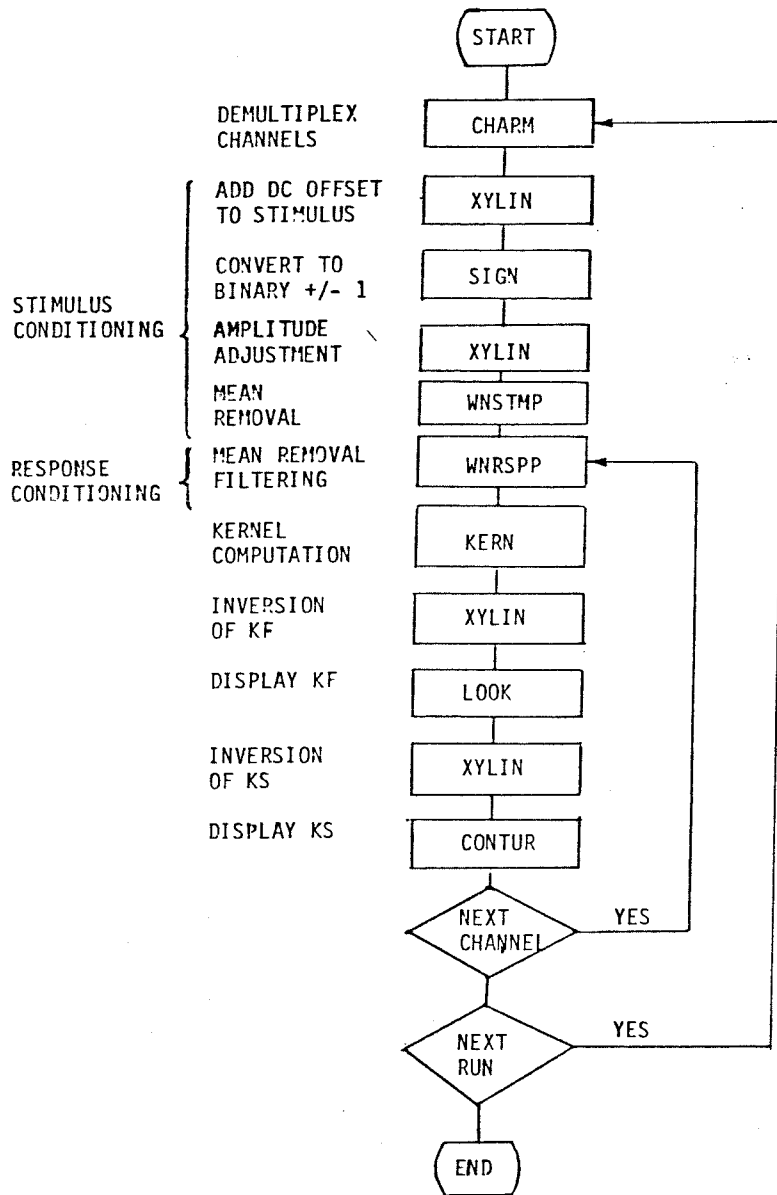


Fig. 4.1.2. The flow-chart of signal processings for first- and second-order kernels.

second step was to condition the stimulus and response (EEG) channels. The stimulus channel had to be rescaled, mean removed, and base-line noise cleared (Fig. 4.1.4 shows the unprocessed and processed stimulus channel). High-pass filtering at 2 Hz was done on all of the EEG channels. Also, means of the response channels were removed. These signal-conditioning steps were performed before correlation was done. Cross-correlation between processed EEG channels with the processed stimulus was done in the KERN program. This correlation procedure generated multiple traces of first order kernels (as well as second-order kernels) as a function of time from multiple scalp locations. In essence, correlation is a signal-to-noise enhancement by summing up weak but correlated signals from uncorrelated background (ongoing EEG, interference etc.).

To ensure that the stimulus was white, auto-correlation was often done on the processed stimulus channel. Fig. 4.1.3 shows this function in one experiment. An impulse of predicted height and tolerable base-line fluctuations assured that the stimulus was close to white-noise in behaviour.

TEST OF STATIONARITY OF EEG

I have tested the stationarity of the EEG by using a program on the GAS system which tests the stationarity of signals. This program performs the following operations: (1) The record was divided into a specified number of segments of equal length. (2) Mean and variance were computed on each segment. (3) The median of each statistic was found. (4) For each statistic, the number of runs above and below the mean for that statistic was found. (5) The number of runs was compared with an internal table to determine whether the signal

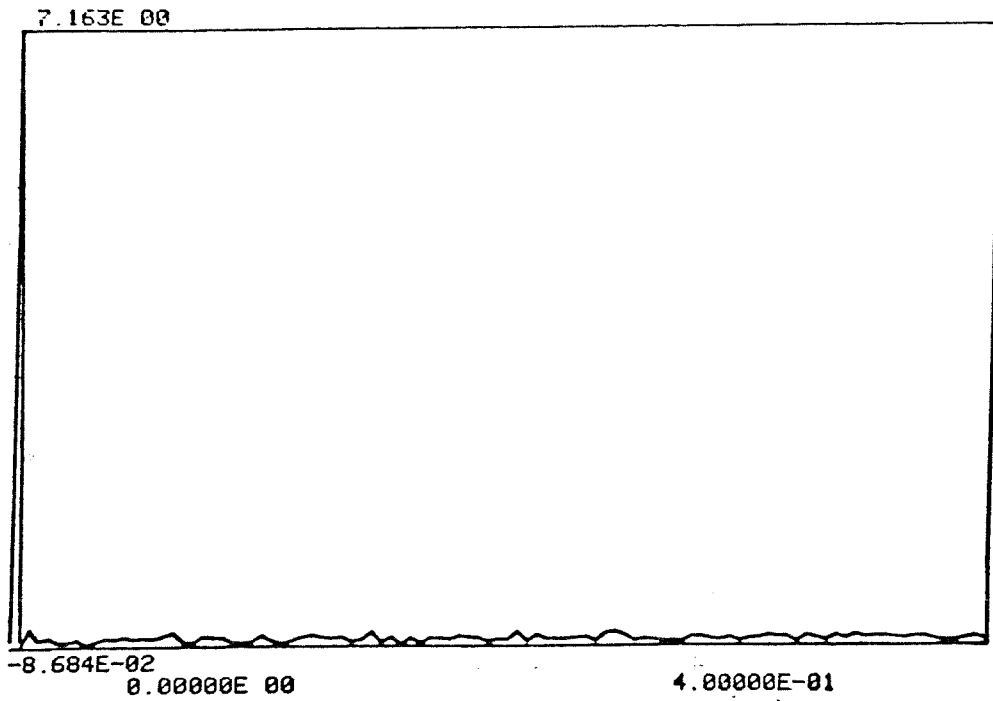


Fig. 4.1.3 Auto-correlation function of the random Poisson impulse train input.

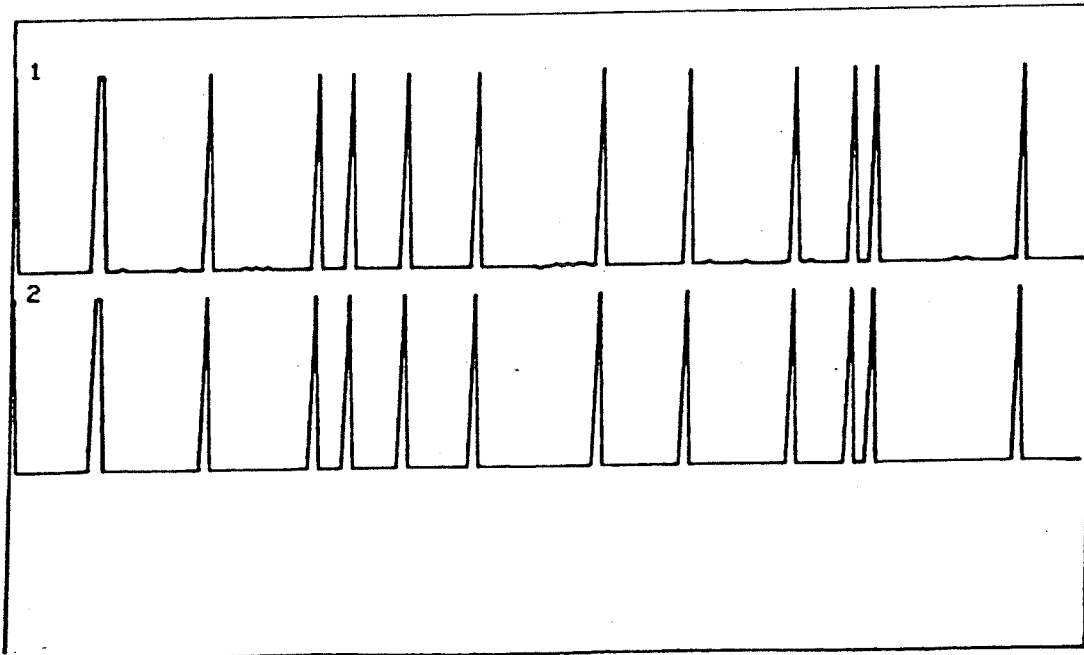


Fig. 4.1.4 The first trace shows the recorded, unprocessed impulse train. The second trace shows the impulse train used for cross-correlation after base-line noise removal, mean removal, and rescaling.

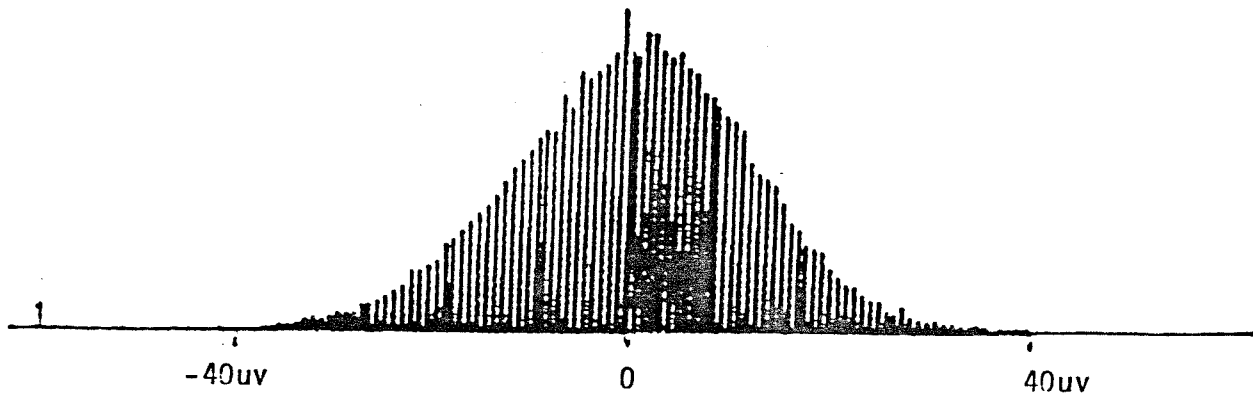


Fig. 4.1.5 Probability distribution function of EEG amplitude for one experimental run from subject 2.

was acceptably stationary. The acceptance criterion was such that 95% of all perfectly stationary signals would be judged stationary. This test was applied to three experimental runs. For a typical three-and-a-half minute run, over 5000 samples were tested in each segment. Usually one experimental run was divided into 10 segments. The results indicated that they were all stationary within the 95% acceptance criterion.

Fig. 4.1.5 shows the histogram done on one experimental run on subject 3. This amplitude distribution function of the EEG shows that the EEG is basically Gaussian in amplitude distribution which confirms the discussions in section 3.2.

Fig. 4.1.0. shows the electrode-map for the series of five-electrode experiments done on the subjects. All the electrodes were placed on the scalp with the support of the helmets strapped on the subjects' heads. The electrode-helmets facilitated repeatable placements of these electrodes on predetermined coordinate locations. The electrodes were placed in a row 15 degrees above theinion plane. The reference and ground locations were on the midline as indicated in the figure.

The magnitudes of the first-order kernels can be obtained by estimating the amplitudes of the peaks and valleys of the waveforms. Take Fig. 4.1.6. for example. Four traces of first-order kernels are shown for electrodes 1, 2, 4 and 5. The horizontal axis indicates time in second. The numbers in front and after TIME(SEC) indicate the starting and ending time (0 and 0.4 sec). For the first trace(electrode 1) of waveform, there are 15 (-

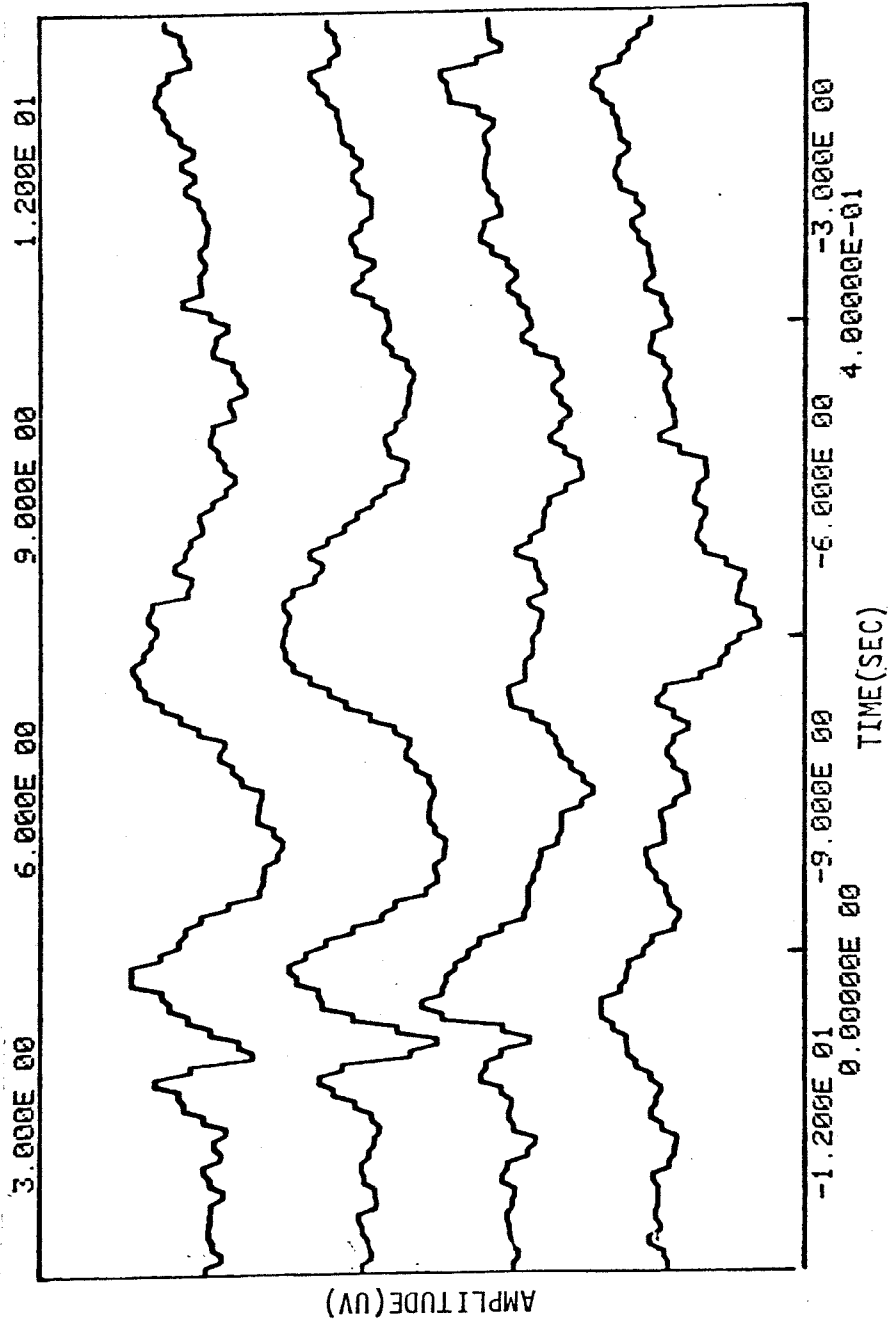


Fig. 4.1.6 Four channels of first order kernels for subject 1.

(one unit on vertical scale = 0.320 uv)

12 to 3) units from bottom to top. The same applies to the second trace (electrode 2, -9 to 6), the third and the fourth trace. Since electrode 1 spans about 3 units and one unit is 0.320 uv, it is easy to estimate that the first-order kernel is about 1 uv in magnitude.

Starting from Fig. 4.1.6, a series of the first-order kernels from electrodes 1, 2, 4, and 5 for all four subjects will be shown. Electrodes 1 and 2 were placed on the subjects' left hemisphere. Electrodes 4 and 5 were on the right as shown in Fig. 4.1.0. Using a left-half patterned field, polarity reversal(or less distinct phase shift in some subjects) was reported for the two major peaks(Nakamura and Biersdorf, 1971; Darcey, 1979) by using conventional averaging. Darcey et al(1980) showed this property most clearly in their spatiotemporal equipotential maps. They established that the mapping between the visual field and the visual cortex could be reflected in the potential distribution and the results also interpretable in terms of equivalent dipole sources. The well-known intersubject variability in the calcarine cortex(Brindley, 1972) may account for the lack of total polarity reversal in some subjects. Although white-noise was used, this property was confirmed in all four subjects. This observation revealed the fact that first-order kernels possess some of the important features which are obtainable from conventional signal averaging.

For subject 1 (Fig. 4.1.6), phase shift can be seen starting at the first major negative peak(72 msec) for electrodes 1, 2, 4 and the first major positive peak for channel 5. This shift extends to around 300 msec. At around 200 msec, polarity reversal can be seen. Fig. 4.1.7 shows the results from

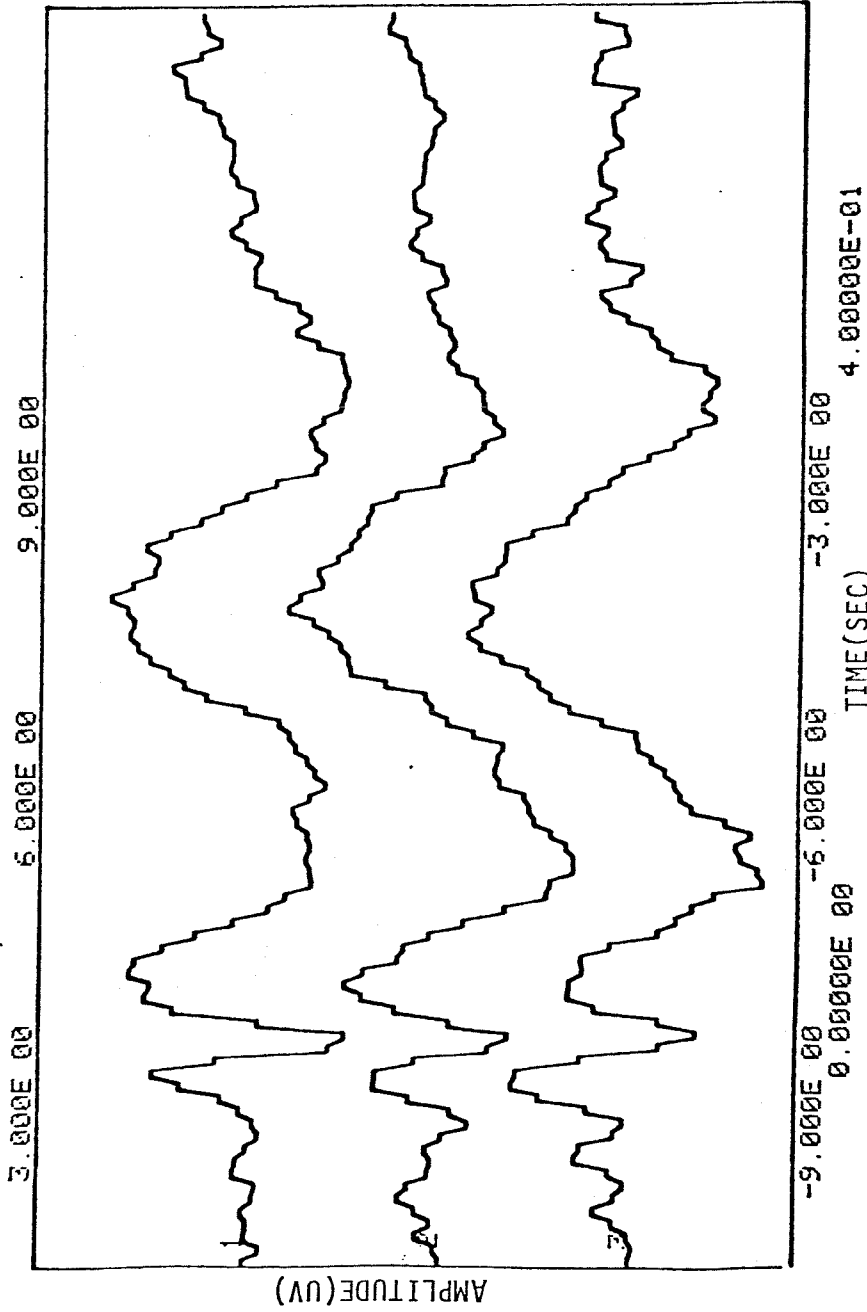


Fig. 4.1.7 First-order kernels from subject 1, runs 1, 2, and 3 (electrode 3).
 The high degree of reproducibility is clearly seen in this figure.
 (One unit on vertical scale is about 0.35 uv)

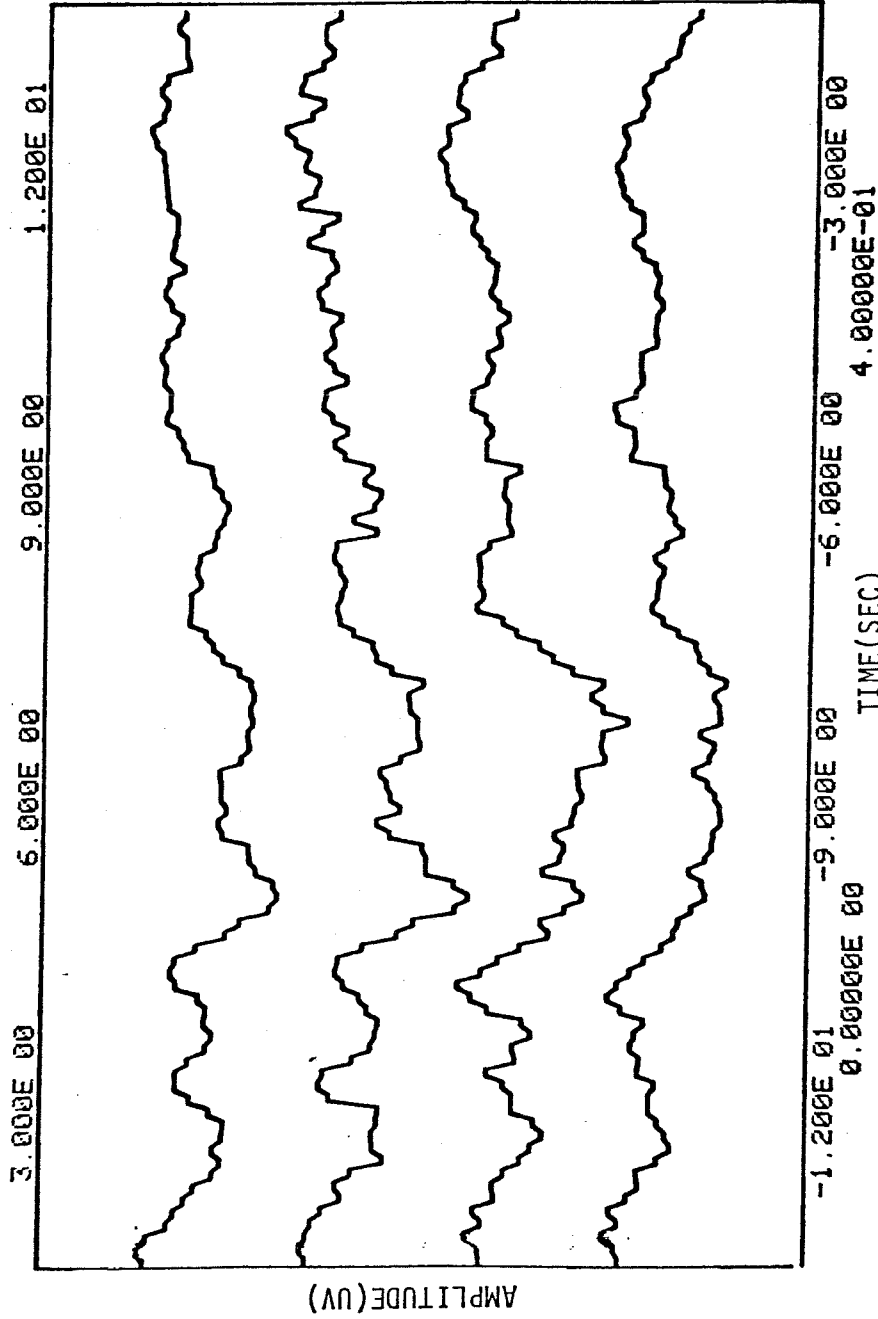


Fig. 4.1.8 Four channels of first-order kernels for subject 2.

(One unit on vertical scale = 0.352 uv).

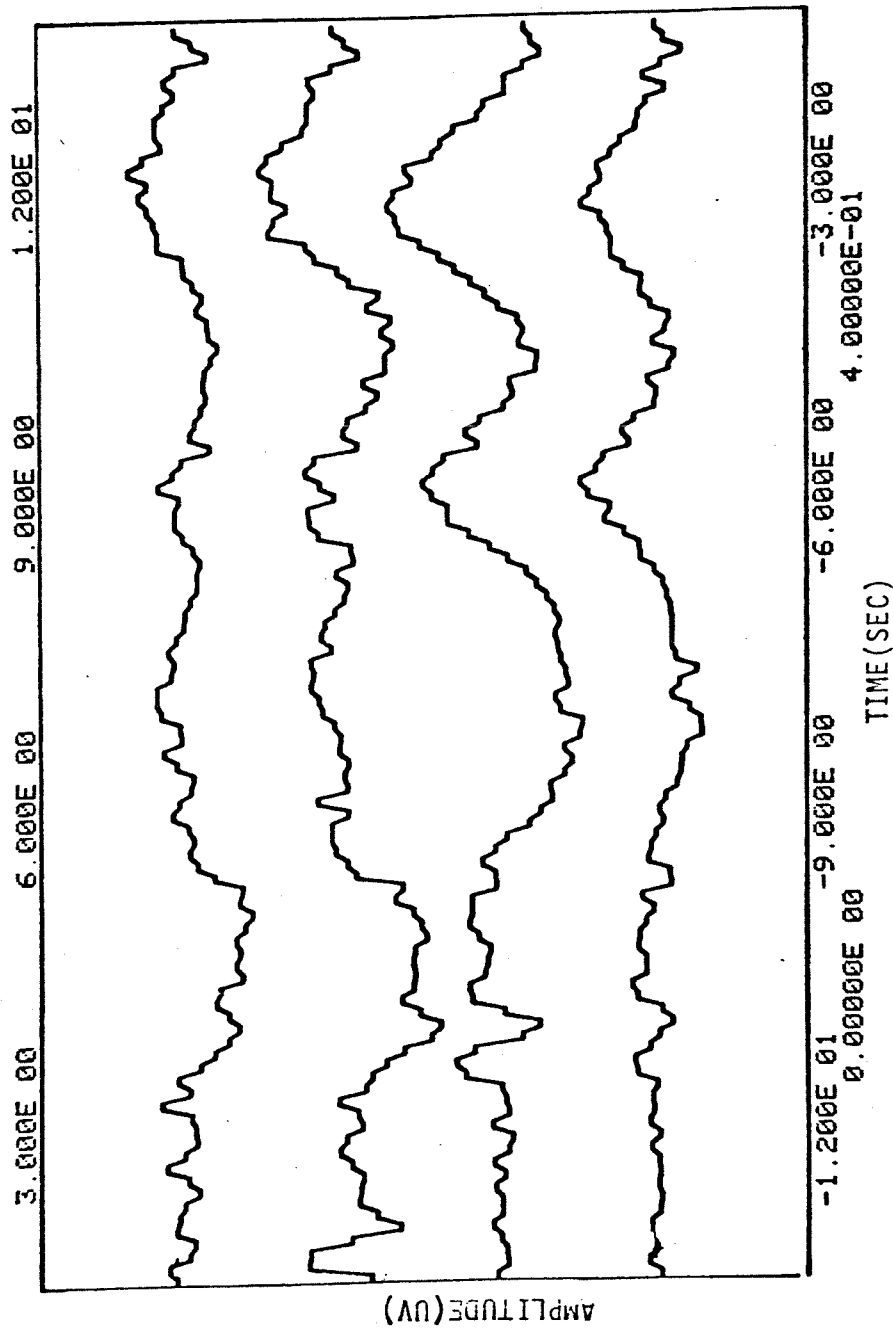


Fig.4.1.9 Four channels of first order kernels for subject 3.

(One unit on vertical scale= 0.228uv).

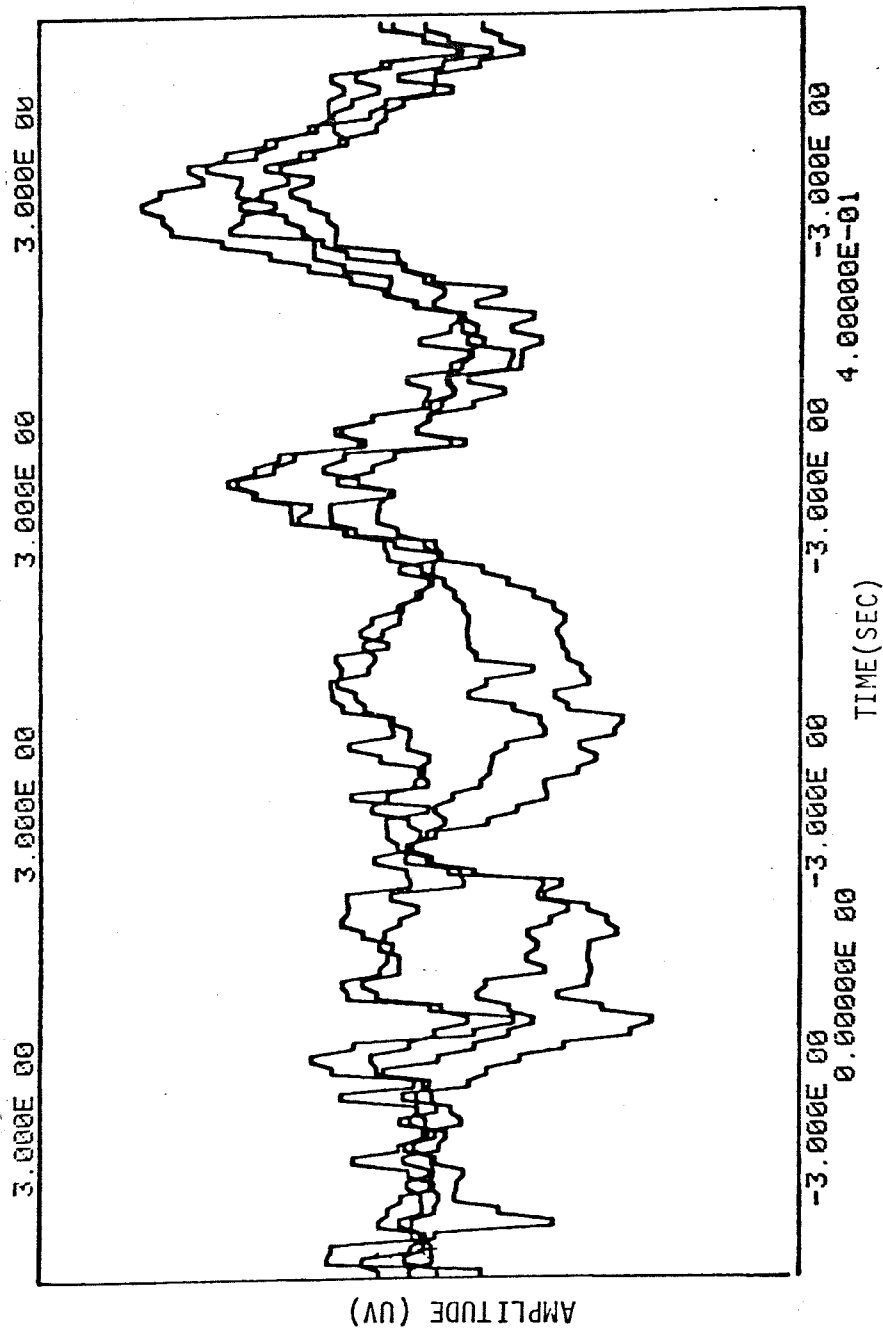


Fig. 4.1.10 Four channels of first order kernels overplotted for subject 3.
(One unit on vertical scale = 0.208 uv).

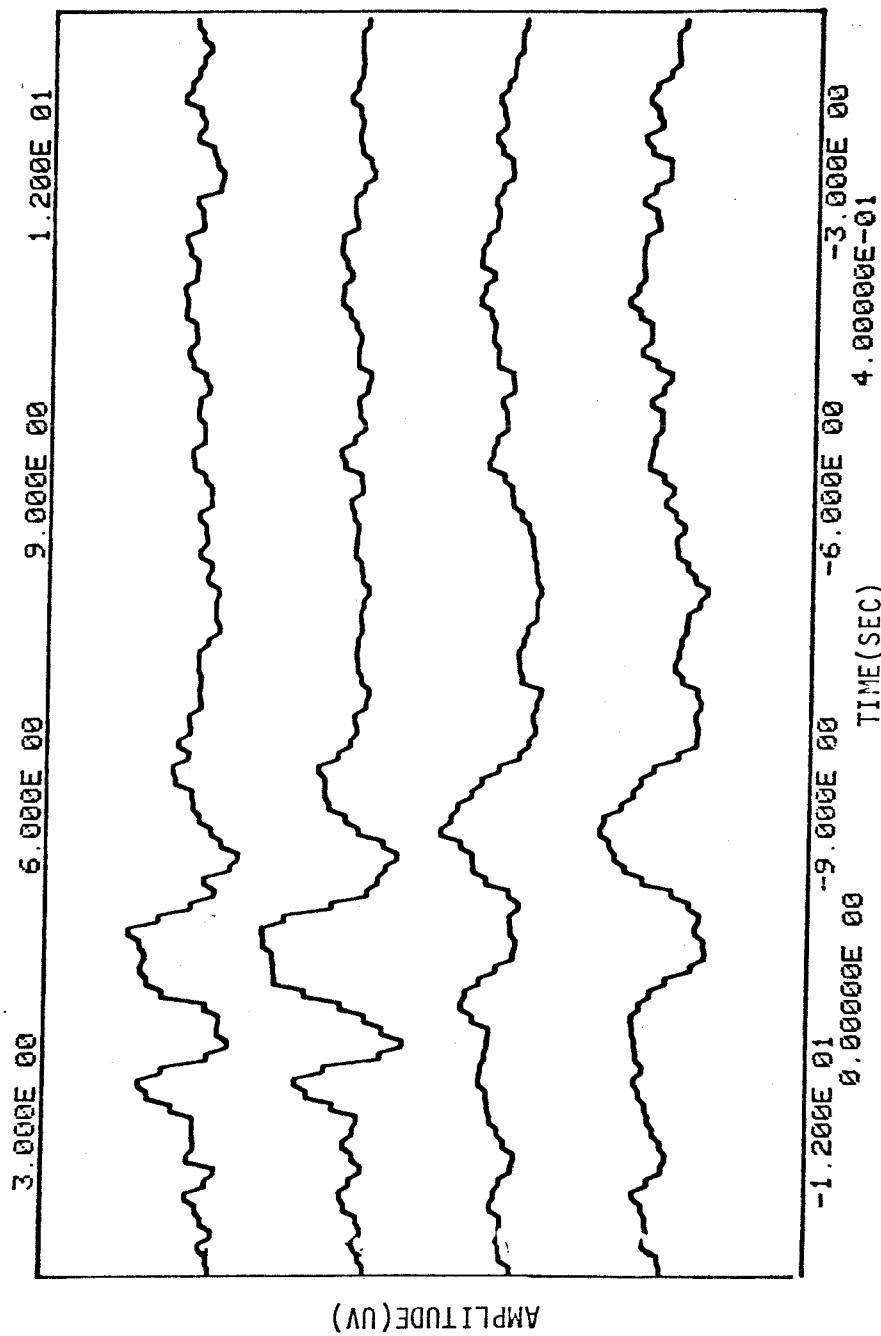


Fig. 4.1.11 Four channels of first order kernels for subject 4.

(One unit on vertical scale = 0.338 uv).

three runs for electrode 3. The high degree of reproducibility of the first-order kernels is clearly seen here. Subject 2 shows phase-shift and reversal from around 70 msec to 200 msec (Fig. 4.1.8). A distinct pattern of left-right reversal in polarity is observed for subject 3 (Figs. 4.1.9 and 4.1.10). Fig. 4.1.10 is the overplotted version of Fig. 4.1.9. with a 2.5 times magnification. The polarity-reversal is also noticeable in subject 4 (Fig. 4.1.11).

The stationarity of the VESP system under study can be assessed by comparing the first-order kernels from several runs of the same or different experiments. Habituation, drowsiness, and boredom are several causes of non-stationarity. Since all of the runs in the present study were done in 3.5 minutes, the stationarity of the subjects could in general be better maintained in comparison with the same experimental situations performed under conventional averaging. The first-order kernels are generally highly reproducible and stationary for all subjects.

Since the first-order kernels can be considered as a special form of averaged evoked potentials, the interpretations of these kernels can follow conventional methods used in evoked potentials. First order kernels are functions of time, therefore implicit-times (latencies) and amplitude measurements of prominent peaks and valleys are valid criteria for determining the timing and fluctuations of underlying intracranial activities.

It is now generally known that the waveform, the timing of each peak and trough, and the duration of evoked potentials are all uniquely related to a large number of conditions. Any change in stimulus parameter, in form,

color, luminance etc. may influence the waveform to a significant extent. In controlled situations, EP can be reproducible to a certain extent. The intrasubject variability can also be reduced in a well-planned and controlled situation. It is this reproducibility that enables us to compare data from different experimental runs among different subjects and to infer their physiological significance.

The first-order kernels shown in the above figures indicate that they possess most of the basic features as seen in conventionally averaged evoked potentials. The latencies of the major peaks are about the same. The distribution of the potentials reflects effects due to half field stimulation. They in general display a high degree of stability in waveforms from different runs. Because of seemingly improved signal-to-noise ratio, early peaks are clearly recognizable and repeatable. This feature may be utilized to investigate in-depth sources such as lateral geniculate nucleus(Chen and Ary, 1979). Because of the high degree of randomness of the stimulus, alpha activities were also rarely observed in the first-order kernels. It seems that the stimulus has better effect in removing alpha activities.

A final reminder is given here for the stimulus used in this study. The somewhat unfamiliar feature of the random flashed checkerboard procedure described here is that the stimuli have interflash intervals which are variable in a pseudorandom manner; they may vary in specified increments from a particular minimum time to a relatively long time. As a typical example, the minimum interflash intervals may be 4 msec, while other intervals may be 8, 12, 16,...msec. The cross-correlation output waveforms (first order kernels)

may be viewed as equivalent VESP waveforms in which the peak and valley values provide measures of the amplitudes of the VESP.

Using a sampling interval of 4 msec and a probability of stimulus occurrence at say, 12.5%, over 6000 repetitions of stimuli can be presented to the subjects in a typical three-and-a-half minute run. If conventional signal averaging is used, assuming an average interstimulus interval of 500 msec, it would take at least 50 minutes to attain the same number of repetitions of the stimuli. Note that in general, the potentials evoked by such rapid stimuli are smaller in amplitude compared with those obtained from the conventional methods which allow the system to return to its resting state.

If a random impulse train is used as the reference waveform (whose spectrum covers a very broad range) then the cross-correlation process will not attenuate the high frequency contents of the evoked responses. This is particularly important if we are interested in early peaks of short durations that are from LGN and other midbrain structures.

The major advantage in using a white noise stimulus over conventional averaging is the greatly reduced experimental time. A much higher informational rate(higher stimulus presentation rate) can be attained by using white noise. This greatly reduces the burden on the subject. Also in general, the shorter the experimental time, the more likely the system would behave as a time-invariant one. Using this method experimental time usually can be reduced ten times. Another advantage lies in the intrinsic nature of the stimulus. This method produces the response to rapidly presented stimuli,

and thus provides an additional parameter for estimation of visual function. In particular, the effect of adaptation due to previous stimulus of very short interval will be discussed in greater detail in the section of second-order kernels.

4.2 EQUIPOTENTIAL MAPS

EEG and EP investigators have been interested in the surface distribution of the electrical potentials of the brain even before digital computers were in general use (reviewed by Petsche, 1973). In order to visualize the salient features from multichannel EEG or EP measurements, number-level plots, contour maps of isopotential lines for single time-frame, spatio-temporal maps for consecutive sampling times (Kavanagh et al, 1978; Darcey, 1979; Darcey et al, 1980 a,b,c), BEAM (Brain Electrical Activity Maps - Duffy et al., 1979), and dot-density topograms (Dubinsky and Barlow, 1980) have been used and reported by other researchers. From such maps, the features of the putative intracranial sources are better revealed. Effects of changes in experimental variables can be detected more easily.

Spatiotemporal equipotential maps will be used as the method for displaying a large number of channels of first-order kernels in this thesis. Fig. 4.2.A shows how these spatiotemporal maps are made. Usually, the average of results from several runs of an experiment under the same experimental condition is plotted. For each time frame, equipotential contour lines computed by an interpolating routine are plotted. This mapping mechanism is a transformation of the 40 traces of averaged first-order kernels into a sequence of equipotential maps at 4 msec intervals. The crosses show the sites of the electrodes. Dotted regions are negative. Fig. 4.2.B shows the top and back view of electrode layout for subject 1. Fig. 4.2.1 shows the back-views of these maps. Not all 40 electrodes are shown since those over the frontal regions of the scalp are out of sight in the back view. For completeness, the

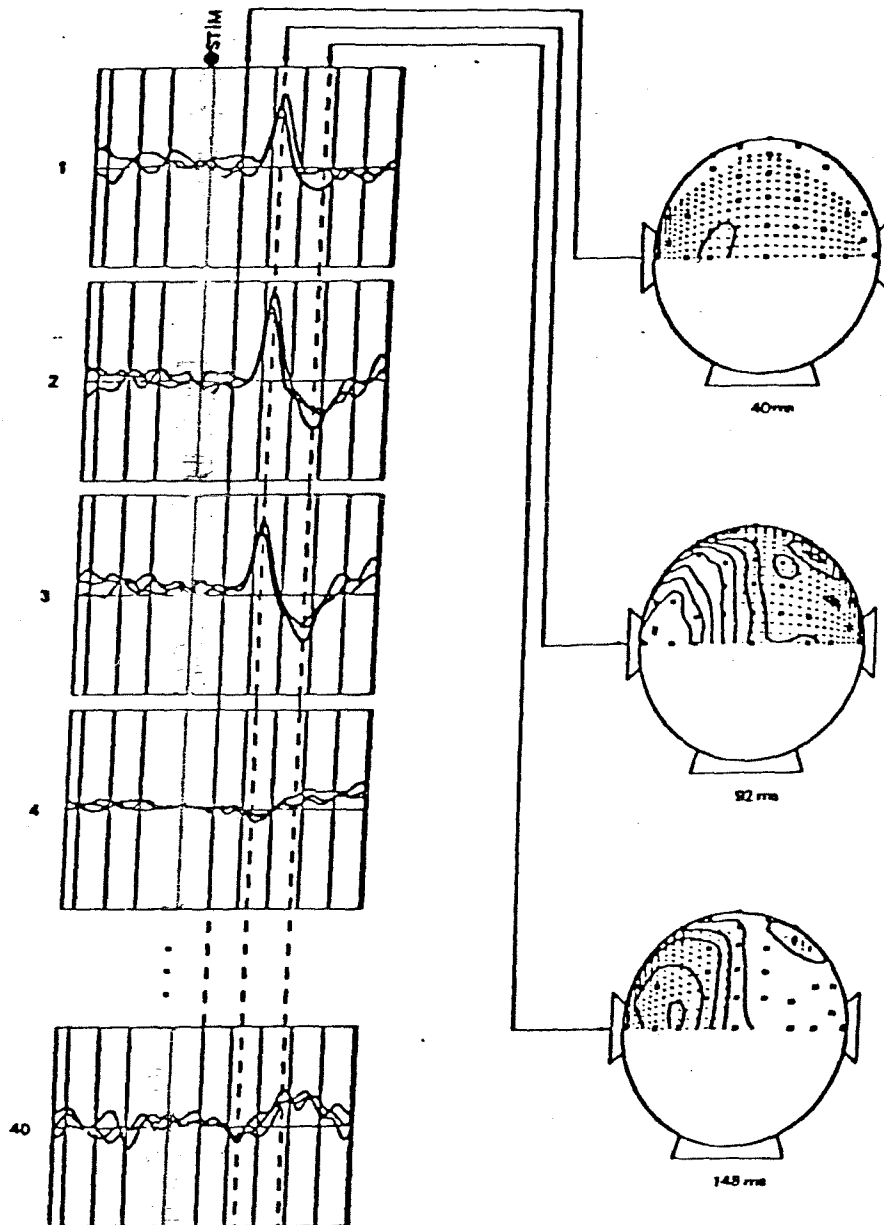


Fig. 4.2.A Equipotential maps of averaged evoked potentials of first-order kernels are made by plotting equipotential contour line for each time frame. The X's indicate electrode locations. Dotted regions are negative.

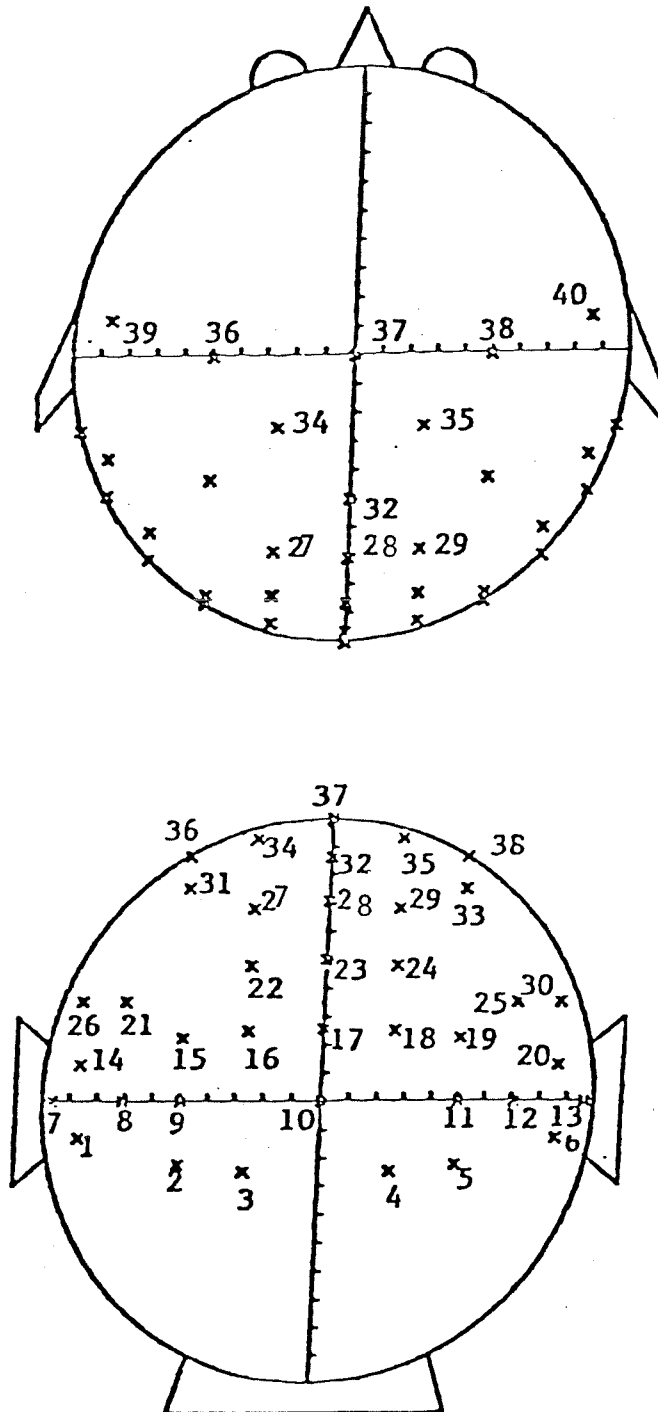


Fig. 4.2.B. Electrode Layout. Top and back view.

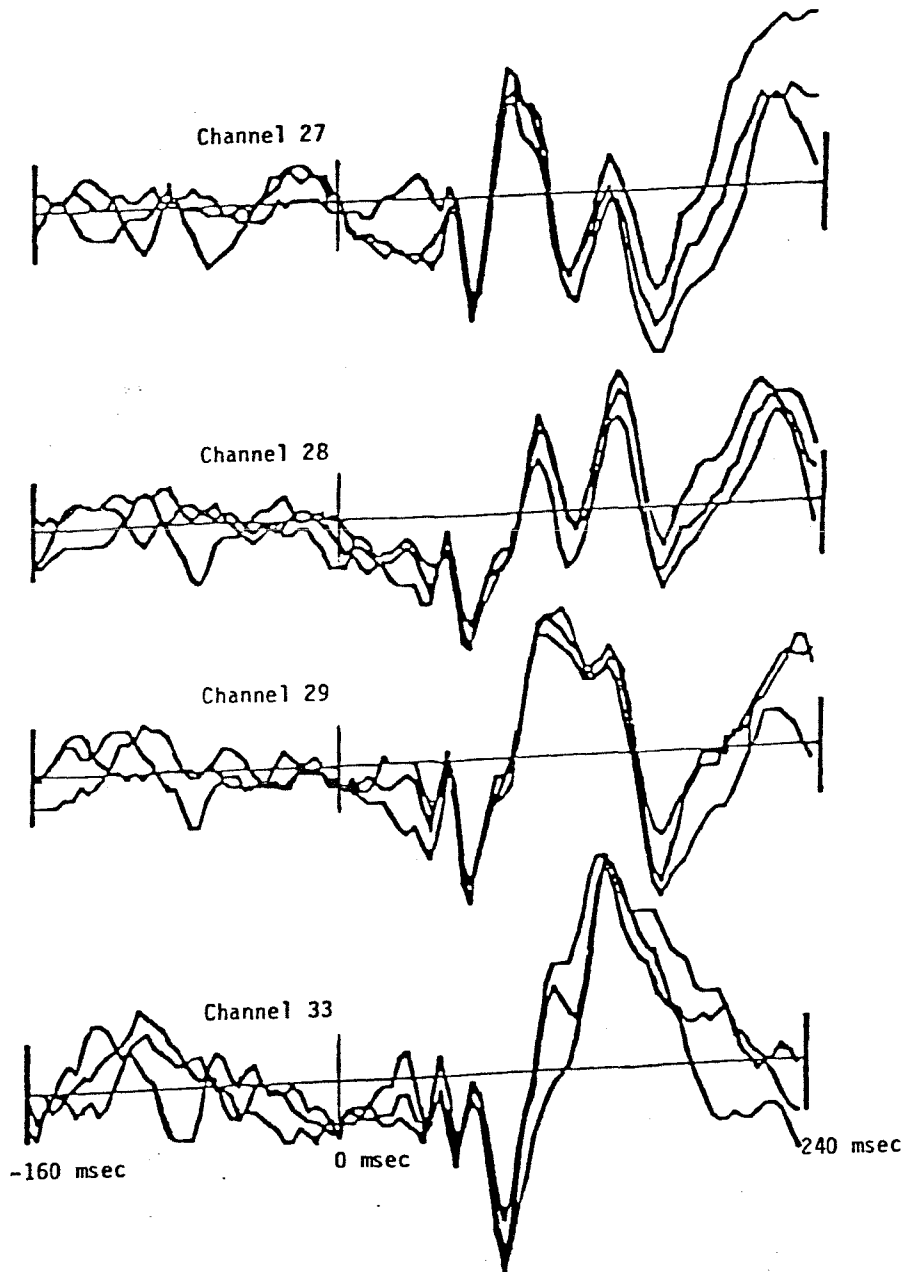


Fig. 4.2.C Four traces of first order kernels from four selected scalp locations. The high degree of reproducibility of three experimental runs is clearly seen. The early peaks overlap with each other and are highly repeatable. They show most clearly in the parietal, close to the midline region.

top views of these maps are shown in Fig. 4.2.2. These maps emphasize the spatial distribution of the first-order kernels. Information in the time-domain can be obtained by inspecting a consecutive sequence of these plots. The stability and reliability of the spatial distribution of the first-order kernels from each individual subject were in general assessed by computer graphics on a Tektronix CRT graphics terminal. Prestimulus values in equipotential maps were good estimations of inherent noise level in responses and the causality of the system.

The data shown in this section were from subject 1, under left-half and right-half field flashed checkerboard stimulation. These time series of equipotential maps were used to capture snapshots of the spatial potential distribution at each time sample. They provided a better way of comprehending spatial relationship among electrodes than by direct inspection of first-order kernel waveforms separately. They made interpretations of underlying brain sources easier. A series of these maps in effect, is a concise display of the complete spatio-temporal course of scalp EP activities. Fig. 4.2.1. shows the equipotential map series of 40 channels of first-order kernels for right-half field stimulation (subject 1). Fig.4.2.2. shows the top view of the same series. Fig. 4.2.3. shows the equipotential map series for left-half field stimulation for the same subject. Fig.4.2.4. shows the same results from top view. When inspecting these maps, it is important to focus attention on identifiable features from one time frame to another. The responses are plotted here starting from 15 samples(60 msec) before the stimulus to 45 samples (180 msec) after. A glimpse of the responses reveals that there is no major

activity before the occurrence of stimulus. The first sign of coherent activity occurs at 48 msec in Fig.4.2.1. Potential distribution begins to show dipole activity starting at around 64 msec. At 92 msec, the distribution is clearly a polarized one with the positive region shown in left hemisphere. Then a different phenomenon appears; at 100 msec the contours of the peak(positive region) starts to migrate across the back of the head from left to right. The potential distribution that was seen at 92 msec is completely reversed by 124 msec. Starting from 128 msec the valley migrates from the left to the right across the head. There is a high degree of similarity between this series of equipotential maps with the results obtained conventionally in terms of the latencies of the major peaks, their polarized distribution, and the migrational phenomenon observed.

Fig.4.2.3 shows the result to left-half field stimulation. There are no major activities before 60 msec. At 96 msec, a distinct left-right polarity is observed with the positive region on the right hemisphere. Starting from 108 msec the valley starts to migrate from left to right across the back of the head. Throughout the whole course, major activities are observed in the right hemisphere.

An optional step in data analysis for first-order kernels was to make reasonable guesses for the source parameters and to perform the source localization routine to choose source parameters whose potential distribution resembles the experimental maps most in a least-square sense. This has been done for selected times after stimulus for some experiments. The results basically agreed with those from other investigators using conventional signal

averaging(Kavanagh,1978; Darcey, 1979).

Darcey et al(1980) suggested that the VESP distributions are interpretable as a combined effect of two schools of thoughts. One school(Lehmann et al, 1969) concentrates on the stability of the potential distributions; it views the head as a volume conductor with spatially stable current sources and assumes that the distribution of the scalp potentials is a function of the strength, location and orientation of the sources. The other school(Childers et al, 1973) concentrates on the change in the potential distributions; it views the movement of potential hills and valleys as a smooth process which reflects the neural propagation of activity in the underlying superficial cortex. Darcey et al speculated that neural propagation as postulated by the latter theory triggers activity in localized populations of neurons, which become the stable sources of the former theory.

When the first-order kernels are studied as time-series of equipotential maps, it is obvious that the hills and valleys move over the head (Fig.4.2.1. to Fig.4.2.4). Recalling the connectivity of the geniculo-striate pathway, this movement might be equated with active propagation along this pathway. The hills and valleys of the equipotential maps of the first-order kernels follow approximately the same paths over the head as the results obtained by using conventional averaging. The first-order kernels on many electrodes are highly correlated in space. This is further evidence for the notion that these evoked potentials are volume-conducted electromagnetic field effects arising from a small number of electric sources at some depth in the head. The amplitude rises and falls in intervals then changes to a new

configuration in a relatively short interval. The figures show that this is a general principle for the major peaks of the first-order kernels. This behaviour was noted in the study by Darcey et al(1980a,b) and the study by Lehmann and Skrandies(1979) using conventional averaging. The most plausible explanation for stably shaped potential distributions varying in magnitude is a group of generators of fixed position and orientation that vary in magnitude with time. Long term stability interrupted by sudden changes may be indicative of relatively slow synaptodendritic processing in one area of the brain followed by rapid axonal transmission to another area.

The equipotential maps for first-order kernels under left- and right-half field pattern stimulation are in many aspects directly comparable with results obtained by conventional signal averaging. This is further evidence that the first-order kernels can be used as an alternative way for displaying prominent features due to partial-field stimulation. The main difference between this approach and the conventional approach is the greatly reduced experimental time to obtain the equipotential maps of reasonable signal-to-noise ratio. Because of improved signal-to-noise ratio, equipotential maps display the potential distribution of early peaks with greater clarity. Some of the early peaks display polarized potential distributions which make dipole-fitting easier(one example, 48 msec in Fig. 4.2.1). This makes it possible for people to investigate in-depth sources such as LGN and other mid-brain structures (Chen and Ary, 1979).

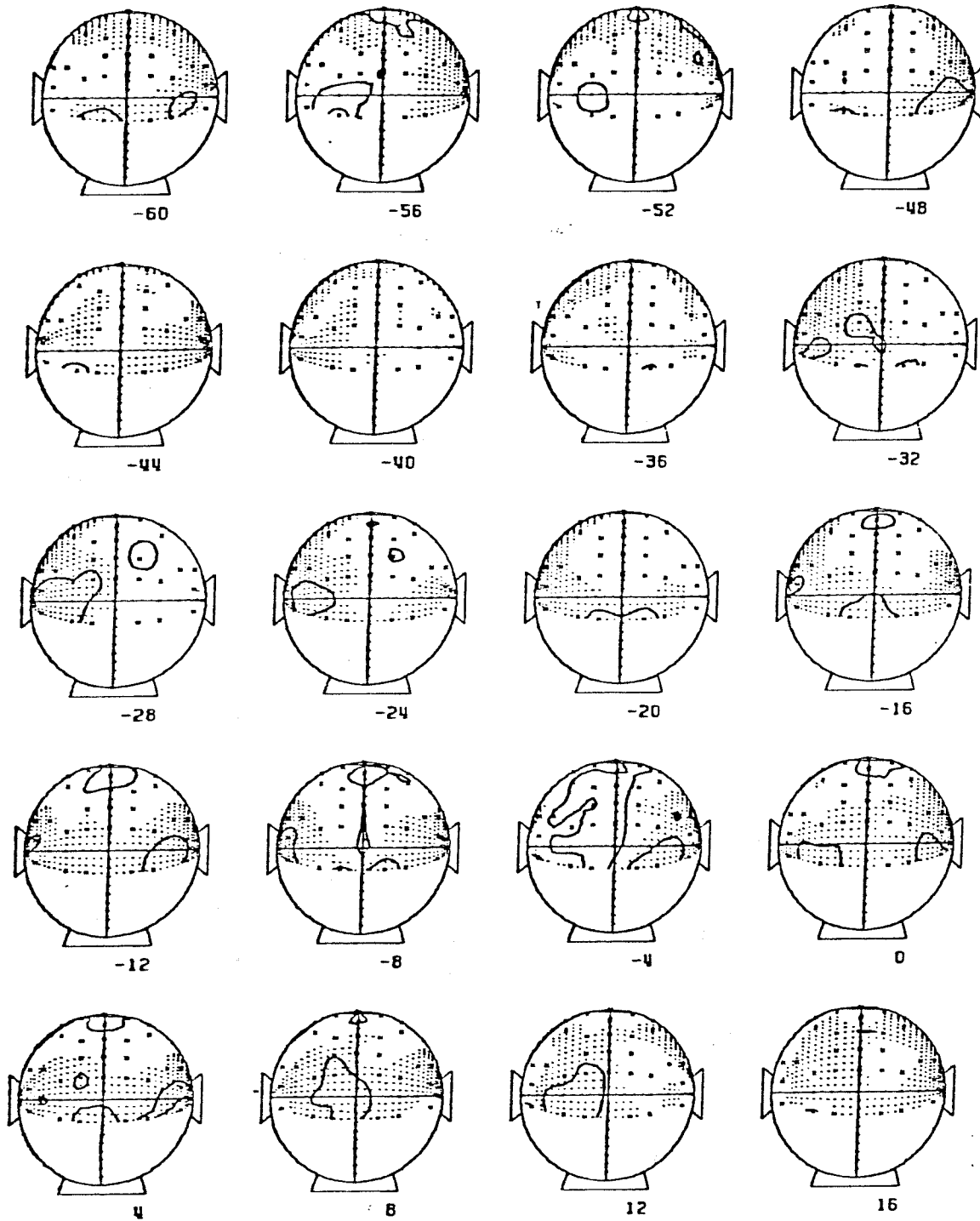


Fig. 4.2.1. Equipotential map series of 40 channels of first order kernels for right half field stimulation.

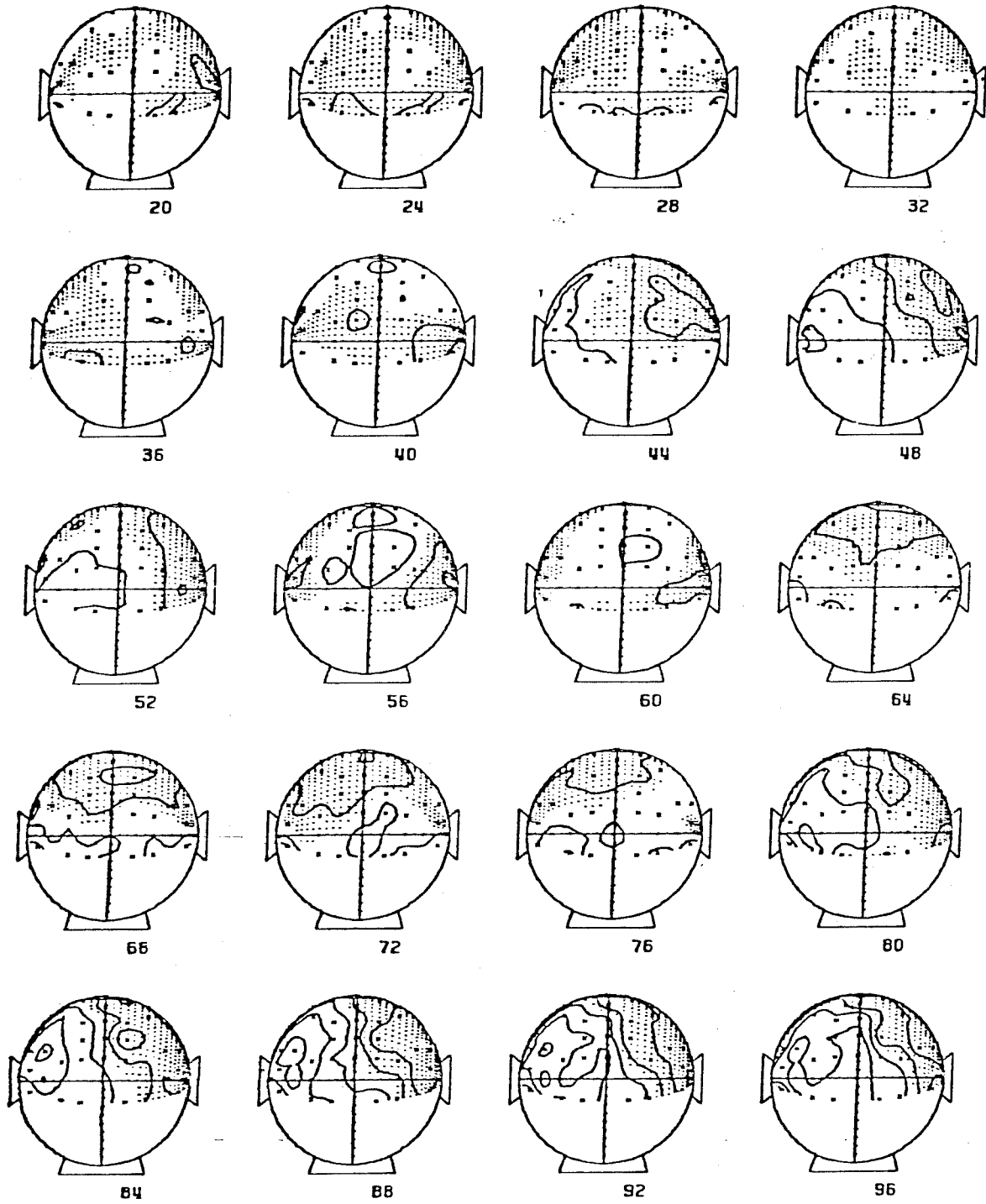


Fig. 4.2.1. (continued)

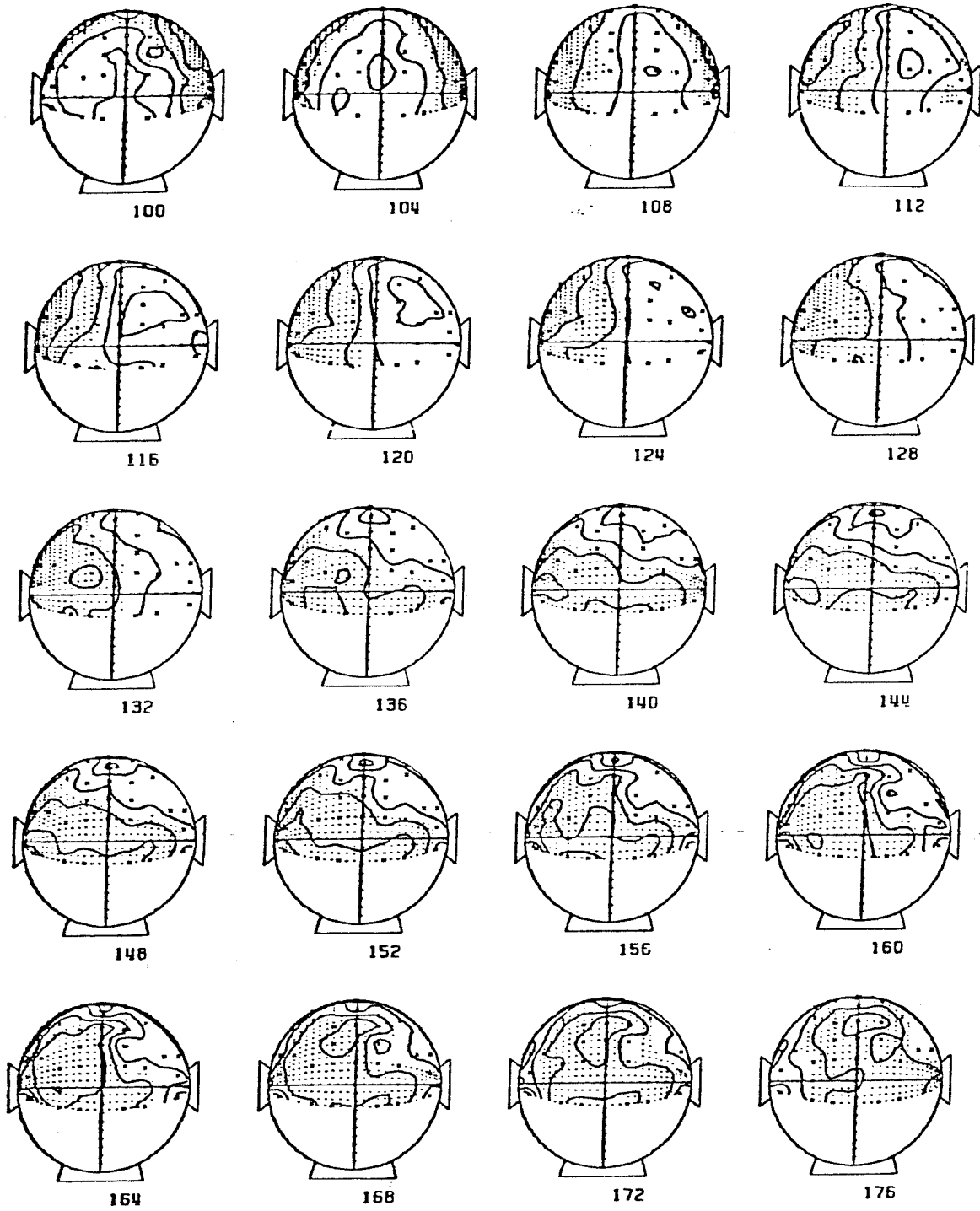


Fig. 4.2.1. (continued)

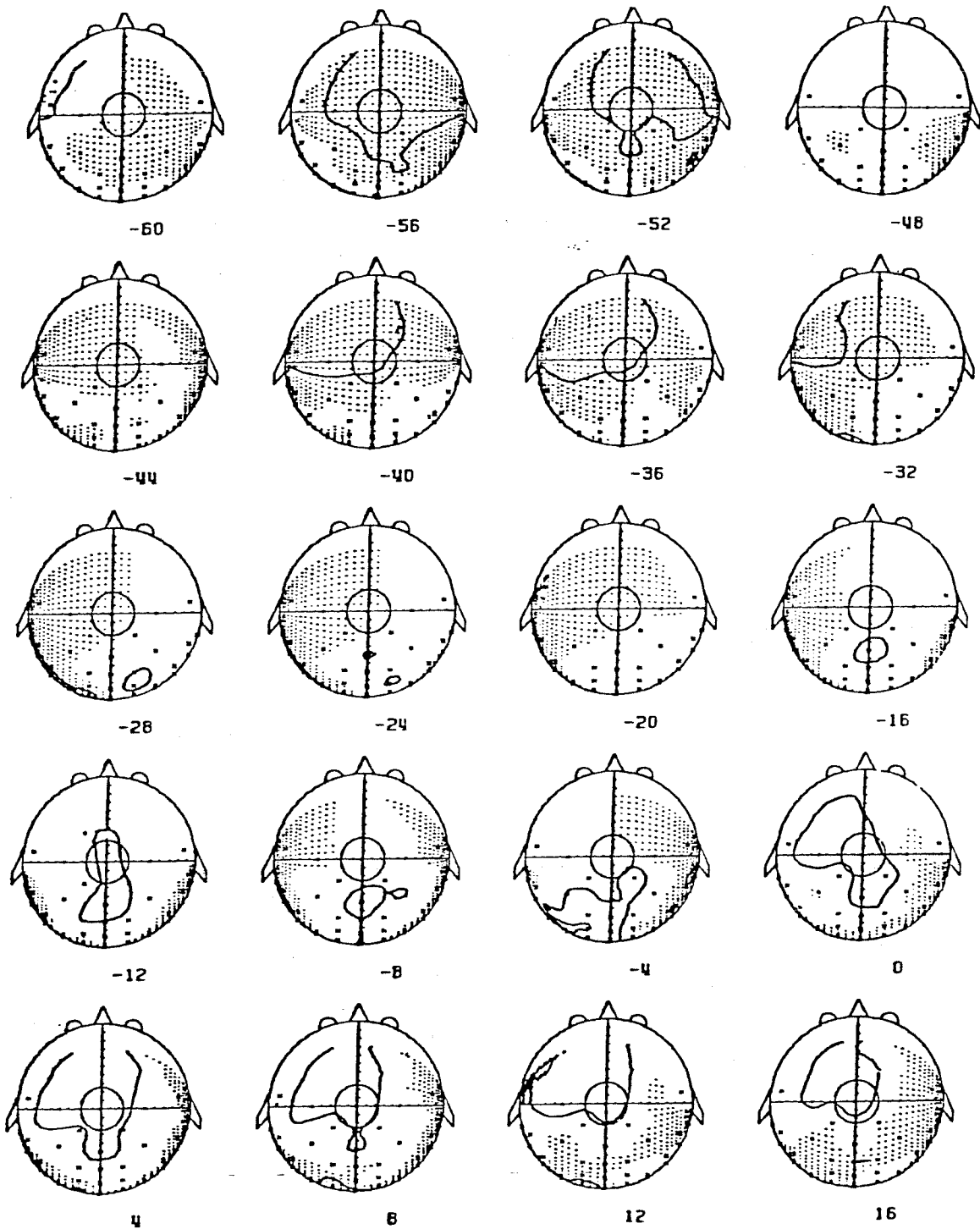


Fig. 4.2.2. Equipotential map series for 40 channels of first order kernels (top view, right half field stimulation).

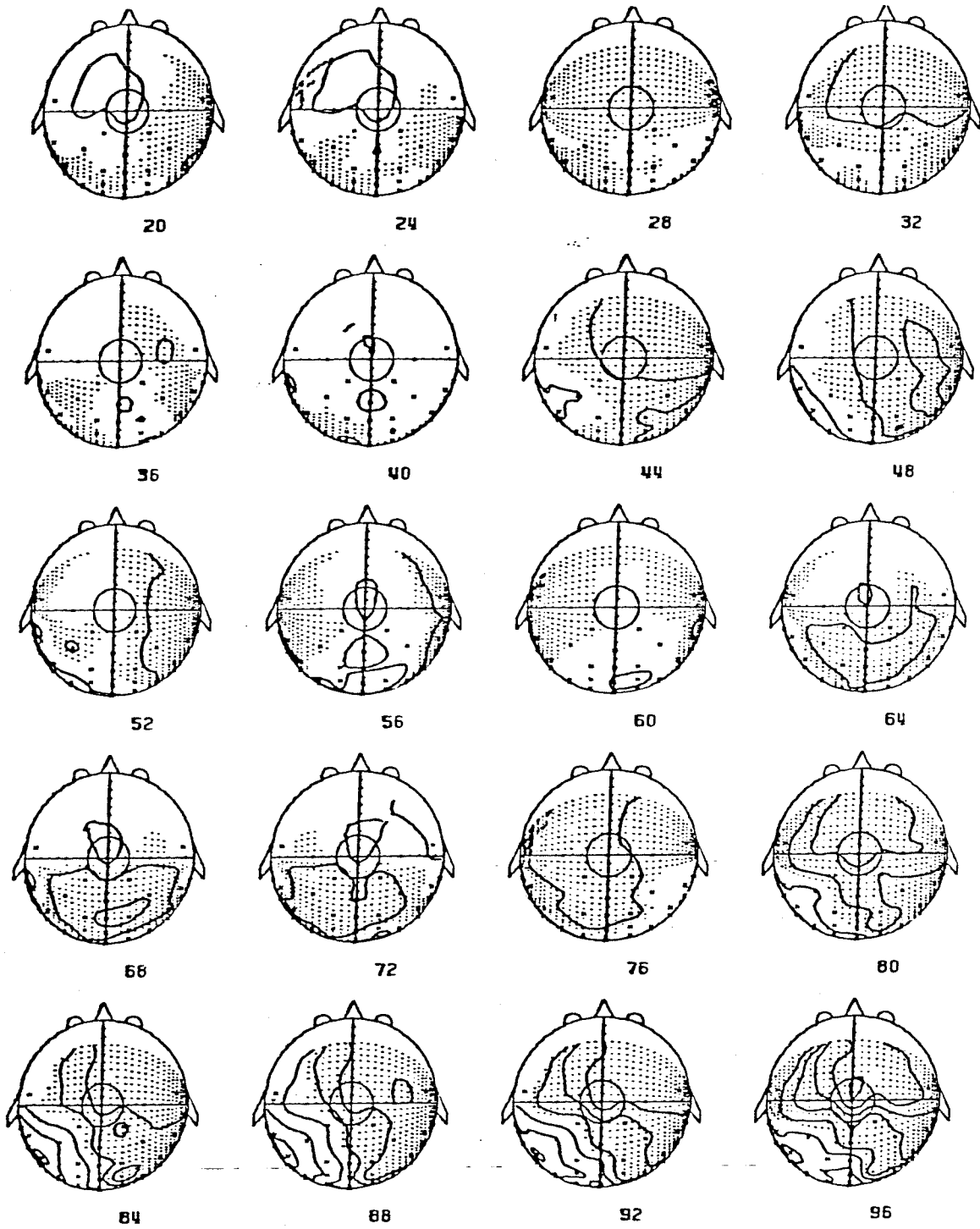


Fig. 4.2.2. (continued)

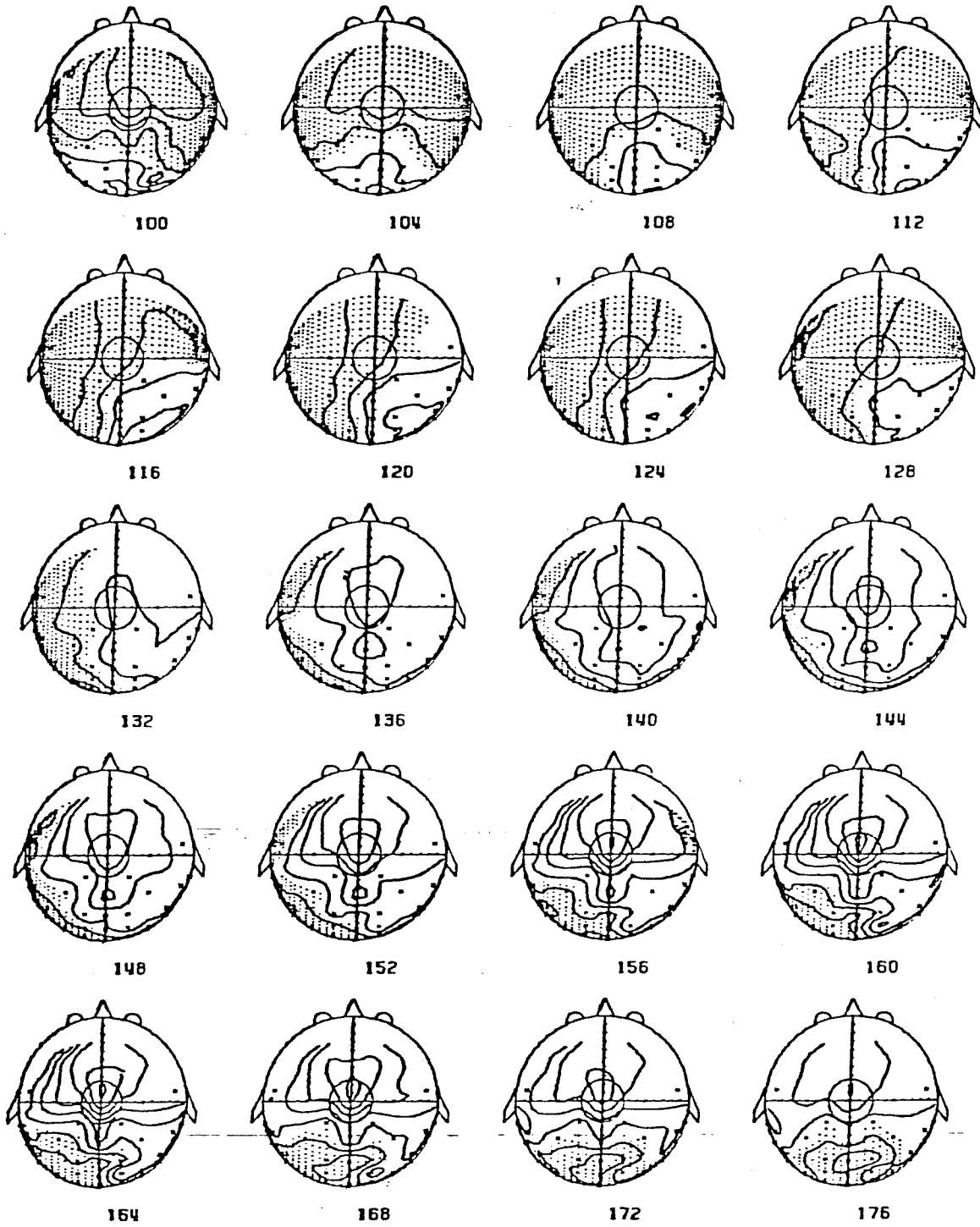


Fig. 4.2.2. (continued)

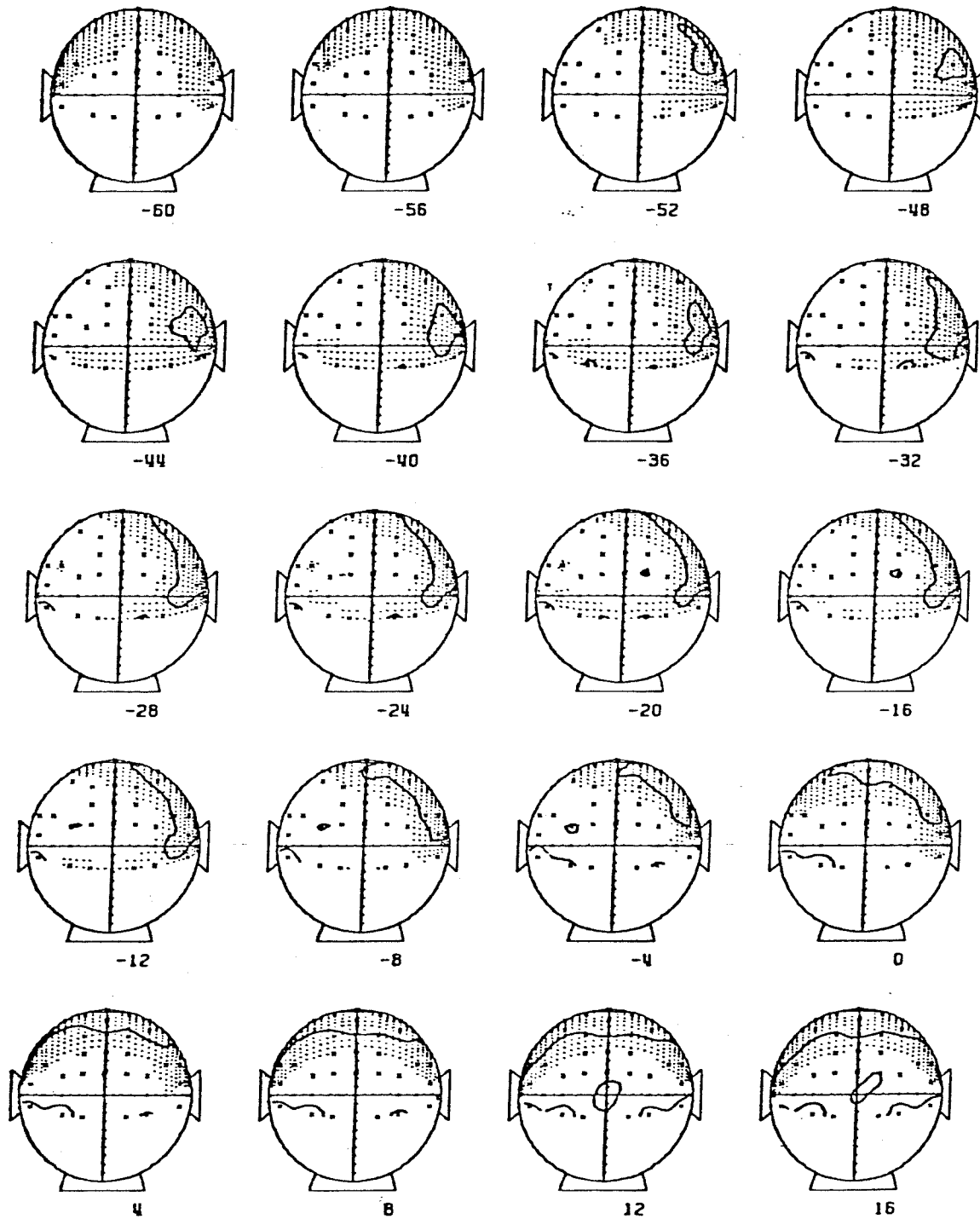


Fig. 4.2.3. Equipotential map series for 40 channels of first order kernels (back view, left half field stimulation).

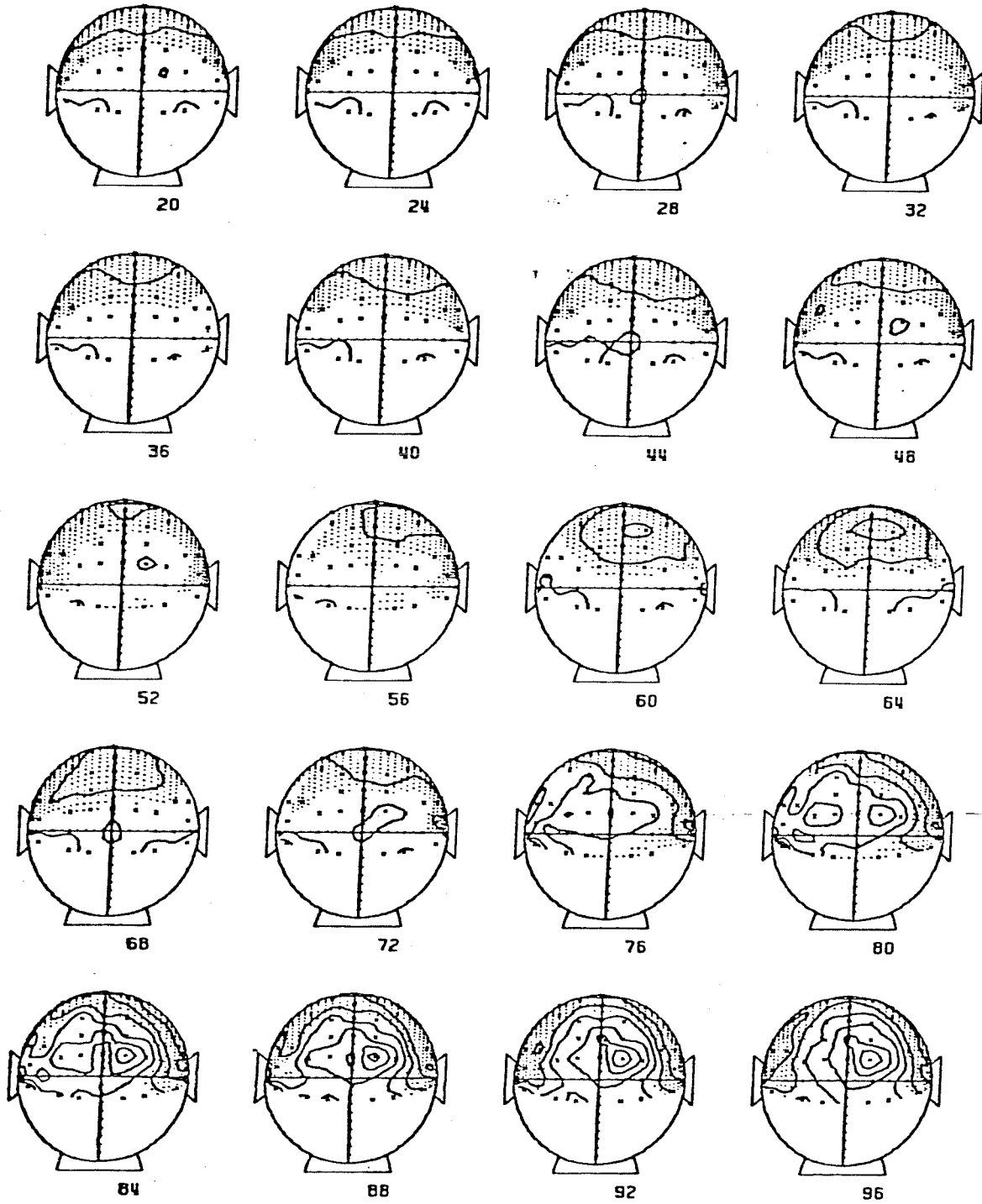


Fig. 4.2.3. (continued)

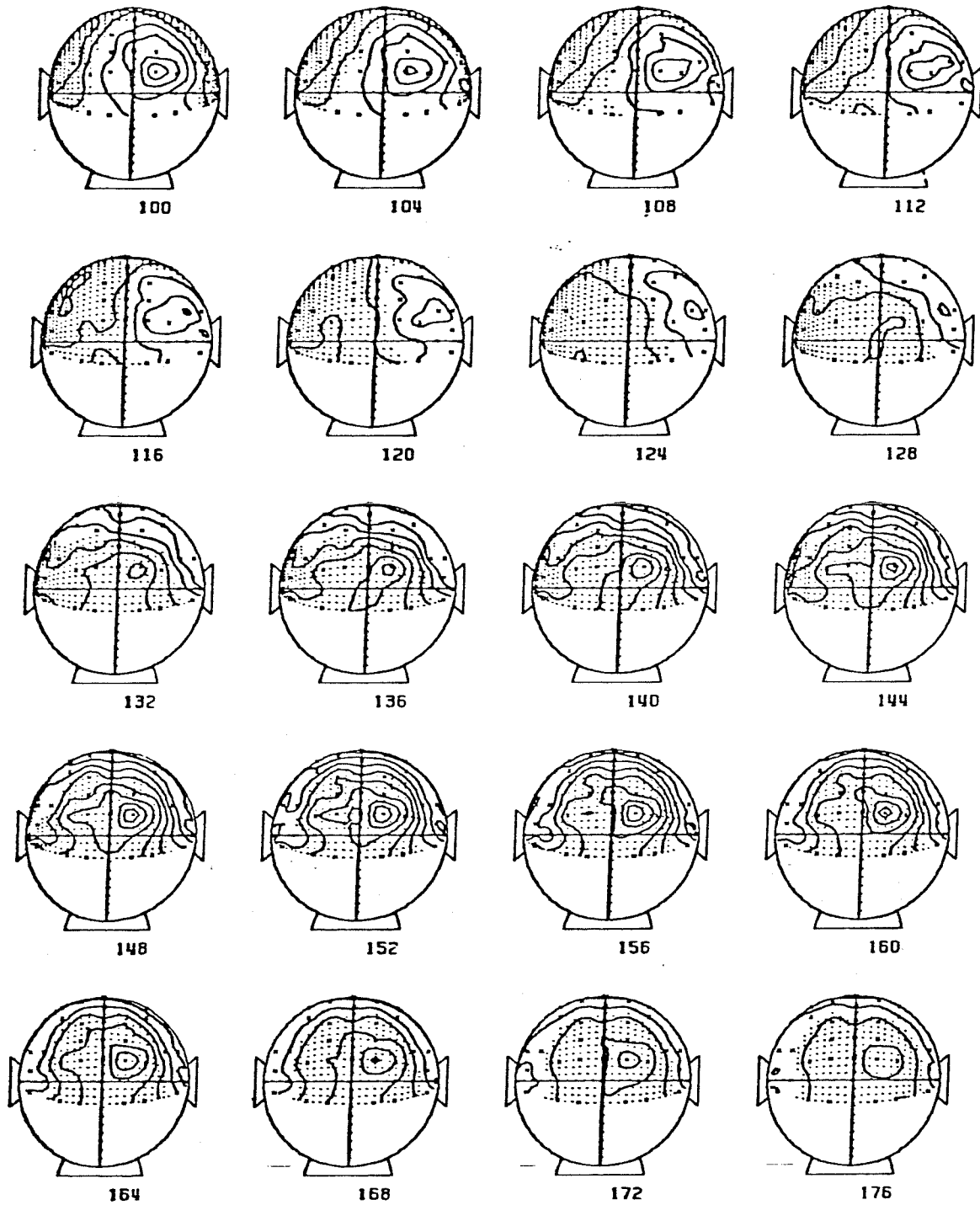


Fig. 4.2.3. (continued)

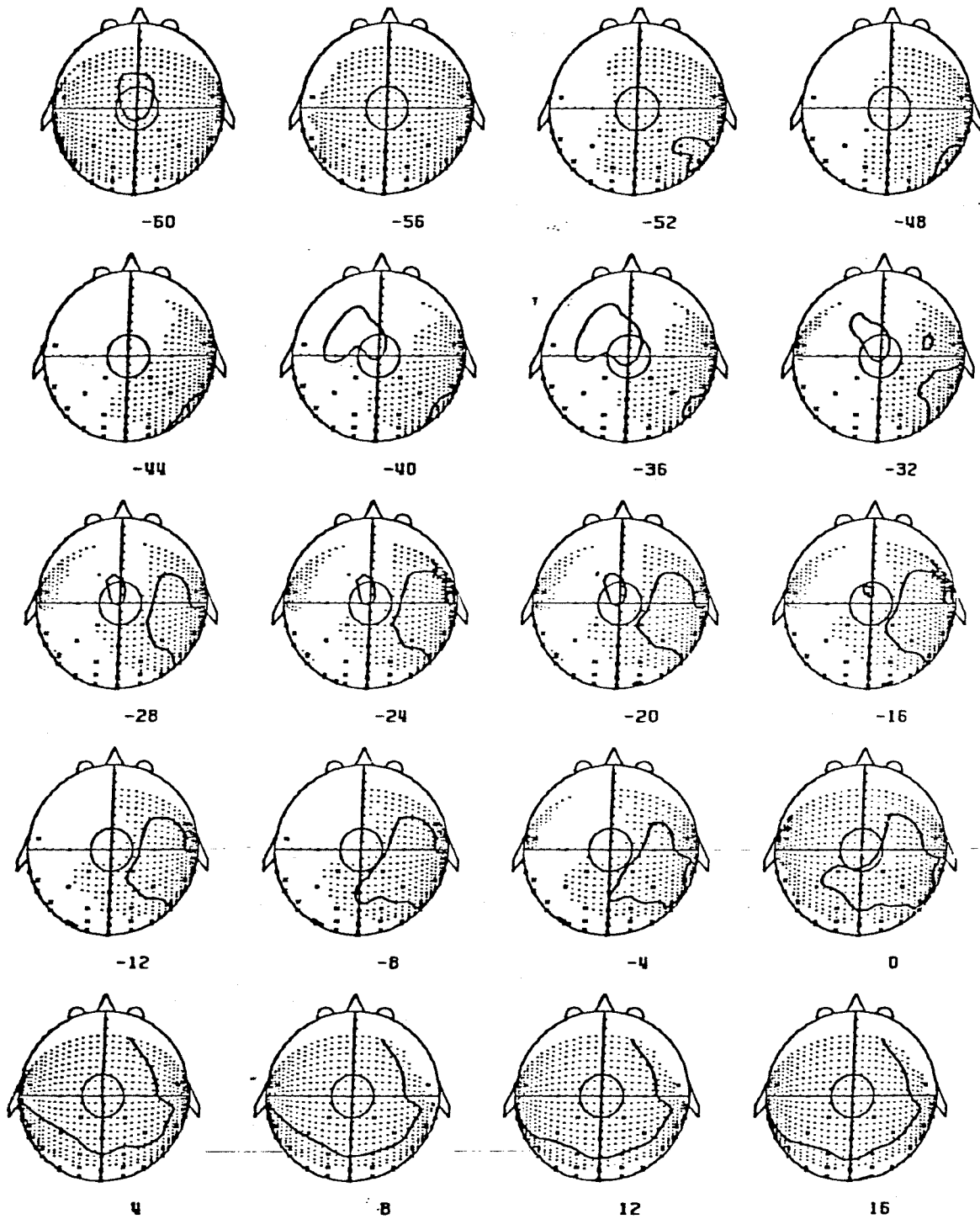


Fig. 4.2.4. Equipotential maps series for 40 channels of first order kernels (top view), left half field stimulation.

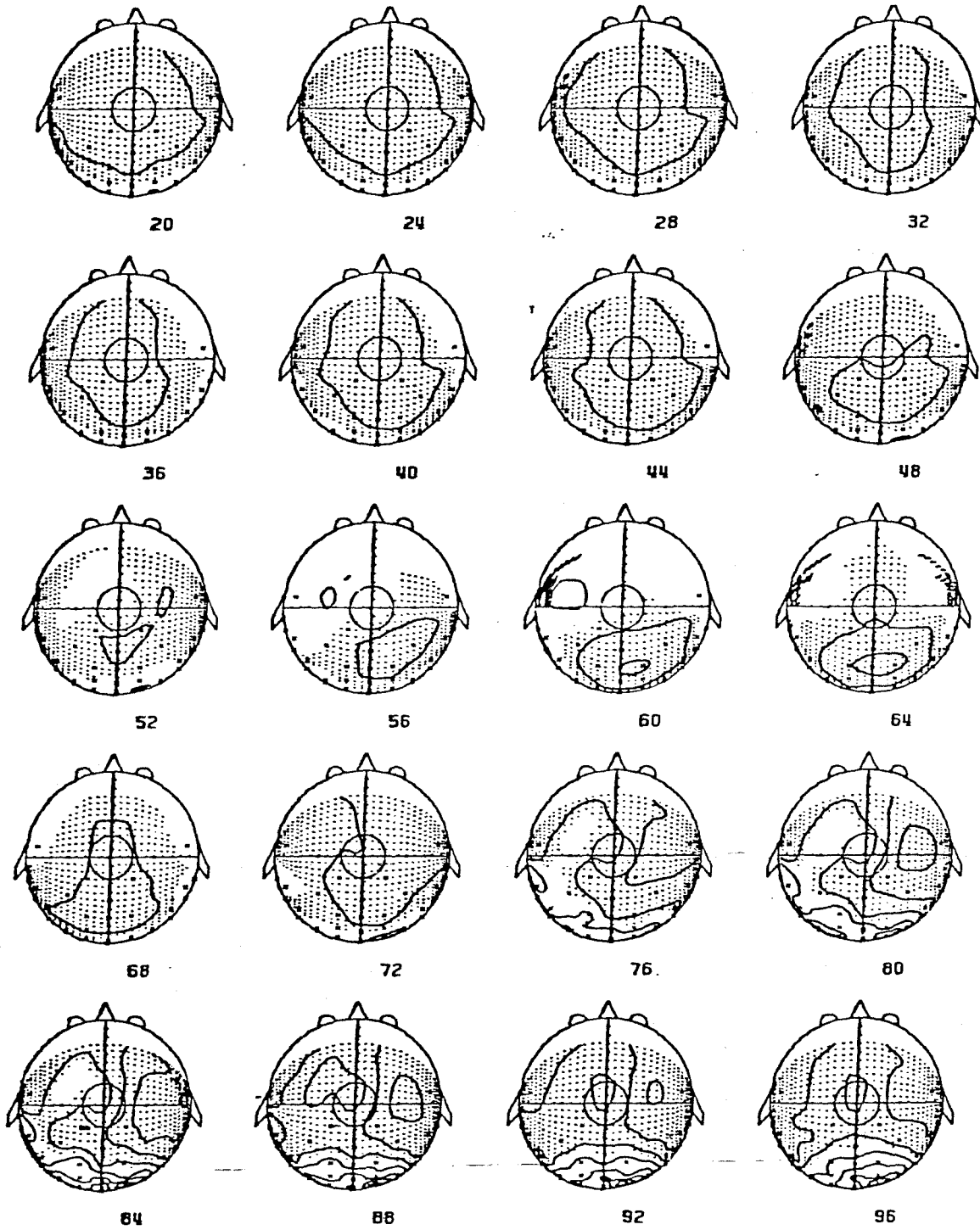


Fig. 4.2.4. (continued)

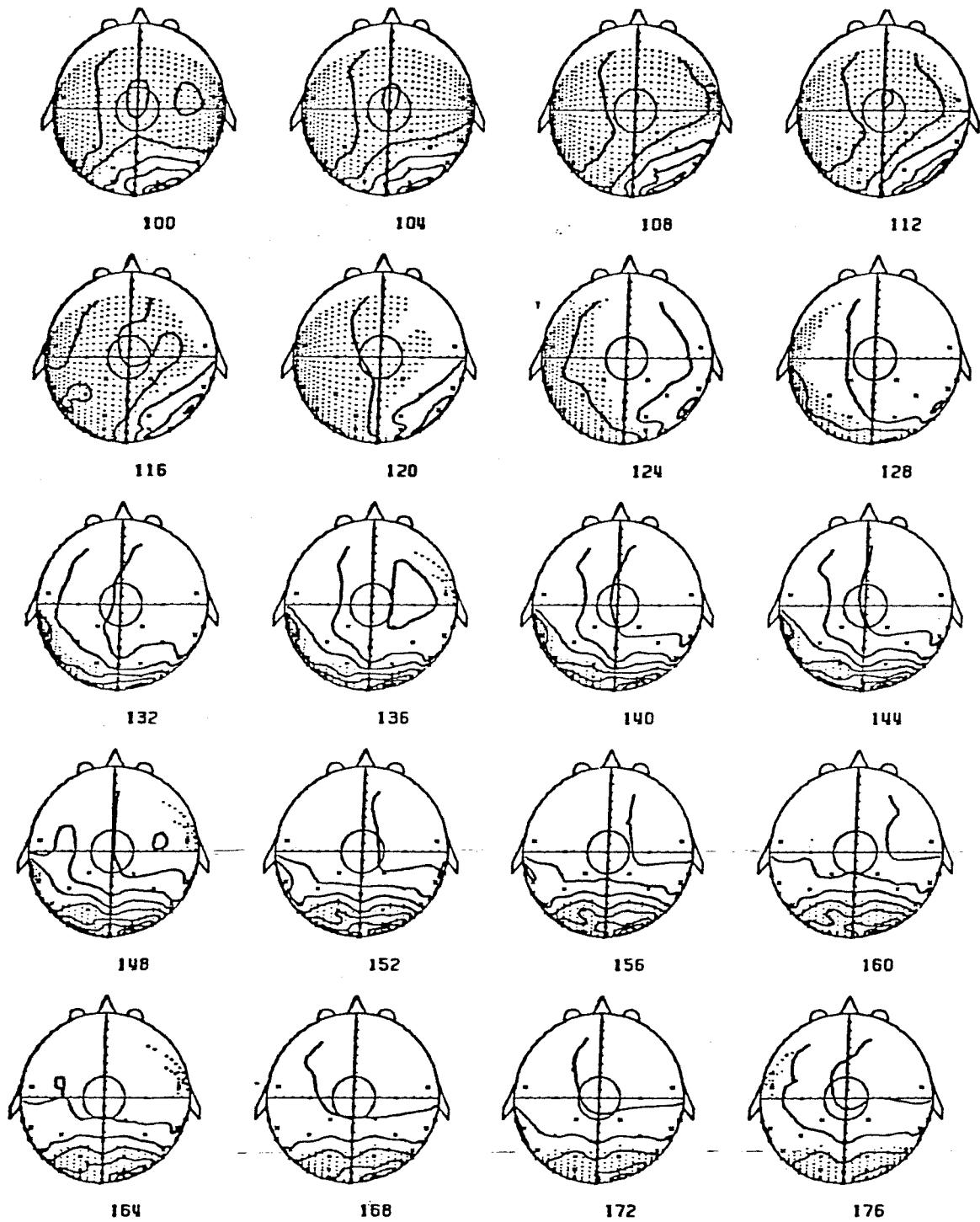


Fig. 4.2.4. (continued)

4.3 LOCALIZATION OF DEEP SOURCES

It is often assumed that scalp-recorded EEG or evoked potential signals represent bioelectric activity which is generated by sources lying immediately below or in very close proximity to the recording site. However, a body of experimental and clinical evidence does support the contention that deep subcortical sources can contribute to scalp potential recordings.

From an interpretation standpoint, it is of some importance to understand the extent to which the activity of such distant sources is reflected at the scalp. If significant contribution is possible, distant sources must be viewed as latent noise generators which might serve to contaminate signals arising from local cortical structures, especially when we are investigating cerebral activities, or localizing cortical sources. Equally important is the proposition that if distant sources can be recorded at the scalp, it should be feasible to develop recording techniques which yield information about thalamic, brainstem, or other in-depth structures. Such information will enable us to trace the route of signal processing in our visual, auditory, somatosensory, olfactory and any other neural modalities which would generate brain activities.

Theoretically, superficial as well as in-depth sources can generate electric field distributions on the scalp according to volume-conduction theory. In a recent study by Hosek(1979), scalp and cortical potential due to implanted, dipole current sources were measured in monkey. A four region spherical model of the head was developed, and scalp potentials due to theoretical radial dipoles were computed and compared with experimental

results. Dipole source locations were chosen to correspond to points along the somatosensory projection pathways to permit comparison of findings with clinical cortical and scalp evoked potential records. Data yielded by the theoretical head model compare well with those obtained experimentally. The results suggest that depth cerebral bioelectric sources do contribute to scalp recorded activity when averaging techniques are used. In their study, the extent to which certain distant sources might contribute to scalp activity was examined experimentally through the analysis of recordings made using externally-driven artificial dipole sources which were chronically implanted in monkey brains. This preparation circumvents many of the restrictions of the straight mathematical model since it leaves the volume conduction medium relatively intact while providing a method of injecting simulated source current of known magnitude, direction and origin.

The feasibility in identifying the peaks and valleys in VESP to their anatomical counterparts is best demonstrated in the results in auditory evoked potentials. Auditory brain-stem responses were recorded by Jewett et al(1970). The result was confirmed by Starr and Achon(1975). Seven short-latency small-amplitude($1/3$ to $1/4$ uv) discrete waves were detected within the first 10 msec after the stimulus click, representing the successive activation of auditory nuclei in the brainstem. Data from human patients with brain lesions of known location have been compared with data obtained by placing recording electrodes within the brain of experimental animals. A widely accepted current interpretation is that as neural signals leave the cochlea, wave 1 is generated by the synchronous firing of nerve impulse in the auditory

nerve, wave 2 coincides with activity in the cochlear nucleus, wave 3 originates in the superior olive, and waves 4 and 5 coincide with the activity in the inferior colliculus. The origin of waves 6 and 7 is not yet known. This correspondence between peaks and valleys in evoked potentials with discrete neural structures in the auditory pathway should apply to the VESP as well.

Corletto et al(1968) studied an epileptic patient who had undergone surgical ablation of the occipital lobe. A comparison was made (1) between the average VER recorded from the scalp and the response from the visual cortex, and (2) between scalp responses recorded before and after surgical removal of the occipital lobe. The result showed that the ablation of the occipital lobe did not affect the initial components(before 60 msec) of the response or the late components (greater than 120 msec), but greatly reduced the amplitude of the waves with peak latencies in the intermediate range. This suggests that the precortical activities which include those from LGN lie in this range. Simultaneous recordings taken from thalamus and scalp in humans by Larson and Sances(1979) suggest that evoked somatosensory signals generated at the thalamic level may be volume conducted to the scalp. This follows from the observation that small inflections seen on the scalp are observed at the same latency in depth (thalamic) recordings.

There is now strong evidence that using Poisson impulse train as a kind of white noise to probe the human visual system makes detecting deep sources easier because of the improved signal-to noise ratio. Early peaks before 70 msec after the stimulus were repeatedly revealed in the first-order kernels across different experimental runs and across different subjects.

Fig. 4.3.1. shows the result of localization on 48 msec time frame for the same experiment as displayed in Fig. 4.2.1. The localization was done by using the same method as described by Kavanagh et al(1978). Equivalent sources for the experimental data are found by taking least-squares estimates of model parameters, minimizing the sum of the squared deviations between the actual scalp potential and scalp potential computed by the model. A homogeneous model was used in this case. The upper back-view of potential distribution shows the experimentally obtained result, whereas the lower figure shows the distribution predicted by the model. Please notice that the source is located centrally in the left hemisphere and the stimulus was a right-half field. If the dipole location indicates the approximate locality of active neural aggregation, then this might indicate that the location is in the middle part of the brain, probably from midbrain or thalamus. There is a possibility that this is actually from the response of the left lateral geniculate nucleus. More investigation along this line is necessary before any conclusive remarks can be made at this point. I am convinced that there are responses originating from deep subcortical sources because of the high degree of reproducibility of these early peaks although their anatomical identification is not established yet. Fig.4.3.2 and Fig.4.3.3 show the results of localization done on 84 and 120 msec time frame from the same experiment. The dipole locations were found to be in the left hemisphere(due to a right-half field stimulation) probably from a cortical origin. The feasibility and the power of this approach is clearly demonstrated here.

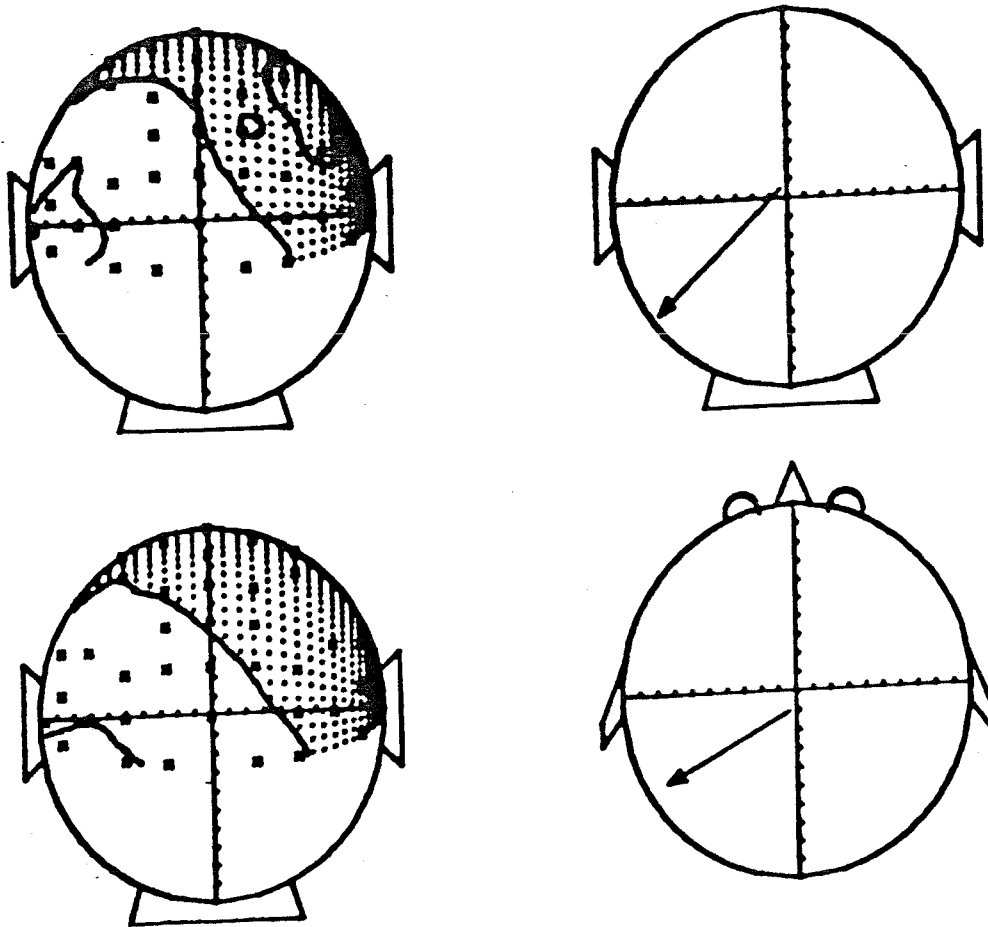


Fig. 4.3.1 Equivalent dipole localization using homogeneous model for the 48 msec peak(refer to Fig.4.2.1). The experiment was done with right-half field flashed checkerboard pattern on subject 1.

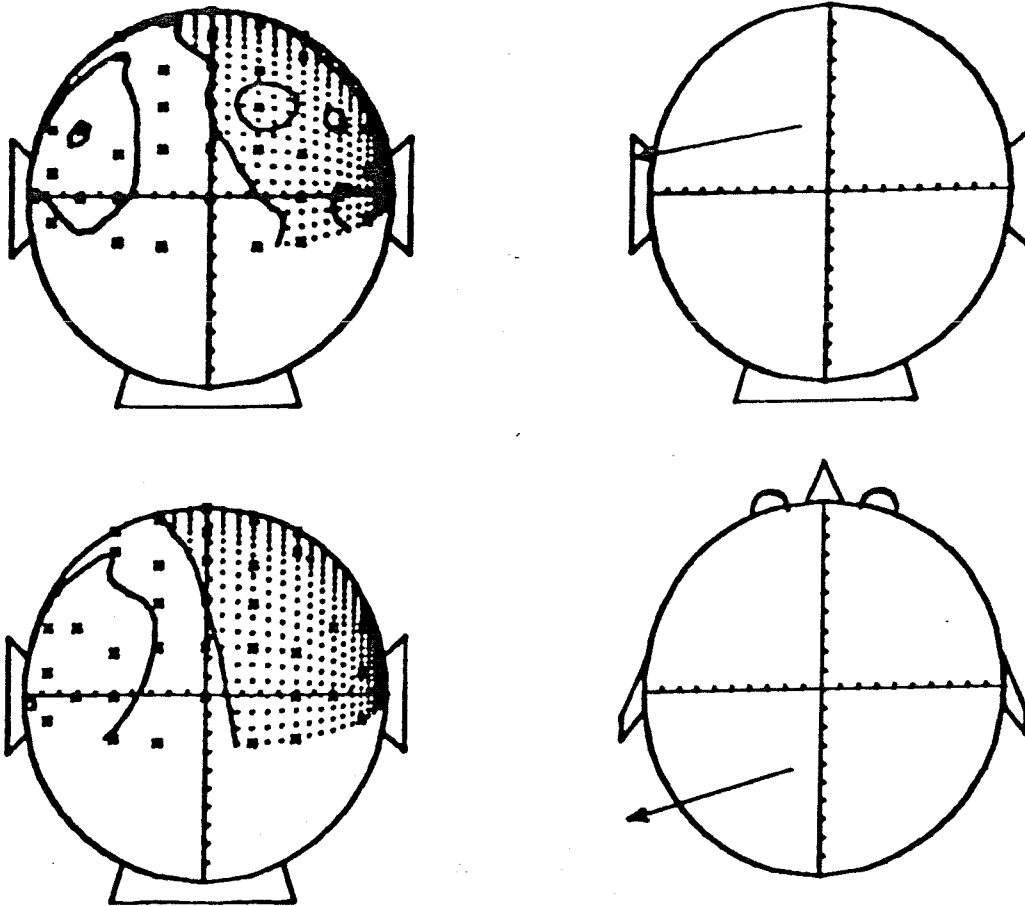


Fig. 4.3.2. Equivalent dipole localization using homogeneous model for the 84 msec time frame as shown in Fig.4.2.1. The experiment was performed with right-half field flashed checkerboard pattern on subject 1.

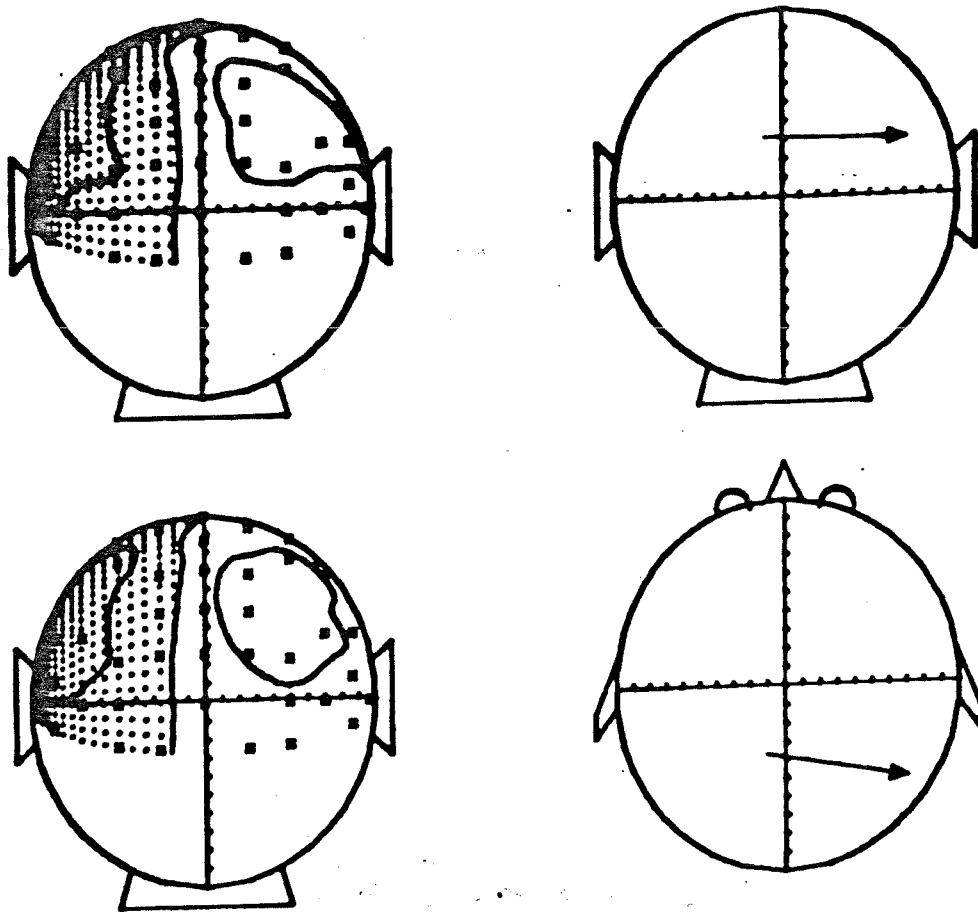


Fig. 4.3.3). Equivalent dipole localization using homogeneous model for the 120 msec time-frame as shown in Fig.4.2.1. The experiment was done with right-half field flashed checkerboard pattern on subject 1.

4.4 INTERPRETATIONS OF SECOND ORDER KERNELS

Fig. 4.4.1 shows the nonlinear interaction between the responses of two impulses in a nonlinear dynamic system. In the upper diagram the impulse response for the first impulse is shown by the solid line. If the system were linear the second impulse would generate an identical impulse response, also shown by a solid line, with a time delay equal to the interpulse interval. Again, if the system were linear, the total response to the two impulses would be the linear sum of the two impulse responses. This is indicated by the dashed line. However, suppose that an actual double-impulse experiment gives results as shown by the dotted line. If this is different from the dashed line in any way, the system is nonlinear. One way of measuring the nonlinearity is to calculate the difference between predicted and the actual responses, as shown by the hatched area and by the lower diagram. Note that the nonlinear effects do not appear until after the second impulse. A nonlinear interaction which reduces the actual output of the system might be known as inhibition, saturation, response compression or adaptation.

Fig. 4.4.2 shows the method of displaying the second-order kernels in this thesis. The first-order kernels are always displayed together with the second-order kernels. This makes interpretations of second-order kernels easier. The horizontal axis of both first- and second-order kernels indicates time(msec) after the test-impulse. The vertical axis of the second-order kernel indicates the time between stimuli(the conditioning stimulus and the test stimulus). Therefore, a horizontal cut across the kernel at a specific "time-between stimuli " would give a profile corresponding to the curve in the

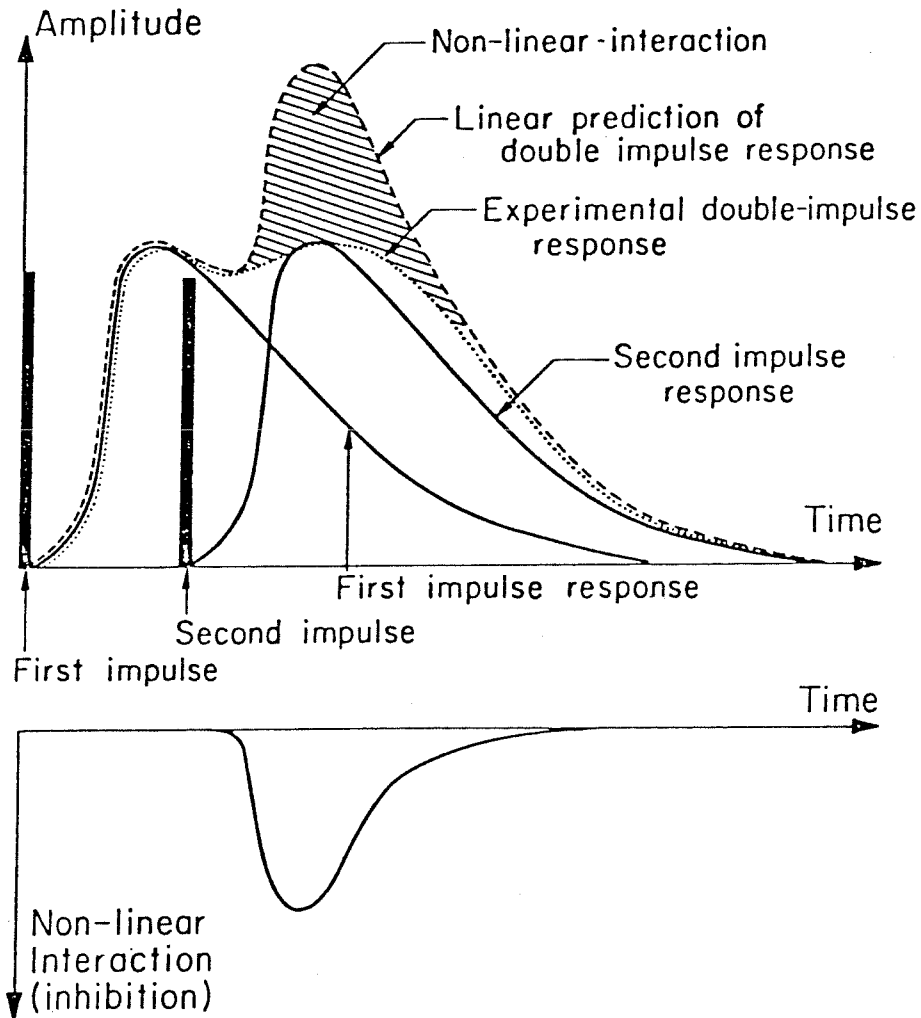


Fig. 4.4.1. In the upper diagram the impulse response for the first impulse is shown by the solid line. If the system were linear, the second impulse would generate an identical impulse response. The dotted line indicates the actual response of a nonlinear system. One way of measuring nonlinearity is to calculate the difference between the predicted and the actual responses.

lower diagram of Fig. 4.4.1. In the display of the second-order kernels, the dotted area indicates negativity in sign.

A closer inspection will tell us that for each peak and trough in the first-order kernel, there is a corresponding region with the approximate time-delay in the second order kernel. By inspection of Fig. 4.4.2, it is easy to find that there is a prominent peak at about 70 msec which corresponds to the valley at the approximate latency in the first-order kernel. Another important thing that can be easily observed is the trend of reversal in sign in the first-order and second-order kernels. This tells us that in general, the nonlinear interaction effect for two impulses separated by different intervals is inhibitory. For a positive peak in the first-order kernel, a negative valley in the second-order kernel is considered as inhibitory. Similarly, for a negative valley in the first-order kernel, a positive peak in the second-order kernel is considered as inhibitory since its effect is still to offset or decrease the magnitude of the first-order kernel. The inhibitory effect at around 70 msec seems to have a short memory. The term memory is used here to describe in the second-order kernels the "length of time-between-stimuli" that shows a reproducible pattern of facilitation or inhibition with respect to the first-order kernel. The time-between-stimuli is displayed in the figures only to 60 msec since beyond this range no distinct reproducible patterns have been observed. It is also noticeable from Fig. 4.4.2 that this inhibitory effect has different memory-lengths for different corresponding peaks and troughs in the first-order kernel. The most distinct region of this inhibition occurs after 100 msec on the time(horizontal) axis.

For the positive peak at 140 msec in the first-order kernel, there is an elongated valley which extends downward to around 60 msec in the second-order kernel. A similar observation applies to the valley at around 180 msec in the first-order kernel.

Starting from Fig. 4.4.3, the first- and second-order kernels for all five electrodes for subject 1 will be displayed. They show basically the same inhibitory effect. Take Fig. 4.4.4. as an example. The peak at around 70 msec still shows a short memory. For the elongated peak that corresponds to the valley at 120 msec latency in the first-order kernel, it still shows an inhibitory effect and a longer memory. The left-right polarity-reversal due to the half-field effect as explained in section 4.1 for electrodes 1, 2 and 4, 5 is also observable in the second-order kernels, particularly in the regions from 175 msec to 200 msec. Refer to Fig.4.4.3 and Fig.4.4.7. This left-right polarity reversal due to half-field effect is again observed in the second-order kernels. For the negative region from 175 to 200 msec in Fig. 4.4.3, there is a positive region shown in Fig.4.4.7 in the same time range.

By careful inspection of the figures, we can observe other reproducible subtleties. One example is shown in a comparison between Fig.4.4.2 and Fig. 4.4.3 to Fig.4.4.8. The elongated valley(100-150 msec in time, Fig.4.4.2) and peaks (same range for other figures) show about the same memory-lengths and interestingly peak at approximate time-between-stimuli, about 18 msec. Other reproducible fine points can be observed between subject 1 and subject 2.

The use of functional power series to characterize human visually evoked response is investigated and is very powerful. This type of analysis provides a measure of the nonlinear interaction in the brain caused by prior inputs. By utilizing this property, in addition to gaining insights into the facilitatory and inhibitory effects, we might be able to draw a dividing line between the cortical and subcortical sources through a better understanding of the second-order kernels.

The amount of facilitation/inhibition in a two-pulse experiment can be predicted to a certain degree if the kernels of the system are known. Experiments using double pulse as visual stimuli have been performed by a number of investigators. Because of the differences in the stimulus modality (flash versus pattern etc), direct comparison of the two approaches should be dealt with carefully. These experiments serve as an indirect comparison to partially explain the second-order kernels. Bartley(1936) has shown in animals that the VESP to the second of a pair of photic stimuli was smaller in amplitude(inhibitory) than the response to the first stimulus unless a certain interstimulus interval(ISI) was used. The duration of the ISI necessary to produce equal and maximal responses to both stimuli was found to be equal to one cycle of the EEG's spontaneous alpha rhythm. Vaughan (1966) recorded human VESP's for various ISI values and studied the relationship between perceptual discrimination performance and the magnitude of the response to the second pulse. He found that the recovery of the response to the second pulse exceeded discrimination performance over the ISI range of 60-100 msec. In a similar way, Inoue(1968) found facilitatory and inhibitory effects in double

pulse and triple flash VESP's according to the ISI. Bartlett and White(1965) used paired flashes as stimuli, varied the interval within each pair while maintaining a constant interval between the sets. Using variations of 9, 16, and 25 msec between the pairs caused the subjects to report that the 9 msec sets appeared brightest most often as opposed to those for the 25 msec interval which were generally reported as being least bright. In addition, a greater amplitude for both positive and negative waves was obtained for the 9 msec interval stimuli.

The following is a summary of the information disclosed by second order kernels using white noise stimulus in EP experiments. (1) It enables us to find out the facilitory and/or inhibitory effect from the conditioning stimulus upon the test stimulus. This can be applied to different stimulus modalities: visual, auditory, somatosensory etc. (2) It tells us about the memory lengths for this nonlinear dynamic interaction. In other words, it tells us what range of the ISI has the most significant or noticeable effect and the limit of the ISI over which this kind of interaction exists. (3) It reveals the 'maximum-interaction ISI'. White-noise analysis provides us with this information very handily. If conventional signal averaging is used, a set of evoked potentials must be measured as a function of different ISIs. (4) If plotted in graphical contour-map form as done in this thesis, the second-order kernels provide us with a possible new tool in disentangling brain sources. Since the EP reflects a substantial amount of hard-wired neural activity, there are reasons to believe that different anatomical structures(such as the LGN, primary visual cortex, secondary visual cortex)

would have different lump together potentially independent processes. By inspection of the second-order kernel for subject 2 in Fig. 4.4.3, it is easily seen that the memory lengths for 72 msec and 92 msec and subsequent peaks and valleys are different. It is logical to think that they might indicate neural activities from different brain structures.

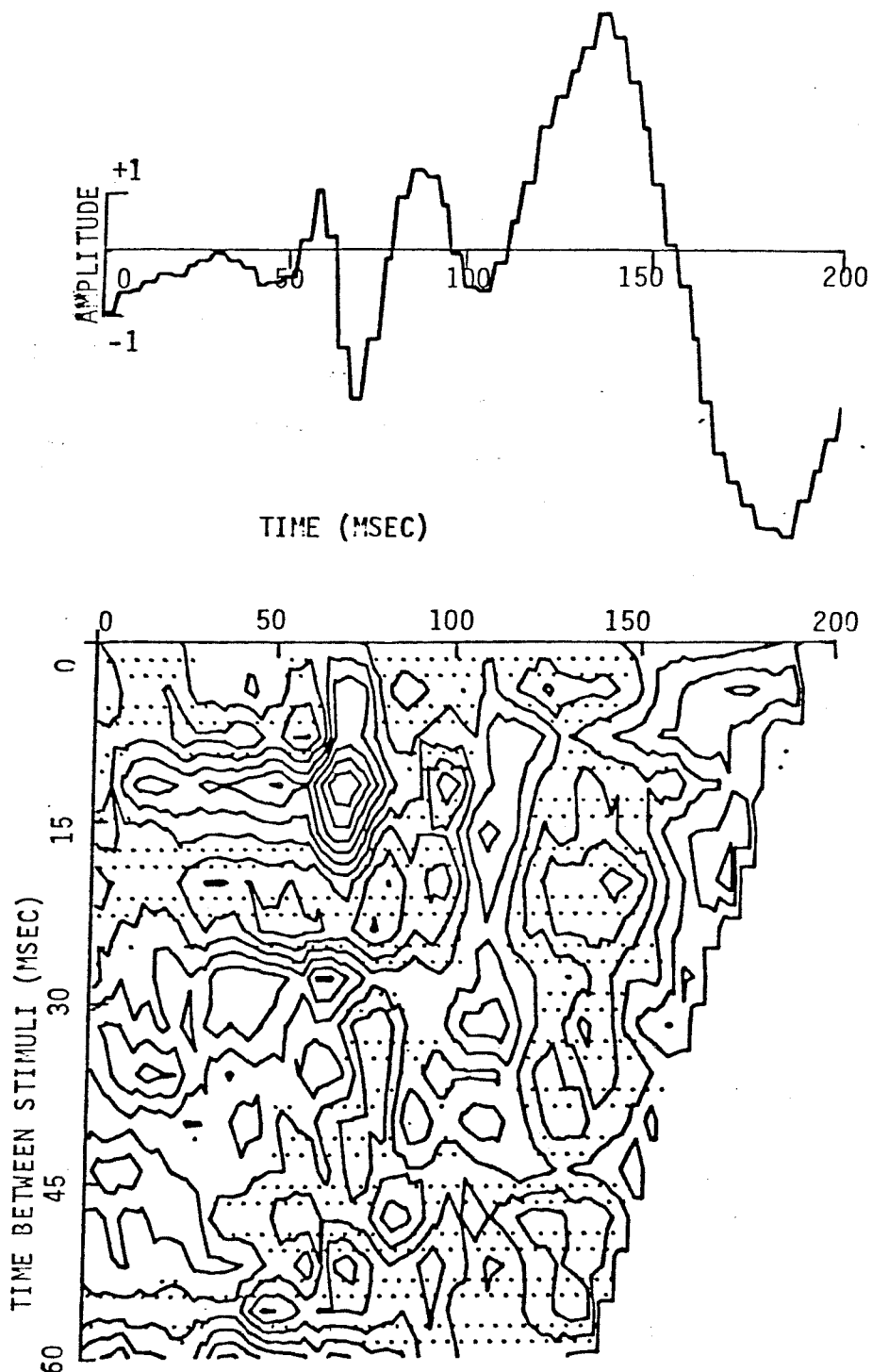


Fig. 4.4.2 One method of displaying the second-order kernel. A horizontal cut across the kernel at a specific 'time-between-stimuli' would give a profile corresponding to the curve in the lower diagram of Fig. 4.3.1 (Subject 2, 1 unit for $KF = 0.338 \mu V$, 1 contour for $KS = 0.044 \mu V$)

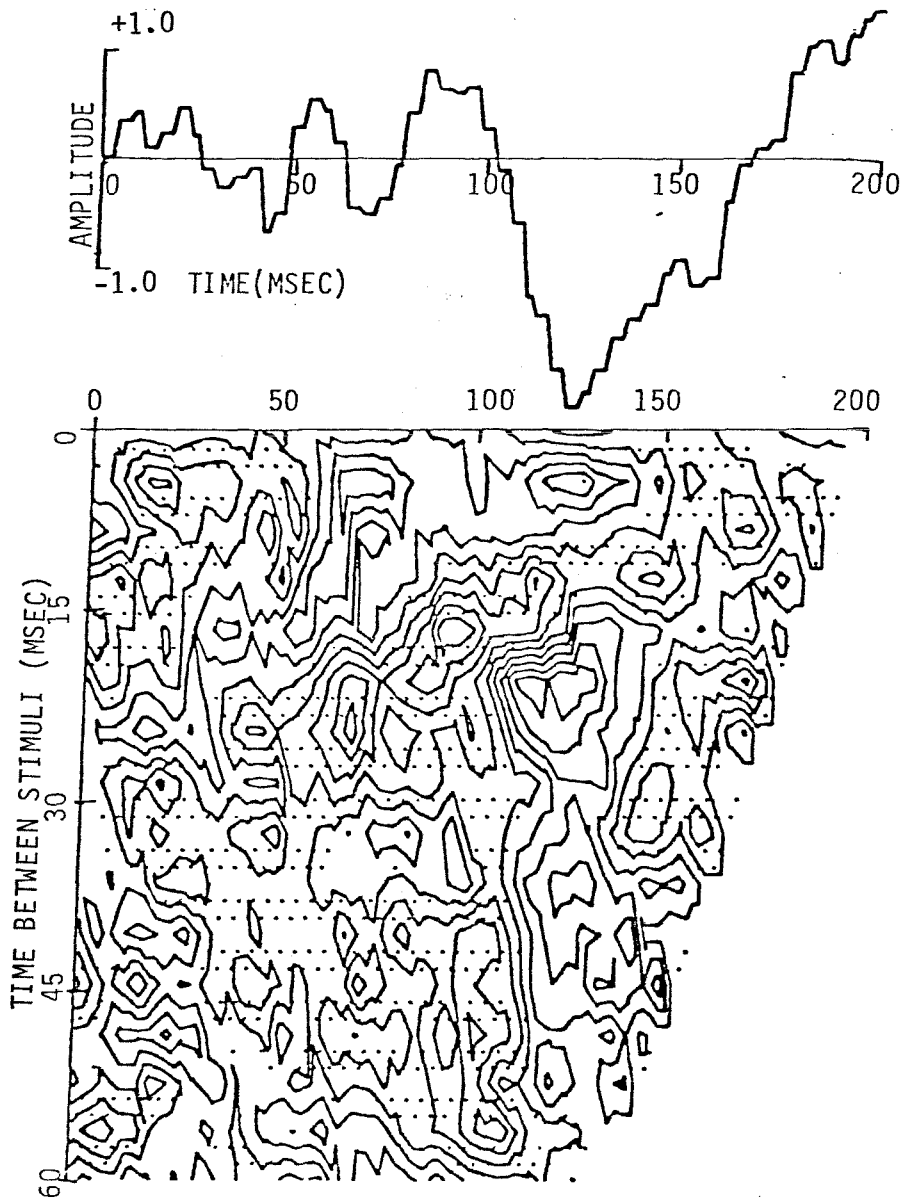


Fig. 4.4.3 The first- and second-order kernel for subject 1, electrode 1, second run. The inhibitory effect of the second-order kernel is seen most clearly in the region of 90 - 200 msec. (One unit for $KF = 0.377$ uv, one contour for $KS = 0.029$ uv)

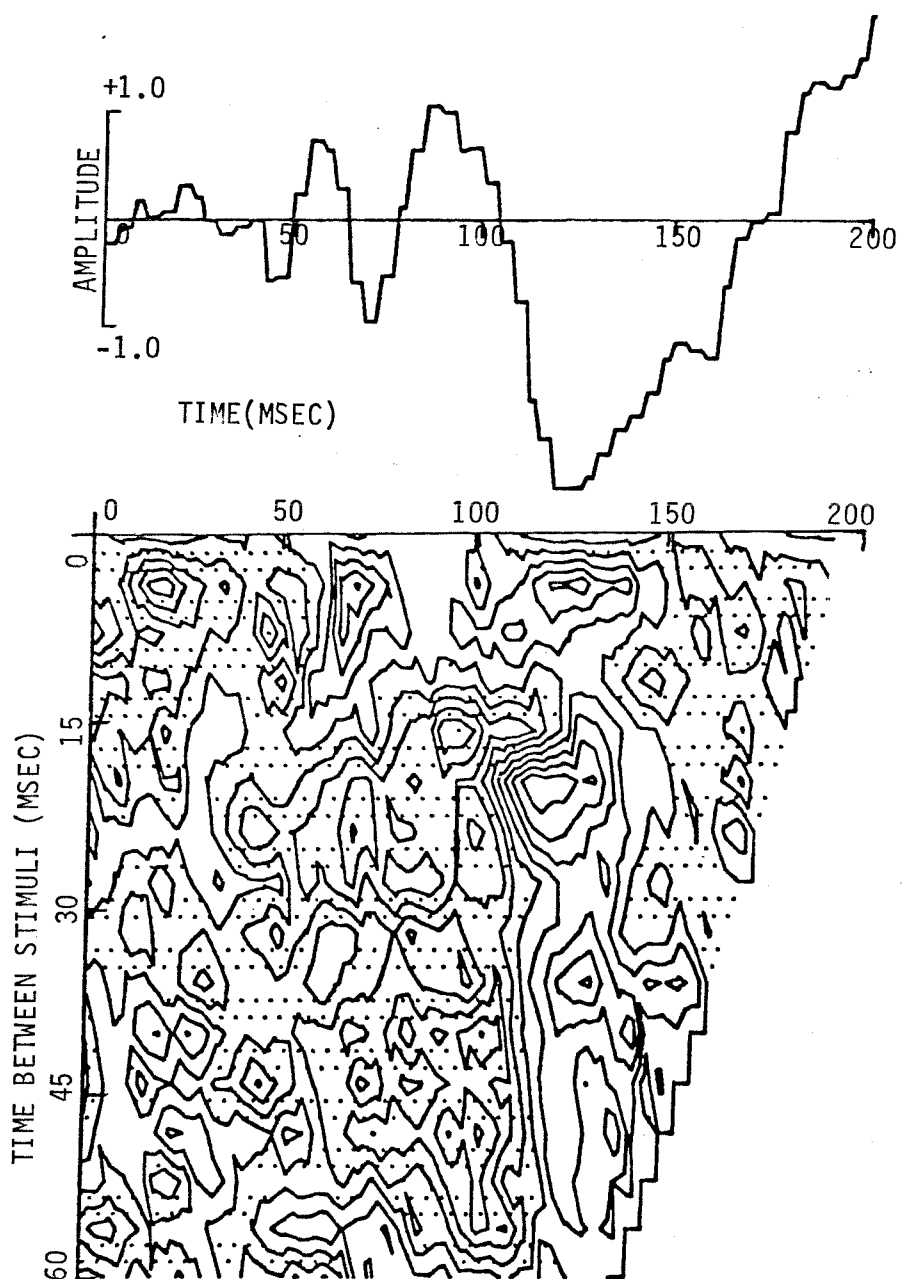


Fig. 4.4.4. The first- and second-order kernel for subject 1, electrode 2, second run. One unit for $KF = 0.377$ uv, one contour for $KS = 0.030$ uv)

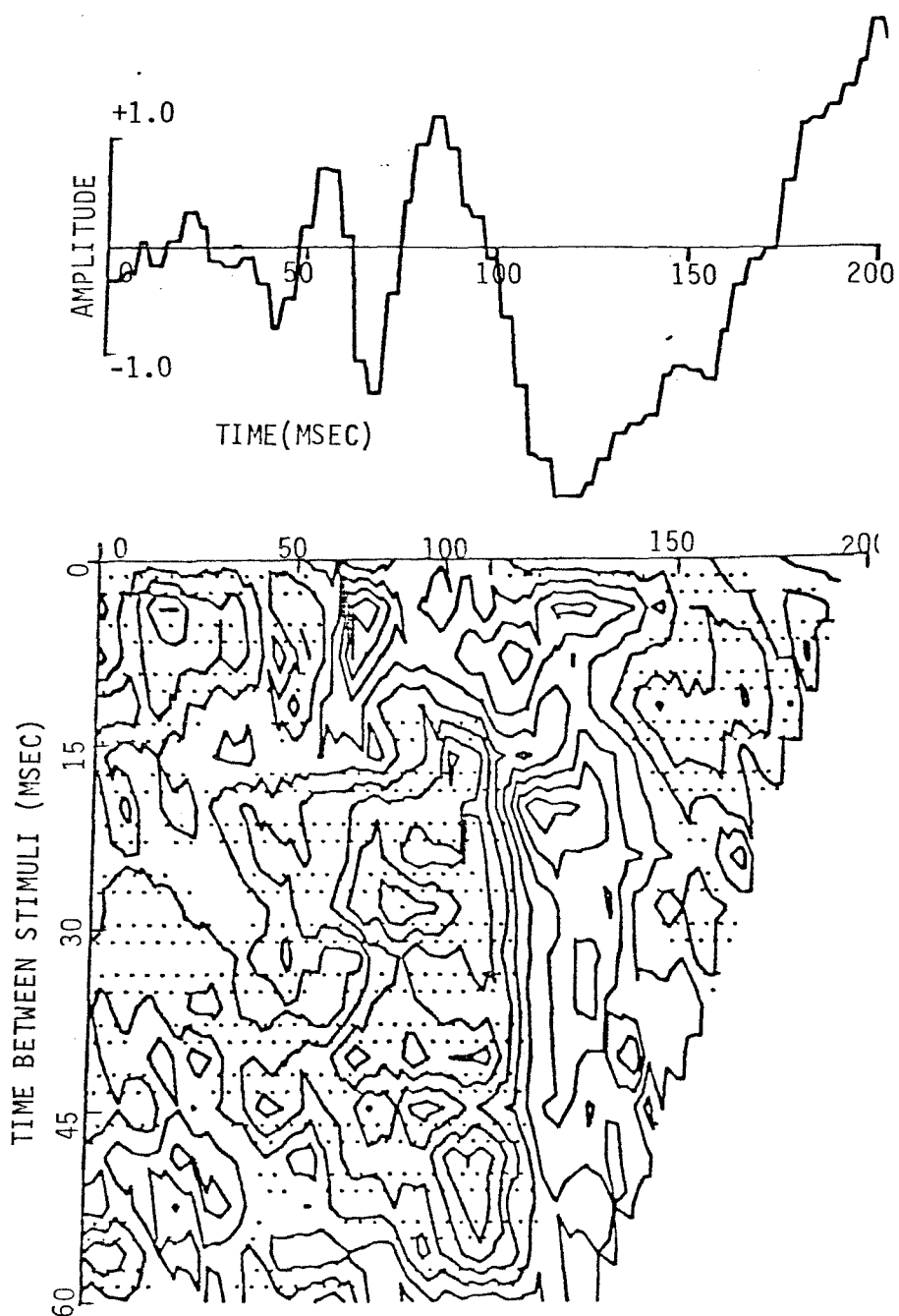


Fig. 4.4.5 The first- and second-order kernel for subject 1, electrode 3, second run. (One unit for KF = 0.377 μ v, one contour for KS = 0.033 μ v)

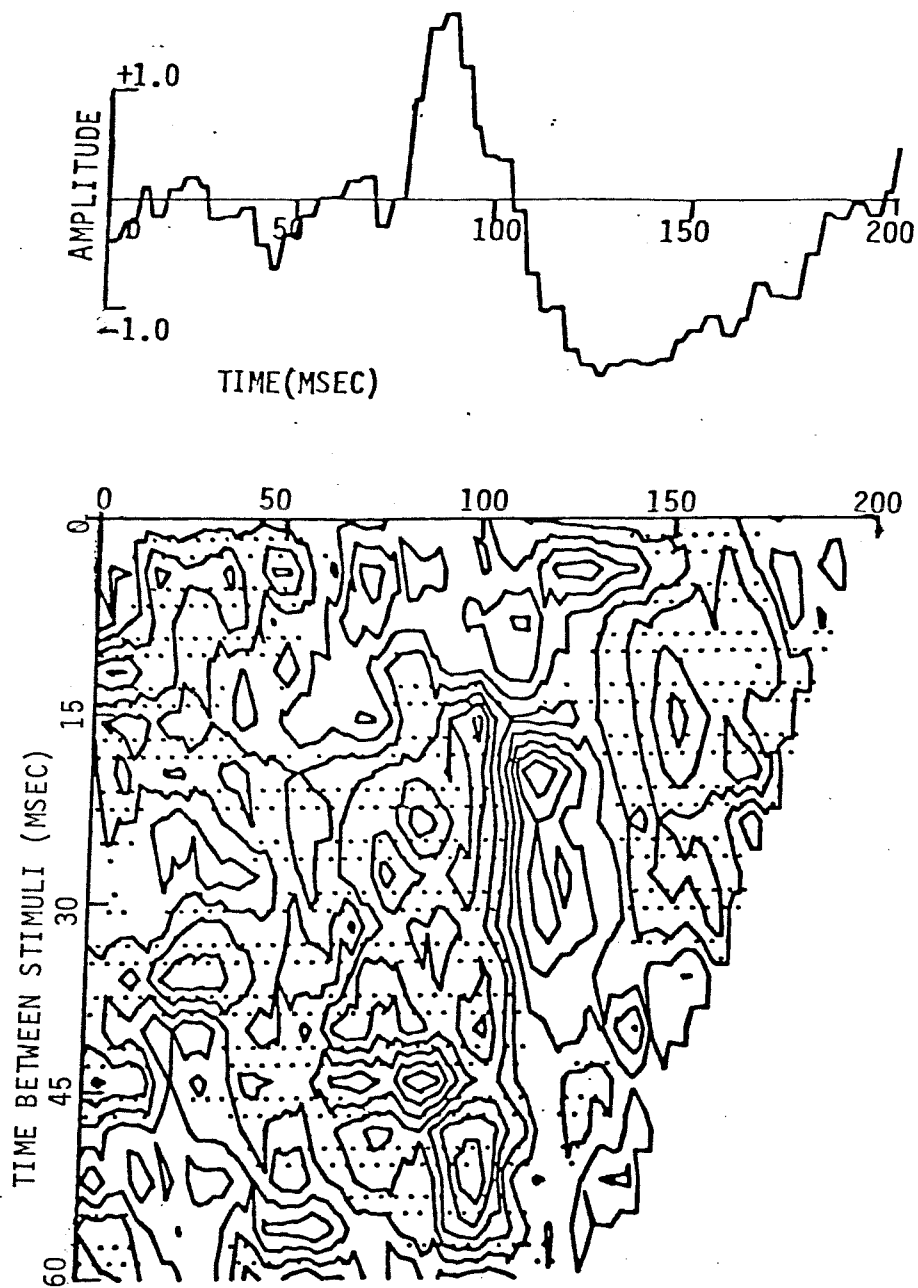


Fig. 4.4.6 The first- and second-order kernel for subject 1, electrode 4, second run. (One unit for KF = 0.377 uv, one contour for second-order kernel = 0.030 uv)

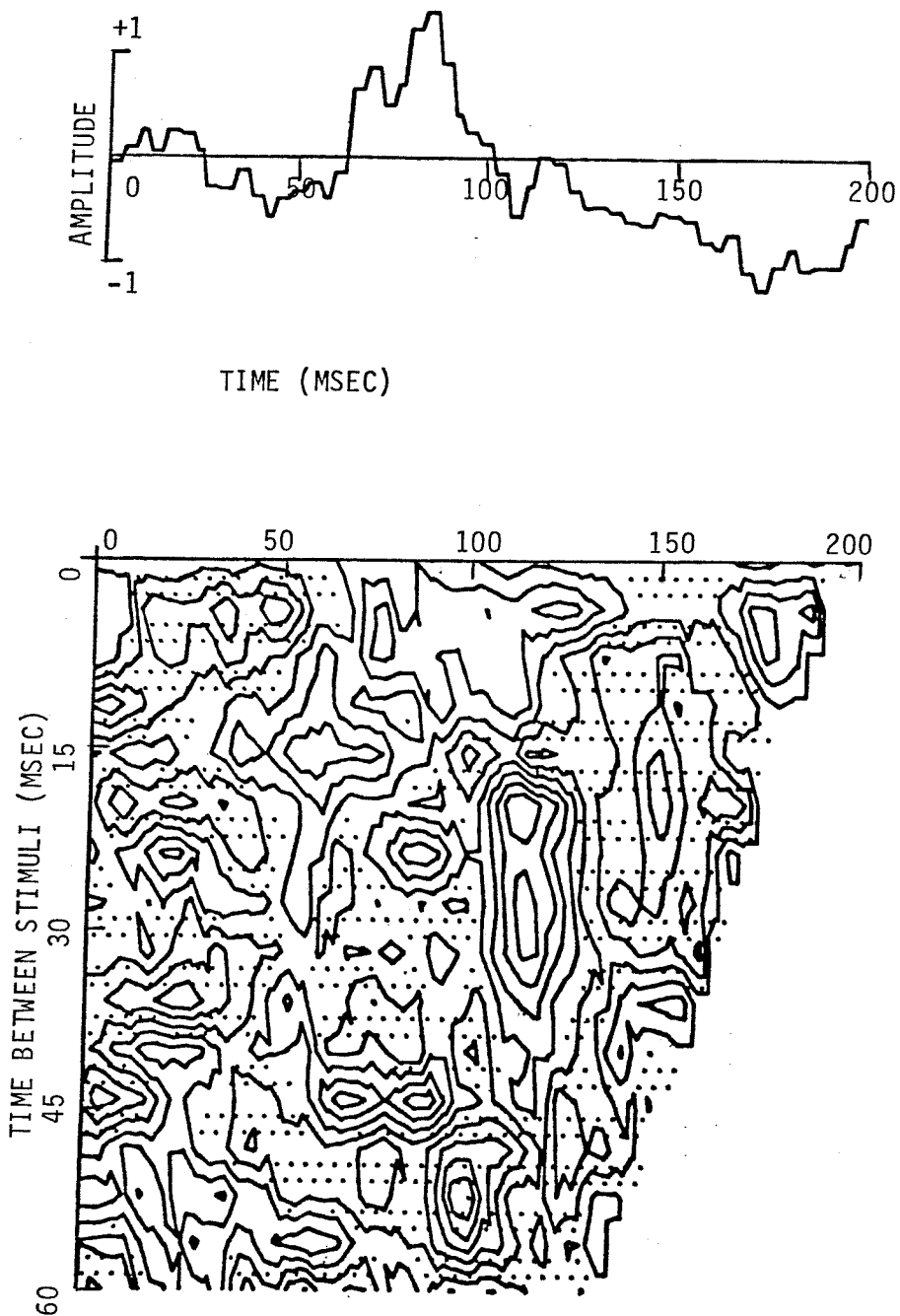


Fig. 4.4.7 The first- and second-order kernel for subject 1, electrode 5, second run. (One unit for KF = 0.377 μ V, one contour for KS = 0.033 μ V)

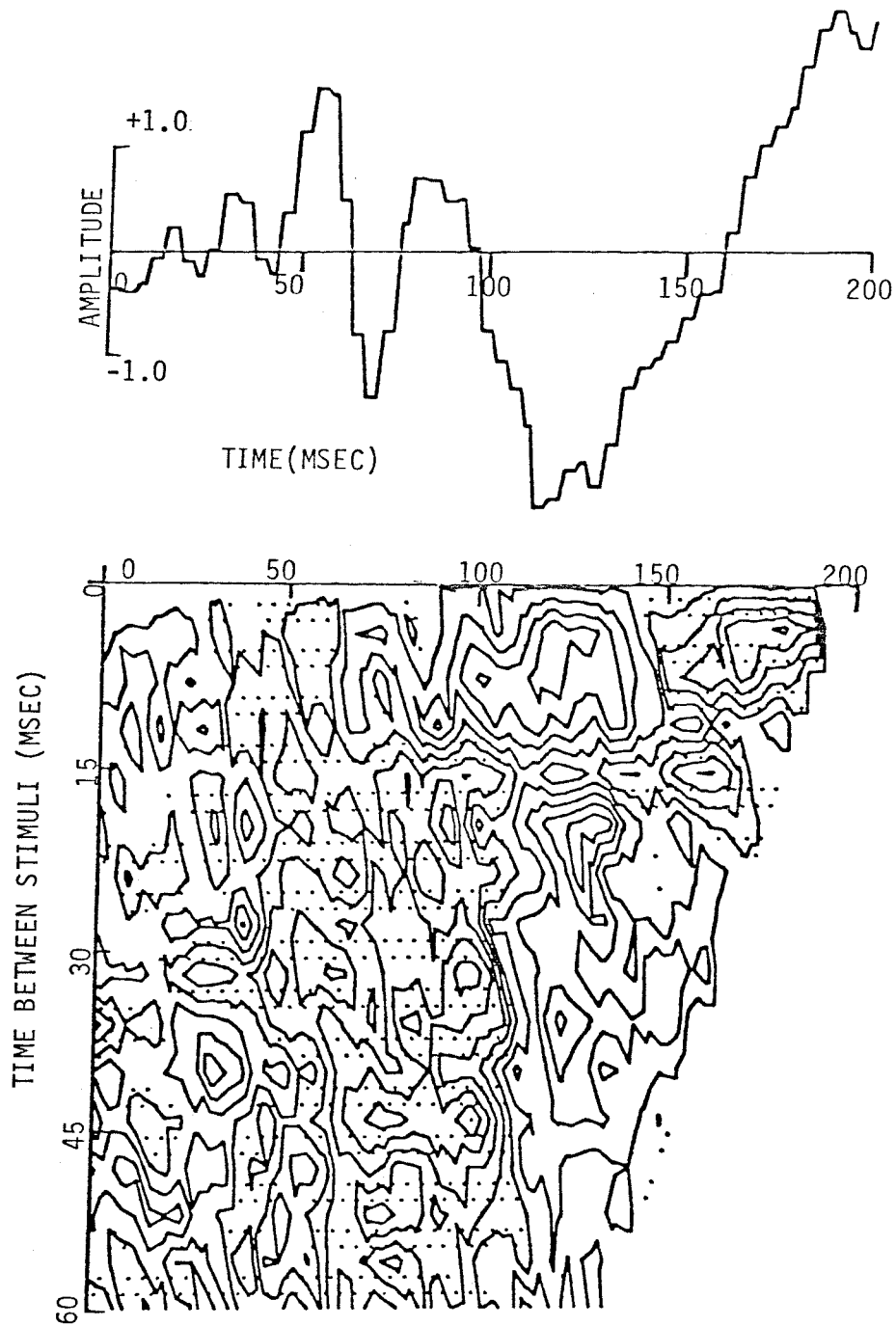


Fig. 4.4.8 The first- and second order kernel for subject 1, electrode 3, the third run. (One unit for KF = 0.329 uv, one contour for KS = 0.032 uv)

CHAPTER 5

Discussion and Conclusion

Changes in surrounding lights will evoke scalp potentials (VESP) and these events constitute an input-output, stimulus-response relationship that makes a systems-analysis approach appropriate. Wiener's nonlinear system identification method provides the theoretical background for this approach. In this thesis, a checkerboard-pattern transilluminated by a randomized flash sequence was chosen as the system probing signal. A single impulse is sufficient to evoke a response which will characterize a linear system. For nonlinear, time-invariant, finite-memory systems, white-noise is a theoretically valid probing signal(Chapter 2) to characterize the system.

Among different kinds of white-noise signals, the Poisson-impulse-train possesses the advantage of high power. This kind of white-noise stimulus has not been extensively used in the past partly because its kernel-estimation algorithm was developed only recently (Krausz, 1975; Kroeker, 1977) in comparison with the derivations of cross-correlation methods for Gaussian white-noise inputs following the approach of Lee and Schetzen(1965). Kernels have been difficult for conventional biologists, clinicians, and some evoked-potential researchers to understand because of their mathematical complexity and vagueness in physical meanings. As a matter of fact, it was not until the last few years that the physical meaning of kernels became generally understood. Some VESP researchers who were interested in white-noise, started by using (band-limited)Gaussian white-noise because that is the most commonly known probing signal.

In general, there have been very few attempts to use Volterra- Wiener kernels to characterize the VESP system in comparison with conventional signal averaging and steady-state evoked potentials which use sinusoids as the probing signals. This study is one of the few efforts in experimenting with this new method. The following are the original contributions of this work. (1) This is the first spatiotemporal approach in white-noise VESP studies. A large number of channels of first-order kernels were displayed in equipotential-map format. By doing so, the spatial potential distribution is clearly revealed. In the past, Beatty (1971), Reits (1975), Trimble and Phillips(1978), and Coppola (1979) have tried white-noise methods. They all used a small number of electrodes. No detailed spatial potential maps were generated. (2) This is the first trial to correlate first- and second-order kernels with underlying neural sources. Because of greatly improved S/N ratio and by combination of source-localization method and usage of large array of electrodes, this method has been proposed (Chen and Ary,1979) and data shown as a powerful probe to thalamic, subcortical and other indepth sources. (3) This is the first attempt to use light-modulated patterns (in particular, flashed checkerboard) instead of noise-modulated light as the stimulus. In comparison with noise-modulated light, pattern is a much stronger stimulus in producing more repeatable and definitive responses(chapter 1). Trimble and Phillips(1978) reported a memory length of 20 msec for the VESP. My data indicate that memory-lengths vary with the latencies of the peaks and valleys. The memory-lengths shown in chapter 4 indicate that they may extend to 60 msec (or slightly beyond). I speculate that these discrepancies may be explained by the fact that I used a stronger stimulus(Poisson as opposed to

GWN, pattern as opposed to luminance). Also my data (particularly, second-order kernels) show a better signal-to-noise ratio than previous results. None of the previous results showed detailed contour maps. Trimble and Phillips displayed their results in dot-density maps which are difficult to see distinct features. This, I believe, was caused by their noisier data and weaker responses. (4) This is the first attempt in using a Poisson-impulse-train as the stimulus in VESP studies. Sciabassi et al. (1977) used this stimulus to obtain somatosensory responses in the study of multiple sclerosis. Krausz (1975) mentioned using this stimulus to analyze auditory evoked potentials.

In general, Poisson-impulse-train proves to be a powerful stimulus to evoke a brain response. By a suitable selection of stimulus probability (a high probability makes the process approach Gaussian which is a psychophysically weaker stimulus; a probability too low makes event-pairs and event-triplets too rare to generate reliable kernel estimates), this stimulus was proved to be an effective system-probing signal. First- and second-order kernels reveal the system's response to single impulse and temporally-separate double impulses. They together constitute the major portion of the system's nonlinear response. First-order kernels are interpretable with respect to their underlying sources. Second-order kernels provide us with an additional tool to differentiate the underlying dynamic neural mechanisms. A suggestion for future study is an extensive study on many subjects by combining the source localization technique with multichannel first-order kernels to investigate the early peaks which are from LGN and other indepth sources. This

would open a new dimension in VESP studies. In addition to the basically inhibitory effect, the other subtleties revealed in the second-order kernels will be a challenge to future investigators.

REFERENCES

- Adrian, E. D.: Afferent discharges to the cerebral cortex from peripheral sense organs. *J. Physiol.*, 100(2):159-191, 1941.
- Anderson, P. and Anderson, S. A.: Physiological basis of the alpha rhythm. Appleton-Century - Crofts, New York, pp. 235, 1968.
- Ary, J. P.: The effect of color on the localization of the sources of human visual evoked response. Ph.D. Dissertation, Ohio State University, 1976.
- Ary, J. P.: A head-mounted 24-channel evoked potential preamplifier employing low-noise operational amplifiers. *IEEE Trans. Biomed. Engrg.*, BME-24: 293-297, 1977.
- Ary, J. P.; Klein, S. A.; Fender, D. H.: Location of sources of evoked scalp potentials: correction for skull and scalp thicknesses. *IEEE Biomed. Engrg.* Vol.BME-28, No.6, June, 1981.
- Barlow, J. S. and Brazier, M. A. B.: A note on a correlator system for brain potentials. *Electroenceph. Clin. Neurophysiol.*, Vol 6, pp.321-325, 1954.
- Barlow, J. S.: An electronic method for detecting evoked responses of the brain and for reproducing their average waveforms. *Electroenceph. Clin. Neurophysiol.*, 9:340-343, 1957.
- Barlow, J. S.: Computerized clinical electroencephalography in perspective. *IEEE Trans. on Biomed. Engrng.*, Vol. BME-26, No.7, July, 1979.
- Barrett, J.: The use of functionals in the analysis of nonlinear physical systems. *J. Electr. Control*, 15:567-615, 1963.
- Bartlett, N. R.; White, C. T.: Evoked potentials and correlated judgments of brightness as functions of interflash intervals. *Science*, 148:908-981, 1965.
- Bartley, S. H.: Comparison of electrogram of optic cortex with that of the retina. *Am. J. Physiol.*, 117:338, 1936.
- Beatty, J.: Measuring the Wiener kernels of CNS subsystems: a general method for systems analysis, paper presented at the 4th Ann. Winter Conf. on Brain Res., 1971.
- Beatty, J.: Applications of Wiener kernels analysis in psychology: the problem of manual control. *Proc. 1st Symp. on Test and Identification of Non-*

- linear Systems., pp.339-352, 1975.
- Becker, E. D. and Farrar, T. C.: Fourier transform spectroscopy. *Science*, 11:789-799, 1972.
- Bedrosian, E. and Rice, S. O.: The output properties of Volterra systems (non-linear systems with memory) driven by harmonic and Gaussian inputs. *Proc. IEEE*, 59:1688-1707, 1971.
- Bedrosian, E. and Rice, S.: Applications of Volterra-system analysis. *Proc. First Symp. on Test and Identification of Nonlinear Syst.*, pp.339-352, 1975.
- Berkhout, J.; Walter, D.: Temporal stability and individual differences in the human EEG: An analysis of variance of spectral values. *IEEE Trans. on Biomed. Engrng.*, Vol. BME-15, No.3, July, 1968.
- Biersdorf, W. : Cortical evoked response from stimulation of various regions of the visual field. XI ISCERG Symposium, *Doc. Ophth. Proc.*, Ser. 3:249-259, 1974.
- Biersdorf, W., Nakamura, F.: Localization studies of the human visual evoked response. Xth ISCERG Symposium, *Doc. Ophth. Proc.*, Ser. 2:137-144, 1973.
- Borda, R.; Frost Jr. J.: Error reduction in small sample averaging through the use of the median rather than the mean. *Electroenceph. Clin. Neurophysiol.*, 25:391-392, 1968.
- Bose, A.: A theory of nonlinear systems. *Res. Lab. Electron., MIT, Cambridge, Mass.*, Tech Rep.309, 1956.
- Brazier M. A.: Computer techniques in EEG analysis. Elsevier Publishing Company, 1961.
- Brenner, D., Williamson, S., Kaufman, L.: Visually evoked magnetic fields of the human brain. *Science*, Vol.190, Oct. 1975.
- Brilliant, M.: Theory of the analysis of nonlinear systems, *Res. Lab. Electronics. M.I.T., Cambridge, Mass.*, Tech. Rep. 345, 1958.
- Brindley, G. S.: The variability of human striate cortex. *J. Physiol.*, 225:1p-3p, 1972.
- Cameron R. and Martin W.: The orthogonal development of nonlinear functionals in series of Fourier-Hermite functionals. *Ann. Math.* 48:385-392, 1947.
- Carlson A.B.: Communication systems: An introduction to signals and noise in

- electrical communication. 2nd edition, McGraw-Hill, Inc., 1975.
- Caughey, T.: Nonlinear analysis, synthesis and identification theory. Proc. 1st Symp. on Test and Identification of Nonlinear Systems, pp. 1-14, 1975.
- Chen, M. J. and Ary, J. P.: LGN and deep source localization through evoked potentials. 1979 Annual Meeting Report. American Academy of Optometry.
- Chesler, D. A.: Nonlinear systems with Gaussian inputs. Technical Reports 336, Research Lab of Electronics, MIT, Feb. 15, 1960.
- Childers, D.G.; Mesa, W.; Halpeny, O. S.: A neuronal model for stimulation of spatio-temporal evoked EEG. IEEE Trans. Syst., Man and Cybern., SMC-3, 1973.
- Ciganek, L.: The EEG response (evoked potentials) to light stimulus in man. Electroenceph. clin. Neurophysiol., 13(2):165-172, 1961.
- Clynes, M. and Kohn, M.: Recognition of visual stimuli from the electric responses of the brain. In Kline, N.S. and Laska, E. (Eds.), 'Computers and Electronic Devices in Psychiatry', Grune, N.Y., 1968.
- Clynes, M. and Kohn, M.: Spatial VEP's as physiologic language elements for colour and field structure. EEG Journal, Suppl. 1, 26:82-96, 1967.
- Clynes, M., Kohn, M. and Lifshitz, K.: Dynamics and spatial behavior of light evoked potentials. Ann. N.Y. Acad. Sci., 112, 468-509, 1964.
- Cobb, W.: On the form and latency of the human cortical response to illumination of the retina. Electroenceph. Clin. Neurophysiol., 2:104, 1950.
- Cobb, W.A., Ettliger, G. and Morton, H.B.: Visual evoked potentials in binocular rivalry. Electroenceph. clin. Neurophysiol., Suppl. 26, pp. 100-107, 1967.
- Cooley J. and Tukey, J.: An algorithm for the machine calculation of complex Fourier series. Math. Comput. 19:297-301, 1965.
- Coppola, R.: A system transfer function for visual evoked potentials. Human Evoked Potentials, Applications and Problems. Edited by Lehmann and Callaway, Plenum Press, 1979.
- Corletto, F., Gentilomo, A., Rosadini, G., Rossi, G. F. and Zattoni, T.: Visual evoked potentials as recorded from the scalp and from the visual cortex before and after surgical removal of the occipital pole in man. Electroenceph. Clin. Neurophysiol., 22:378-380, 1967.
- Cruikshank, R.M.: Human occipital brain potentials as affected by intensity-

- duration variables of visual stimulation. *J. Exper. Psychol.*, 21:625-641, 1937.
- Crum, L.: Simultaneous reduction and expansion of multidimensional Laplace transform kernels. *Proc. 1st Symp. on Test and Identification of Non-linear Systems*, pp.89-105, 1975.
- Darcey, T. M.: Methods for localization of electrical sources in the human brain. Ph.D. Thesis, Caltech, 1979.
- Darcey, T. M.; Ary, J. P. and Fender, D. H.: Spatio-temporal visually evoked scalp potentials in response to partial-field patterned stimulation. *Electroenceph. and Clin. Neurophysiol.*, 50:348-355, 1980.
- Darcey, T. M.; Ary, J. P. and Fender, D. H.: Methods for the localization of electrical sources in the human brain, motivation, motor and sensory processes of the brain. *Progr. in Brain Res.*, Vol. 54., 1980.
- Darcy, T.M., Ary J.P., Fender, D.H.: Multichannel evoked scalp potentials: data analysis, display, and interpretation. 1980.
- Dawson, G. D.: A summation technique for the detection of small evoked potentials. *Electroenceph. Clin. Neurophysiol.*, 6:65-84, 1954.
- De Lange: Attenuation characteristics and phase-shift characteristics of the human fovea-cortex system in relation to flicker phenomena. Thesis, Technical University, Delft, The Netherlands, 1957.
- Donker, D. N. J.: Harmonic composition and topographic distribution of responses to sine wave modulated light (SML), their reproducibility and their interhemispheric relation. *Electroenceph. Clin. Neurophysiol.*, 39:561-574, 1975.
- Doty, R. W.: Ablation of visual areas of the central nervous system. In R. Jung (Ed.) *Handbook of Sensory Physiology. Vol.713B - Central Processing of Visual Information*, Springer-Verlag, New York, 1973.
- Dubinsky, J. and Barlow, J. S.: A simple dot-density tomogram for EEG. *Electroenceph. Clin. Neurophysiol.*, 48, 473, 1980.
- Duffy, F. H.; Burchfiel, J. L.; Lombroso, C. T.: Brain electrical activity mapping (BEAM), a method for extending the clinical utility of EEG and evoked potential data. *Ann. Neurol.*, 5:309, 1979.
- Elul, R.: Gaussian behaviour of electroencephalogram: Changes during performance of mental task. *Science*, Vol.164, p.328-331, Apr.-June, 1969.
- Eykhoff, P.: *System identification: parameter and state estimation*. Wiley, N.Y., pp. 94-104, 1974.

- Fender, D. H.: Watching the brain at work. Engineering and Science, April, California Institute of Technology, 12-16.
- Frechet, M.: Sur les functionals continues. Ann. Ec. Norm. Sup. 27:193-219 1910.
- French, A. S.; Butz, E. G.: Measuring the Wiener kernels of a nonlinear system using the fast Fourier algorithm. Int. J. Control 17, 529-539, 1973.
- French, A. S.; Butz, E. G.: The use of walsh functions in the Wiener analysis of nonlinear systems. IEEE Trans. on Computers, Vol.C-23, No.3, 1974.
- Fricker, S. J. and Sanders III, J. J.: Clinical studies of the evoked response to rapid random flash. Electroenceph. and Clin. Neurophysiol., 36:525-532, 1974.
- Galampos, R. and Davis, H.: The response of single auditory-nerve fibers to acoustic stimulation. J. Neurophysiol., 6(1): 39-57, 1943.
- Galampos, R. and Hallowell D.: The response of single auditory-nerve fibers to acoustic stimulation. J. Neurophysiol., 6:65-84, 1954.
- George, D.: Continuous nonlinear systems. Res. Lab. Electron., M.I.T., Cambridge, Mass., Tech. Rep. 355, 1959.
- Gevins, A.S.; Yeager, C.; Diamond, S.; Spire, J.; Zeitlin, G.; and Gevins, A.: Automated analysis of the electrical activity of the human brain(EEG): A progress report. Proc. IEEE, Vol.63, pp.1382-1399, Oct., 1975.
- Glass, A.: Changes in the amplitude probability function of the EEG under varying normal conditions. Electroenceph. Clin. Neurophysiol., Vol.26, pp.538, 1969.
- Goldman, D.: The clinical use of the "average" reference electrode in monopolar recording. EEG Clin. Neurophysiol., 2:211-214, 1950.
- Guyton, A.: Organ Physiology, Structure and Function of the Nervous System.
- Henderson, C. J.; Butler, S. R.; Glass, A.: The localization of equivalent dipoles of EEG sources by the application of electrical field theory. Electroenceph. and Clin. Neurophysiol., 39, 1975.
- Henderson, C. J.; Butler, S. R. and Glass, A.: Abstract of presentation given at EEG Society meeting in London on 15 Jan., 1977.
- Hida, T. and Ikeda, T.: Analysis on Hilbert space with reproducing kernel arising from multiple Wiener integral. Proc. of 5th Berkeley Symp. on Mathematical Statistics and Probability. 2:1:117-143, University of California Press, Berkeley and Los Angeles, 1965.

- Ho, D.: Functional identification and modelling of the human visual systems, Ph.D. thesis, Univ. of Calif., Berkeley, 1973.
- Hosek, R. S.; Sances Jr., A.; Jodat, R. W.; Larson, S. J.: The contribution of intracerebral currents to the EEG and evoked potentials. IEEE Trans. on Biomed. Engrng., Vol.BME-25, No.5, Sept., 1978.
- Hubel, D. H. and Wiesel, T. N.: Receptive fields, binocular interaction and functional architecture of the cat's visual cortex. J. Physiol., 160:106-154, 1962.
- Hubel, D. H. and Wiesel, T. N.: Receptive fields and functional architecture of two nonstriate visual areas(18 and 19) of the cat. J. Neurophysiol., 28:1041-1059, 1965.
- Hubel, D. H. and Wiesel, T. N.: Receptive fields and functional architecture of monkey striate cortex. J. Physiol., 195:215-243, 1968.
- Huber, P., Kleiner, B., Gasser, T., and Dumormuth: Statistical methods for investigating phase relations in stationary stochastic processes. IEEE Trans. on Audio and Electroacoustics. AU-19 (1), 78-86, March, 1971.
- Hung, G.; Stark, L.; and P. Eykhoff: On the interpretation of quadratic kernels.: I. Computer simulation of responses to impulse-pairs. Ann. Biomed. Eng., 5:130-143, 1977.
- Hung, G.; Brillinger, R. and Stark, L.: On the physiological interpretation of kernels: II. Essentially negative 1st and 2nd degree kernels of the human pupillary system. Ann. Biomed. Eng. 5, 1977.
- Hung, G. and Stark, L.: On the physiological interpretation of kernels: III. Positive off-diagonal kernels as kernel correlates of physiological process of pupillary escape. (unpublished paper) 1977.
- Hung, G. and Stark, L.: The kernel identification method - review of theory, calculation, application and interpretation. Math. Biosci., 37:135-190, 1977.
- Inoue, J.: Visual evoked potentials by monocular and binocular flashes, with double and single flashes. Acta Soc. Ophthal., Japan, 235.
- Jacobson, J. H., Kawasaki, K. and Hirose, T.: The human electroretinogram and occipital potential in response to focal illumination of the retina. Invest. Ophthal., 8(5): 545-556, 1969.
- Jeffreys, D. A.: Cortical source locations of pattern-related visual evoked potentials recorded from the human scalp. Nature, 229:502-504, 1971.

- Jeffreys, D. A. and Axford, J. G.: Source locations of pattern-specific components of human visual evoked potentials. II. Component of extrastriate cortical origin. *Exp. Brain Res.*, 16:22-40, 1972 b.
- Jeffreys, D. A.: A magnetic recording method of averaging evoked biological potentials. Thesis, University of London. 1968.
- Jewett, D. L.; Romano, M. N.; Williston, J. S.: Human auditory evoked potentials: possible brain stem components detected on the scalp. *Science*, Vol.167, pp.1517-1518, 1970.
- Johnson, T. L.; Wright, S. C.; Segall, A.: Filtering of muscle artifact from the electroencephalogram. *IEEE Trans. on BME*, Vol. BME-26, No.10, Oct. 1979.
- Kaiser, E.; Petersen, I.; Selden, N. and Kagawa, N.: EEG data representation in broad band frequency analysis. *Electroenceph. Clin. Neurophysiol.*, Vol.17, pp.76-80, 1964.
- Kamp, Sam-Jacobsen, Storm van Leeruwen and Van der Tweel: Cortical responses to modulated light in the human subject. *Acta Physiol. Scand.*, 48, 1-12, 1968.
- Kavanagh, R.; Darcy, T.; Lehmann, D.; Fender, D.: Evaluation of methods for three-dimensional localization of electrical sources in the human brain. *IEEE Trans. on Biomed. Engrng.*, Vol. BME-25, No.5, Sept., 1978.
- Klein, S.; Yasui, S.: Nonlinear system analysis with non-Gaussian white stimuli: general basis functionals and kernels. *IEEE Trans. on Information Theory*, Vol.II-25, No.4, July, 1979.
- Klein, S.: Interpreting nonlinear systems: the third order kernel of the eye movement control system. Published in Vogt and Mickle (editors). Tenth Annual Pittsburgh Conference on Modeling and Simulation, University of Pittsburgh, 1979.
- Koblaz, A. and Fender, D.: Nonlinear analysis of the human ERG: double pulse versus pseudo-random stimuli. Tech Rep., California Institute of Technology, 1975.
- Kooi, K. A.: *Fundamentals of Electroencephalography*. New York: Harper and Row, 1971.
- Kooi, K. A. and Bagchi, B. K.: Visual evoked responses in man: normative data. *Annals N.Y. Acad. Sci.*, (1):254-269, 1964.
- Krausz, H.: Identification of nonlinear systems using random impulse train inputs. *Biol. Cybernetics*, 19:217-230, 1975.

- Krausz, H. and Friesen, W. O.: Identification of discrete input nonlinear systems using Poisson impulse trains. Proc. 1st Symp. on Testing and Identification of Nonlinear Systems, 1975.
- Kroeker, J. P.: Wiener analysis of nonlinear systems using Poisson-Charier cross-correlation. Biol. Cybernetics 27:221-227, 1977.
- Ku, Y. H. and Wolf, A. A.: Volterra-Wiener functionals for the analysis for nonlinear systems. J. Franklin Inst., 281, No. 1, pp.9-26, Jan.,1966.
- Larkin, R. M.: Photopic rapid adaptation in the electroretinogram: A white noise analysis. Ph.D. Thesis, Caltech, 1979.
- Larkin, R. M.; Klein, S.; Ogden, T. E.; Fender, D. H.: Nonlinear kernels of the human ERG. Biol. Cybernetics 35:145-160, 1979.
- Larsen, H. and Lai, D.: Walsh spectral estimates with applications to the classification of EEG signals. IEEE Trans. on BME, Vol. BME-27, No.9, Sept., 1980.
- Larson, S. J. and Sances Jr., A.: Averaged evoked potentials in stereotaxic surgery. J. Neurosurg., Vol. 28, pp. 227-232, 1968.
- Lee, Y. W., Statistical theory of communication. Wiley and Sons, N.Y., 1960.
- Lee, Y. W., and Schetzen M.: Measurement of the Wiener kernels of a nonlinear system by cross-correlation. Int. J. Control 2:237-254, 1965.
- Lehmann, D.; Kavanagh, R.N.; Fender, D. H.: Field studies of averaged visually evoked EEG potentials in a patient with a split chiasm. Electroenceph. Clin. Neurophysiol., 26:13-199, 1969.
- Lehmann, D., Beeler, G. W., Jr. and Fender, D. H.: EEG responses to light flashes during the observation of stabilized and normal retinal images. Electroenceph. Clin. Neurophysiol., 22(2):136-142.
- Lehmann, D. and Fender, D. H.: Monocularly evoked electroencephalogram potentials: Influence of target structures presented to the other eye. Nature (London), 215:204-205.
- Lehmann, D.: Multichannel topography of human alpha EEG fields. Electroenceph. Clin. Neurophysiol., 31:439-449, 1971.
- Lehmann, D. and Skrandies W., Multichannel mapping of spatial distributions of scalp potential fields evoked by checkerboard reversal to different retinal areas. In D. Lehmann and E. Galloway (Eds.), Human Evoked Potentials-Applications and Problems; Plenum, London, pp.201-214, 1979.
- Marmarelis, P. Z.: Nonlinear dynamic transfer functions for certain retinal

- neuronal systems. Ph.D. Thesis, Caltech, 1971.
- Marmarelis, P. Z., Naka, K. I.: White-noise analysis of a neuron chain: An application of the Wiener theory. *Science*, Vol.175, pp 1276-1278, 1972.
- Marmarelis, P. Z., McCann G. D.: Development and application of white-noise modeling techniques for studies of insect visual nervous system. *Kybernetik*, 12:74-89, 1973.
- Marmarelis, P. Z., Naka, K. I.: Experimental analysis of a neural system: Two modelling approaches. *Kybernetik*, 15:11-26, 1974.
- Marmarelis, P. Z. and McCann, G. D.: Errors involved in the practical estimation of nonlinear system kernels. *Proc. Conf. on Testing and Identification of Nonlinear Systems. CIT*, 147-173, 1975.
- Marmarelis, V. Z. and McCann, G. D.: Optimization of test parameters in the identification of spike train responses of biological systems through random test signals. *Proc. Conf. on Testing and Identification of Nonlinear Systems. CIT*, 325-338, 1975.
- Marmarelis, V. Z.: A family of quasi-white random signals and its optimal use in biological system identification. Part I: Theory. *Biol. Cybernetics* 27:49-56, 1977a.
- Marmarelis, V. Z.: A family of quasi-white random signals and its optimal use in biological system identification. Part II: Application to the Photoreceptor of *Calliphora Erythrocephala*. *Biol. Cybernetics*, 27: 57-62, 1977b.
- Marmarelis, V. Z.: Random versus pseudorandom test signals in nonlinear-system identification. *Proc.IEEE*, Vol.125, No. 5, May 1978.
- Marmarelis, P. Z. and Marmarelis, V. Z.: Analysis of physiological systems; the white-noise approach. Plenum Press, N. Y., 1978.
- Matousek, M., Volavka, J., Roubuek, J. and Roth, Z.: EEG frequency analysis related to age in normal adults. *Electroenceph. clin. Neurophysiol.*, Vol. 23, pp. 162-167, 1967.
- McCann, G. D.: Development of nonlinear identification models for a comprehensive representation of insect visual nervous systems. Part I. The horizontal motion detection system. *Tech. Rep., Calif. Inst. of Technology*, 1973.
- McCann, G. D.: Nonlinear identification theory models for successive stages of visual nervous system of flies. *J. Neurophysiol.*, 37:869-895, 1974.
- McEwen, J. A. and Anderson, G. B.: Modeling the stationarity and Gaussianity

- of spontaneous electroencephalography activity. IEEE Trans. on BME, Vol. BME-22, No.5, September 1975.
- McGillem, C. D., Aunon, J. I.: Measurements of signal components in single visually evoked brain potentials. IEEE Trans. on Biomed. Engineering, Vol. BME-24, No.3, May 1979.
- McShane, E. J.: Stochastic integrals and nonlinear processes. J. of Math and Mechanics. 2:235-283, 1962.
- Michael, W. F. and Halliday, A. M.: Differences between the occipital distribution of upper and lower field pattern-evoked responses in man. Brain Res., 32:311-324, 1971.
- Milner, B.A., Regan, D., Heron, J.R.: Theoretical models of the generation of steady-state evoked potentials, their relation to neuroanatomy and their relevance to certain clinical problems, in Arden GB (ed.): The Visual System: Neurophysiology, Biophysics and their Clinical Applications, Vol. 24, Advances in Experimental Medicine and Biology. New York, Plenum Press, 1972.
- Montagu, J. D.: The relationship between the intensity of repetitive photic stimulation and the cerebral response. Electroenceph. Clin. Neurophysiol., 23:152-161, 1967.
- Moore, G.; Reinking, R.; Stauffer E. and Stuart D.: White noise analysis of mammalian muscle receptors. In Proc. 1st Symp. on Testing and Identification of Nonlinear Syst., pp. 316-324, 1975.
- Nakamura, F. and Biersdorf, W. R.: Localization of the human visual evoked response. Early components specific to visual stimulation. Amer. J. Ophth., 72:988-997, 1971.
- Narayanan, S.: Transistor distortion analysis using Volterra series representation. The Bell System Technical Journal, May-June 1967.
- Obriest, W.D. and Henry, C.E.: Frequency analysis of aged psychiatric patients. Electroenceph. clin. Neurophysiol., Vol. 10, pp. 621-632, 1958.
- Offner, F. F.: The EEG as potential mapping: the value of the average monopolar reference. EEG Clin. Neurophysiol., 2:215-216, 1950.
- Ogura, H.: Orthogonal functionals of the Poisson process. IEEE Trans. on Information Theory, Vol.11, No. 4, pg. 18, July, 1972.
- Osselton, J. W.: Acquisition of EEG data by bipolar, unipolar and average reference methods: A theoretical comparison. EEG Clin. Neurophysiol., 19:527-528, 1965.

- Padmos, P. and Norren, D.V.: The vector voltmeter as a total to measure electroretinogram spectral sensitivity and dark adaptation. *Invest. Ophthalm.*, 11:783-788, 1972.
- Palm, G. and Poggio, T.: Wiener-like system identification in physiology. *J. Math. Biol.*, 4:375-381, 1977.
- Palm, G. and Poggio, T.: Stochastic identification methods for nonlinear systems: An extension of the Wiener theory. *SIAM. J. Appl. Math.*, 34:524-534, 1978.
- Perry, N. W., and Childers, D. C.: The human visual evoked response. Charles C. Thomas, Springfield, Illinois, 1969.
- Petsche, H.: Handbook of electroencephalography and clinical neurophysiology. EEG Topography, A. Remond(Ed.) Elsevier, Amsterdam, Vol 5B, 1973.
- Ratliff, F., Victor, J., Shapley, R.: Nonlinear analysis of visual evoked potentials in the human. 1978 Annual Meeting, Optical Society of America.
- Reddy, N. and Kirilin, R.: Spectral analysis of auditory evoked potentials with pseudorandom noise excitation. *IEEE Trans. on Biomed. Engrng.*, Vol.BME-26, No.8, Aug. 1979.
- Regan, D.: Evoked Potentials. Chapman and Hall; London, 1972.
- Reits, D.: Potentials in man evoked by noise modulated light. Ph.D. Thesis, University of Amsterdam, 1975.
- Reitveld, W. J.; Tordoir, W. E. M.; Hagenouw, J. R. B.; Lubbers, J. A. and Spoor, Th. A. C.: Visual evoked responses to blank and to checkerboard patterned flakes. *Acta Physiol. Pharmacol. Neurol.*, 14:259-285, 1967.
- Rosner; Burton, S.; Allison, T.; Swanson, E.; Goff, W.: A new instrument for the summation of evoked responses from the nervous system. *Electroenceph. Clin. Neurophysiol.*, 12(3):745-747, 1960.
- Rushkin, D. S.: An analysis of average response computations based upon aperiodic stimuli. *IEEE Trans. Biomed. Engrng.*, BME-12, 87-94, 1965.
- Sandberg A. and Stark, L.: Wiener G-Function analysis as an approach to nonlinear characteristics of human pupil light reflex. *Brain Res.* 11: 194-211, 1968.
- Schneider, M. et Gerin, P.: Une methode de localisation des dipoles cerebraux. *Electroenceph. Clin. Neurophysiol.*, 28:69-78, 1970.

- Sciabassi, R.; Risch, H.; Hinman, C.; Kroin, J.; Enns, N. and Namerow, N.: Complex pattern evoked somatosensory responses in the study of multiple sclerosis. Proc. of the IEEE, Vol.65, No.5, May 1977.
- Segundo, J.; Bryant H. and Brillinger D. R.: Identification of synaptic operators. In Proc. 1st Symp. on Testing and Identification of Nonlinear Systems., pp. 221-226, 1975.
- Shetzen, M.: Measurement of the kernels of a non-linear system of finite order.
- Sokol, S.: Visually evoked potentials: Theory, techniques and clinical applications. Survey of Ophthalmology., Vol 21, No.1, July-Aug 1976.
- Spekreijse: Analysis of EEG response in man. Junk Publishers; The Hague, The Netherlands, 1966.
- Spekreijse and Oosting: Linearizing, a method for analyzing and synthesizing nonlinear systems. Kybernetik, 7:22-31, 1970.
- Spehlmann, R.: The averaged electrical response to diffuse and to patterned light in the human. Electroenceph. clin. Neurophysiol., 19:560-569, 1965.
- Sprague, J. M., Berlucchi, G. and Rizzolatti, G.: The role of the superior colliculus and pretectum in vision and visually guided behavior. In R. Jung (Ed.) Handbook of Sensory Physiology- Vol.7/3b - Central Processing of Visual Information. Springer-Verlag. New York, 1973.
- Starr. A. and Achor, L. J.: Auditory brain stem responses in neurological diseases. Arch. Neurol., Vol. 32, pp.761-768, 1975.
- Trimble, J. and Phillips, G.: Nonlinear analysis of the human visual evoked response. Biol. Cybernetics 30:55-61, 1978.
- Van der Tweel, L. H.: Some problems in vision regarded with respect to linearity and frequency response. Ann. N.Y. Acad. Sci., 89:829-856, 1961.
- Van der Tweel, L.H. and Verduyn-Lunel, H.F.E.: Human visual responses to sinusoidally modulated light. Electroenceph. Clin. Neurophysiol., 18:587-598, 1965.
- Van der Tweel, L.H. and Spekreijse, H.: Signal transport and rectification in the human evoked response system. Ann. N.Y. Acad. Sci., 156:678-685, 1969.
- Van Trees, H. L.: Volterra series representation of optimum nonlinear control systems. MIT Press, Cambridge, Mass., 1962.

- Vaughan, H. G.: The perceptual and psychologic significance of visual evoked responses recorded from scalp in man. *Vision Research (Suppl)*, 211, 1966.
- Volterra, V.: *Theory of Functionals*. Blackie and Sons, Glasglow, 1930.
- Walter, D. O. and Adey, W. R.: Analysis of brain wave generators as multiple statistical time series. *IEEE Trans. Biomed. Eng.*, Vol. BME-12, pp. 8-13, Jan. 1965.
- Watanabe A. and Stark, L.: Kernel method for nonlinear analysis: identification of a biological control system. *Math. Biosci.* 27:99-108, 1975.
- Wennberg, A. and Zetterberg L. H.: Application of a computer-based model for EEG analysis. *Electroenceph. and Clin. Neurophysiol.* 31:457-468, 1971.
- Whalen, A. D.: *Detection of signals in noise*. Academic Press, N.Y., 1971.
- White, C.T.: Evoked cortical responses and patterned stimuli. *Am. Psychol.*, 24, 212-216, 1968.
- Wiener, N.: *Extrapolation, interpolation and smoothing of stationary time series*. J. Wiley and Sons, New York, 1949.
- Wiener, N.: *Nonlinear problems in random theory*. New York, J. Wiley, 1958.
- Yasui, S. and Fender D.: Methodology for measurement of spatial-temporal Volterra and Wiener kernels for visual systems. In *Proc. 1st Symp. on Testing and Identification of Nonlinear Systems*, pp.366-383, 1975.